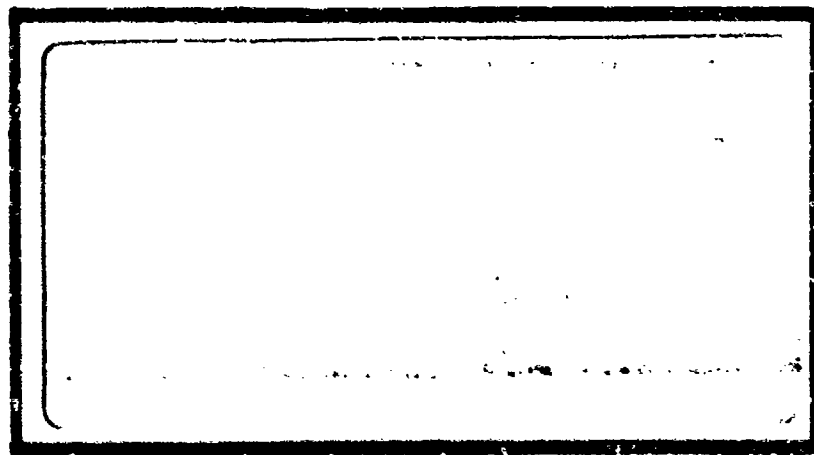


DTIC FILE COPY

AD-A189 843



DTIC

LECTE

MAR 07 1988

00 H

DEPARTMENT OF THE AIR FORCE
AIR UNIVERSITY

AIR FORCE INSTITUTE OF TECHNOLOGY

Wright-Patterson Air Force Base, Ohio

DISTRIBUTION STATEMENT A

88 3 01 099

AFIT/GE/ENG/87D-50

A MODEL FOR NITROGEN
ATOM RECOMBINATION ON A
SILICON DIOXIDE SURFACE

THESIS

Michael Newman
Captain, USAF

AFIT/GE/ENG/87D-50

Approved for public release; distribution unlimited

DTIC
ELECTE
MAR 07 1988
H

A MODEL FOR NITROGEN
ATOM RECOMBINATION ON A
SILICON DIOXIDE SURFACE

THESIS

Presented to the Faculty of the School of Engineering
of the Air Force Institute of Technology
Air University
In Partial Fulfillment of the
Requirements for the Degree of
Master of Science in Electrical Engineering

Michael Newman, B.S., M.S.
Captain, USAF

December 1987

Approved for public release; distribution unlimited

Preface

The primary objective of this thesis was to develop a model which described the steady-state heterogeneous recombination of atomic nitrogen on a silicon dioxide surface as a function of temperature. The temperature range was 300-2000K. The need to accurately characterize a surface, coupled with a better understanding of the heterogeneous recombination process are especially important with regard to earth orbiting reentry vehicles such as the Space Shuttle Orbiter. The Langmuir-Rideal recombination mechanism was adapted for this thesis and was shown to agree well with the experimental data.

My sincere gratitude is extended to my thesis advisor, Maj Donald R. Kitchen, for his agreeing to assume this task, his unflagging patience, moral support, and technical guidance. An equal amount of gratitude is also extended to Lt Col Eric J. Jumper and Maj W. A. Seward without whom this thesis would not have been possible. My gratitude goes to the additional member of my research committee, Dr. Ernest Dorko.

Additional gratitude goes to Mr. and Mrs. Douglas Rabe who gladly accepted the task of typing this thesis and to the support staff at the AFIT Library and those individuals



For	
A&I	
need	
Classification	
By	
Distribution/	
Availability Co	
Avail and/	
Dist	Special
A-1	

at the AFIT Canteen, especially Mrs. Mary Torry, who provided words of wisdom and encouragement.

This research project is dedicated to my grandparents.

Michael Newman

Table of Contents

	Page
Preface	ii
List of Figures	vi
List of Tables.	ix
Abstract	xi
I. Introduction	1
Background.	1
Purpose of Study	1
Outline of Study	3
Scope.	5
Approach	7
Assumptions	10
Results	11
Sequence of Presentation	12
II. Background	14
Introduction	14
The Thermal Protection System of the Space Shuttle Orbiter	14
Mechanisms of Heterogeneous Recombination	22
Introduction	22
Adsorption.	23
Physical Adsorption	24
Chemical Adsorption	24
The Langmuir Isotherm	28
The Langmuir-Hinshelwood Mechanism	30
The Migration Mechanism	33
The Langmuir-Rideal Mechanism	34
Details of the Model.	38
The Rate Equations from First Principles.	41
Review of the Literature	56
Introduction	56
Discussion of the Literature	57
Summary	69
Silica Surface Structures.	70
Introduction	70
Silicon Dioxide.	70
Silicon Nitride.	73
Silicon Oxynitride	74
Summary	75

III. Analytical	88
Introduction	88
Calculation of the Surface Area	90
Calculation of the Number of Surface Sites Per Unit Area	97
Calculation of the Pressure	103
Calculation of the Activation Energy and Steric Factor	105
Determination of the Dissociation Energy.	110
Values Selected for the Initial Sticking Coefficient	113
Summary	115
IV. Results and Discussion	117
Introduction	117
The Recombination Coefficient of Nitrogen on Silicon Dioxide	118
The Sorption Rates of Nitrogen on Silicon Dioxide	127
The Effect of the Denominator Terms on the Recombination Mechanism	133
The Effect of Varying the Initial Sticking Coefficient on the Recombination Reaction	139
Effect of Holding the Pressure Constant vs. Pressure Being a Function of the Temperature	141
The Fractional Surface Concentration of Nitrogen on Silicon Dioxide	143
The Fractional Surface Concentration of Oxygen on Silicon Dioxide.	146
Summary	154
V. Conclusions and Recommendations	156
Conclusions	156
Recommendations.	157
Appendix A: Computer Routine to Calculate the Recombination Coefficient of Nitrogen on Silicon Dioxide as a Function of Temperature.	161
Bibliography	164
Vita.	172

List of Figures

Figure	Page
1. Thermal Protection System of the Orbiter. Side View	15
2. Thermal Protection System of the Orbiter. Upper and Under Surfaces	16
3. Potential Energy of a System as a Function of the Distance of the Adsorbate from the Surface Relative to Zero Potential Energy of the Adsorbate at an Infinite Distance	26
4. Recombination Coefficients of Atomic Nitrogen on Silica Surfaces	62
5. Relative Volume Expansions of Crystalline and Amorphous Phases of Silica	72
6. Alpha-Quartz (Two Cells), SiO_2 . Low Temperature Phase	76
7. Beta-Quartz (Two Cells), SiO_2 . High Temperature Phase	77
8. Tridymite, SiO_2 . Viewed Along $\langle 110 \rangle$ Direction	78
9. Alpha-Cristobalite, SiO_2 . Low Temperature Phase	79
10. Beta-Cristobalite, SiO_2 . High Temperature Phase	80
11. Silica Glass, SiO_2	81
12. Silicon Nitride, Si_3N_4	82
13. Alpha-Silicon Nitride, $\alpha\text{-Si}_3\text{N}_4$. Low Temperature Phase	83
14. Beta-Silicon Nitride, $\beta\text{-Si}_3\text{N}_4$. High Temperature Phase	84
15. Silicon Dioxide Model Showing Double Bonds at the Surface. Top View, $\langle 110 \rangle$ Direction	85
16. Silicon Dioxide Model Showing Double Bonds at the Surface. Side View.	86

Figure	Page
17. Silicon Dioxide Model Showing Rearrangement of the Double Bonds at the Surface. Stoichiometry is Maintained. Top View, <110> Direction .	87
18. Top View of Quartz Surface	93
19. Side View of the Quartz Surface (View A-A) .	94
20. Calculation of the Surface Area, A.	95
21. Dimensions Used to Determine the Surface Area, A	96
22. The Quartz Configuration Before Simplification	98
23. The Quartz Configuration After Simplification	99
24. A Hexagon Pattern Used to Determine the Number of Sites	100
25. A Lewis Structure for the $\text{Si}_x\text{O}_y\text{N}_z$ Molecule .	111
26. The Recombination Coefficient of Nitrogen on Silicon Dioxide as a Function of Temperature and a Dissociation Energy of 79 Kcal/Mole .	119
27. The Recombination Coefficient as a Function of Temperature for Dissociation Energies of 79 and 105 Kcal/Mole.	121
28. The Sorption Rates vs. Temperature for Nitrogen on Silicon Dioxide at a Dissociation Energy of 79 Kcal/Mole	128
29. The Sorption Rates vs. Temperature for Nitrogen on Silicon Dioxide at a Dissociation Energy of 105 Kcal/Mole	129
30. The Recombination Coefficient as a Function of Temperature for Initial Sticking Coefficients of $0.05 \times \exp(-0.002 \times T)$ and $0.95 \times \exp(-0.002 \times T)$	140
31. The Recombination Coefficient as a Function of Temperature. The Gas Pressure Varied as the Temperature and a Fixed Value of the Pressure	142
32. Fractional Surface Concentration as a Function of Temperature for Nitrogen on Silicon Dioxide	144

Figure	Page
33. Fractional Surface Concentration as a Function of Temperature for Nitrogen on Silicon Dioxide for a Dissociation Energy of 79 and 105 Kcal/Mole.	147
34. Fractional Surface Concentration for Oxygen on Silicon Dioxide	149
35. An Overlay of the Fractional Surface Concentration for Nitrogen onto that of Oxygen on a Silicon Dioxide Surface	151

List of Tables

Table	Page
1. Thermal Protection System of the Orbiter .	17
2. Physisorption and Chemisorption Characteristics	25
3. Recombination Coefficient Data for Atomic Nitrogen on Silicon Dioxide and Pyrex Surfaces	60
4. Order of the Recombination	66
5. Properties of the Phases of Silica. . . .	71
6. Properties of the Phases of Silicon Nitride .	73
7. Recombination Coefficient Versus Temperature.	108
8. Activation Energies and Steric Factors . .	109
9. Steric Factors.	110
10. Input Parameters to Calculate the Recombination Coefficient	115
11. Calculated Values of the Recombination Coefficient, Gamma, for a Dissociation Energy of 79 Kcal/Mole	120
12. Calculated Values of the Recombination Coefficient, Gamma, for a Dissociation Energy of 105 Kcal/Mole	122
13. Calculated Values of the Sorption Rates for a Dissociation Energy of 79 Kcal/Mole . . .	127
14. Calculated Values of the Sorption Rates for a Dissociation Energy of 105 Kcal/Mole . . .	130
15. Calculated Values of the Denominator Terms of Equation (101) for a Dissociation Energy of 79 Kcal/Mole	135
16. Calculated Values of the Denominator Terms of Equation (101) for a Dissociation Energy of 105 Kcal/Mole	136

Table**Page**

- | | |
|--|-----|
| 17. Gamma vs. Temperature for Fixed and Varying Pressure | 143 |
| 18. Input Parameters to Calculate the Fractional Surface Concentration for Oxygen Chemisorption on Silicon Dioxide | 148 |

Abstract

A model which describes the heterogeneous recombination of atomic nitrogen on a silicon dioxide surface in the temperature range 300-2000K was developed. The model accounts for surface participation in the recombination and uses Langmuir-Rideal as a basic mechanism to describe gas phase nitrogen atoms recombining with adsorbed nitrogen atoms. Silicon atoms were assumed to be the active surface sites upon which the nitrogen atoms adsorb. The nitrogen atoms lost by recombination were then replaced by other gas phase nitrogen atoms. The number of surface sites was calculated to be 2.12×10^{14} per cm^2 .

Rate equations were derived from first principles and incorporated into a computer routine which calculated the recombination coefficient and other recombination parameters. The results show that the model agrees satisfactorily with the empirical data obtained from the literature. The other parameters calculated by the routine yield quantitative and qualitative information to foster a better understanding of the kinetics of heterogeneous recombination as a function of temperature.

A MODEL FOR NITROGEN
ATOM RECOMBINATION ON A
SILICON DIOXIDE SURFACE

I. Introduction

Background

→ The heterogeneous recombination of particles (molecular and atomic) upon solid surfaces (metallic as well as nonmetallic) is, in theory, straightforward and understandable. However, because the recombination reaction is heterogeneous, there is a dependency of the efficiency of the reaction on the structure and temperature of the surface. According to Berkowitz-Mattuck (3:3), no model or mechanism exists which can quantitatively predict the recombination rate. In addition, if a solid is catalytic to atomic recombination and undergoes structural changes as the temperature changes, then the catalytic efficiency of the resulting surface may be different from that of the original surface.

Purpose of Study

→ The need to accurately characterize a surface, coupled with a better understanding of the heterogeneous recombination process are especially important with regard to earth orbiting reentry vehicles such as the Space

Shuttle Orbiter, the planned Aeroassisted Orbital Transfer Vehicle (AOTV), and the planned Space Plane. In fact, surface recombination rates are now known to play a major role in heating the surfaces of the Space Shuttle Orbiter (15:2). According to Scott (71:498), however, the initial design of the Space Shuttle completely ignored the effects of a catalytic surface, not to mention the resulting structure changes of the surface with temperature. ←

Compared to the Shuttle, the AOTV is designed to remain at higher altitudes where nonequilibrium flow dominates. Furthermore, the AOTV reenters the atmosphere at higher velocities. Both conditions enhance atomic interactions at the boundary layer and surface. The Space Plane is designed as a small, manned, rapid-response vehicle which can take off from conventional airstrips or be launched by another aircraft. The Space Plane will operate in near-earth orbit and reenter the atmosphere to land on earth.

Since the initial design of the Shuttle, several individuals (Breen and others[5], Gupta[22], Owen[59], Scott[69,70,71]) have investigated the Thermal Protection System (TPS) of the Shuttle, only to uncover new problem areas. The most notable problem is the behavior of the constituents of atmospheric air (primarily nitrogen and oxygen) as they pass through the shock wave and their resulting energetic state(s) following dissociation and reaction with the surface.

The exothermic reaction due to the atomic recombination may transform the crystal structure of the TPS surfaces, and for reentry vehicles that are designed for reuse, the transformed structure may result in either a prolonged or degraded lifetime of the TPS. Experiment and observation have shown, however, that the latter case (degradation) occurs. Scott (71:489) studied the effects of wall catalysis on the heating of the Shuttle for flights STS-2, STS-3, and STS-5. He observed (71:499)

...The normalized heat fluxes measured on the windward centerline of the Orbiter tended to increase from flight to flight. Roughly, a 20% change was noted from STS-2 to STS-5 ... indicating changes in surface properties such as emittance or catalycity.

He noted that "The reason for this difference is not understood,..." (71:491). Thus, some phenomenon is taking place at the surface which tends to make the tiles of the TPS less resistant to heat with each successive mission.

As will be detailed in the next chapter, the tiles of the TPS are primarily silicon dioxide. Hence, developing a possible mechanism for the heterogeneous recombination of atomic nitrogen on silicon dioxide can allow the calculation of the surface temperature of the Shuttle and other reentry vehicles.

Outline of Study

The primary objective of this thesis effort was to develop a model which described the steady-state

heterogeneous nitrogen atom recombination on a silicon dioxide surface in the temperature range 300-2000K. In this regard, a valid prediction of the behavior of surfaces of reentry vehicles required a detailed understanding of the reaction kinetics of the species at the gas/surface interface. Because oxygen molecules dissociate before nitrogen molecules in the upper atmosphere, Seward (72) modelled the behavior of oxygen recombination on silicon dioxide in the temperature range 300-2000K. Since nitrogen and oxygen are present in the upper atmosphere, the next step is to try to gain an understanding of atomic nitrogen on a silica surface. Hence, a need exists to develop a model to describe the behavior of nitrogen as well. The concepts underlying Seward's model (72) will be used as an initial mechanism to describe nitrogen atom recombination on silicon dioxide in the temperature range 300-2000K.

Empirical values of the recombination coefficient (the fraction of atoms that strike the surface and ultimately recombine) exist in the literature. Plotting the empirical recombination coefficients and comparing with the calculated recombination coefficients of the proposed model can allow the determination if the proposed recombination model is a viable mechanism. If this model does not apply, a new model will be proposed.

Scope

Previous investigations of heterogeneous recombination of atomic nitrogen have considered metallic as well as nonmetallic surfaces. The temperature ranges also varied from temperatures less than 300K as well as from 300-2000K and above.

This thesis effort focused on the heterogeneous recombination of atomic nitrogen on a silicon dioxide (nonmetallic) surface in the temperature range 300-2000K. Silicon dioxide transitions between different crystal structures as the temperature changes. For increasing temperature, the transitions are as follows: quartz (alpha and beta) \rightarrow tridymite \rightarrow cristobalite (alpha and beta) \rightarrow liquid \rightarrow gas (77:547). The quartz - tridymite - cristobalite transitions were considered in this thesis effort because each transition forms a different silicon dioxide surface and substructure. The importance of considering the phase transitions of quartz and the subsequent effect on the recombination rate were emphasized by Hinshelwood (30). Thus, since quartz alters its forms as a function of the temperature, the resulting (changed) surface can therefore provide a different number of available active surface sites for gas phase nitrogen with which to react.

This thesis was concerned with nitrogen recombination on uncoated silicon dioxide. Thus, recombination

coefficient values on coated surfaces were not considered as usable data for the analysis in Chapter III.

Seward's analysis (72:50) assumed the number of surface sites were constant with temperature and these sites were equal to the bulk concentration of $5 \times 10^{14} \text{ cm}^{-2}$. In this thesis, this assumption was not made. Crystal models were used with the intention of more closely determining the number of surface sites.

At temperatures less than 300K, the recombination reaction involves physical adsorption (physisorption) of nitrogen rather than chemical adsorption (chemisorption) of nitrogen (79:3). Physisorption was not the recombination reaction addressed in this thesis.

The thermal protection system of the Shuttle consists of approximately 70% (55:48) Reusable Surface Insulation (RSI). Recognizing that the RSI is 96% silica (77:576), the results of this thesis only applied to those areas covered by RSI, which are the bottom, top, and some leading edges (55:48-49).

The recombination reaction can create a fraction of excited molecules (47:125). These excited molecules are also known as "active nitrogen" (84). The issue of "active nitrogen" was beyond the scope of this thesis.

Having placed reasonable limits on the problem, the next step was to define the activities required to accomplish the objective.

Approach

The steps taken to solve the problem in this thesis included the following:

1. Gather data of the recombination reaction.
2. Develop a physical picture and necessary rate equations of the reaction.
3. Gain familiarity with the software routine developed by Seward (72). The routine used in this thesis is described briefly in Chapter III and shown in Appendix A.
4. Substitute different recombination variables into the routine to determine their effect on the model.
5. Compare the results with reality to determine if the proposed model (Langmuir-Rideal) is a valid explanation of the reaction kinetics.
6. Propose a possible mechanism to describe the recombination reaction if that of Langmuir-Rideal was not viable.

Each step is described below. As a starting point, Seward's model (72), described in Chapter II, was used to determine its application to heterogeneous nitrogen recombination on a silicon dioxide surface.

Heterogeneous recombination is typically described in terms of the recombination coefficient, γ , which is defined as the total number of atom wall collisions which ultimately recombine divided by the total number of atoms

that strike the surface (34:43). In addition, the recombination coefficient can be expressed as a function of temperature and pressure (5;24;29-35) which provides a more accurate picture of the dynamics of the reaction. Therefore, the primary goal of the literature survey was threefold:

1. Obtain values of the recombination coefficient of gas phase nitrogen on silicon dioxide as it varied with temperature.
2. Obtain the maximum value of the recombination coefficient at a particular temperature (if a maximum indeed existed).
3. Obtain the order of the recombination process.

To develop a physical picture of the recombination reaction, the number and character of the available surface sites as well as the thermochemical reactions associated with these sites should be determined. The number of possible surface sites was better approximated by building up the surfaces of the crystal models to show the sites for potential recombination. This involved adding a bonded silicon atom to each dangling oxygen atom at the surface as described in Chapter III. Attached to the silicon atom, assumed to be the active surface site, was a doubly bonded nitrogen atom with which other gas phase nitrogen atoms could recombine. The thermochemical reactions and the necessary rate equations were developed according to

kinetic theory arguments (81). The rate equations for atomic nitrogen bonded via the Langmuir-Rideal model consisted of the adsorption rate, the thermal desorption rate, and the recombination desorption rate and are detailed in Chapter II.

Seward (72) used a computer routine for oxygen recombination on silicon dioxide. The output is a set of curves showing the recombination coefficient as a function of temperature. Since this thesis involves nitrogen recombination, Seward's routine (72) was adapted and modified. The modifications involved using different values for the steric factor, sticking coefficient, number of surface sites, and thermal desorption energy. The routine used in this thesis is in Appendix A.

Using the nitrogen routine, the values of the sticking coefficient, steric factor, and thermal desorption energy were sequentially varied to determine their effect on the calculated values of the recombination coefficient. Note that after building up the surface, the number of surface sites was calculated to be in the range 1.80×10^{14} - 2.12×10^{14} per square cm. The variation of the number of sites was an attempt to account for the temperature effects on the quartz crystal structure. Each variable was input to the routine and the results analyzed.

The exercises were reiterated, followed by quantitative and qualitative analysis to determine if any variation or

combination of variations provided a match to the recombination data from the sources. A model which describes the heterogeneous recombination of atomic nitrogen on a silicon dioxide surface was then proposed.

Assumptions

Since the primary goal of this thesis was to develop a model of a possible nitrogen recombination mechanism on a silicon dioxide surface, the following assumptions were made:

1. The experimental data (recombination coefficient, its maximum, and its functionality relative to pressure) used to support this thesis were valid.
2. The surface was ideal, that is free from defects.
3. The influence of impurities was ignored at a quantitative level.
4. Recombination data of nitrogen on pyrex was used since pyrex is a silica-based compound (13:2456; 46:4-1; 57:174; 75:4083) and because its recombination coefficients are similar to those of quartz.
5. Negligible diffusion of atomic nitrogen into the bulk. This is supported by Hinshelwood (30:205).
6. Glass is nonporous to molecular nitrogen (32:1850).
7. The gas phase nitrogen atom forms a double bond to the surface silicon atom.
8. The initial sticking coefficient of nitrogen on

silicon dioxide behaves in a manner similar to that of oxygen on silicon dioxide.

9. Pressure of the atomic nitrogen went as the temperature for a constant number density.

Results

A model which describes the heterogeneous recombination of atomic nitrogen on a silicon dioxide surface in the temperature range 300-2000K was developed using the Langmuir-Rideal recombination mechanism as a basis. The model accounts for surface participation in the recombination to describe gas phase nitrogen atoms recombining with nitrogen atoms that are adsorbed to the silicon dioxide surface. Silicon atoms were assumed to be the surface active sites to which the nitrogen atoms adsorb. The nitrogen atoms lost by recombination were then replaced by other gas phase nitrogen atoms. Rate equations were derived from first principles and incorporated into a computer routine (included as an appendix) which calculated the recombination coefficient and other recombination parameters. The maximum value of the recombination coefficient was calculated to be 0.014 at 1300K. The number of surface sites was calculated to be in the range of 1.80×10^{14} to 2.12×10^{14} per square cm. The results show that the Langmuir-Rideal recombination mechanism agrees satisfactorily with the empirical data.

Sequence of Presentation

This thesis consists of five chapters and one appendix. Chapter I is the Introduction to this thesis effort. It contains the purpose of the study, the importance to the Department of Defense, the limits placed on the problem, the approach taken to address the problem, the assumptions that were made, a synopsis of the results and major accomplishments, and finally, the sequence of the presentation of the material in this thesis.

Chapter II is the Background to this thesis effort and contains information necessary to understand heterogeneous recombination of atomic nitrogen on silicon dioxide. It is divided into four main sections. The first presents a discussion of the Shuttle's Thermal Protection System. The following section deals more with the theory underlying heterogeneous recombination and covers the mechanisms of atomic recombination in terms of the types of adsorption, the various methods used to describe recombination, and the rate equation and its components. A review of the literature is presented next. The final section in Chapter II details the solids addressed in this thesis.

Chapter III is the Analytical section of this thesis. Included in this chapter are detailed discussions of the proposed recombination model, the rate equation, recombination coefficient, and the demonstration of the model.

Chapter IV presents the Results and Discussion of this thesis. It contains a discussion of the experimental results from a quantitative as well as qualitative perspective. Based on the experimental results, the chapter discusses the validity of the model and issues that surround the recombination reaction.

Chapter V discusses the Conclusions and Recommendations to this thesis. The work of this thesis is summarized in this chapter along with a look to some potential applications. These applications would include use by the Department of Defense in conjunction with the National Aeronautics and Space Administration.

Finally, Appendix A contains the Fortran 5 program developed from the rate equations in Chapter II.

II. Background

Introduction

Chapter II presents the information necessary to understand the heterogeneous recombination of atomic nitrogen on a silicon dioxide surface in the temperature range 300-2000K. It is divided into four main sections. The first section discusses the Space Shuttle's Thermal Protection System (TPS) and how it relates to the recombination of nitrogen on silicon dioxide. The next section covers modelling of heterogeneous recombination of atoms in terms of physical and chemical adsorption, the mechanisms used to describe atomic recombination, and the rate equation and its components. The next section is devoted to a review of the current literature as it applies to the heterogeneous recombination of atomic nitrogen on silicon dioxide. The final section presents a discussion of the various nonmetallic solids considered in this thesis.

The Thermal Protection System of the Space Shuttle Orbiter

In 1976, the National Aeronautics and Space Administration (NASA) published a report (55) which detailed the Space Shuttle and the design of its Thermal Protection System (TPS). The TPS protects the Orbiter from the high temperatures (1925K at the nose and leading edges

of the wing and tail and 590K at the leeward surfaces) generated during launch and reentry (55:48,49). The TPS consists of the following (55:48,49): two types of Reusable Surface Insulation (RSI) tiles; a coated fabric (Nomex felt), also termed Flexible RSI (FRSI); a high temperature structure coupled with internal insulation; thermal window panes; and thermal seals. The nose and wing leading edges are covered with Reinforced Carbon-Carbon (RCC). The RSI tiles are of two types (55:48), High-temperature RSI (HRSI), and Low-temperature RSI (LRSI). Figures 1 and 2 show the relative location of these tiles and other TPS components of the Orbiter (55:48,49).

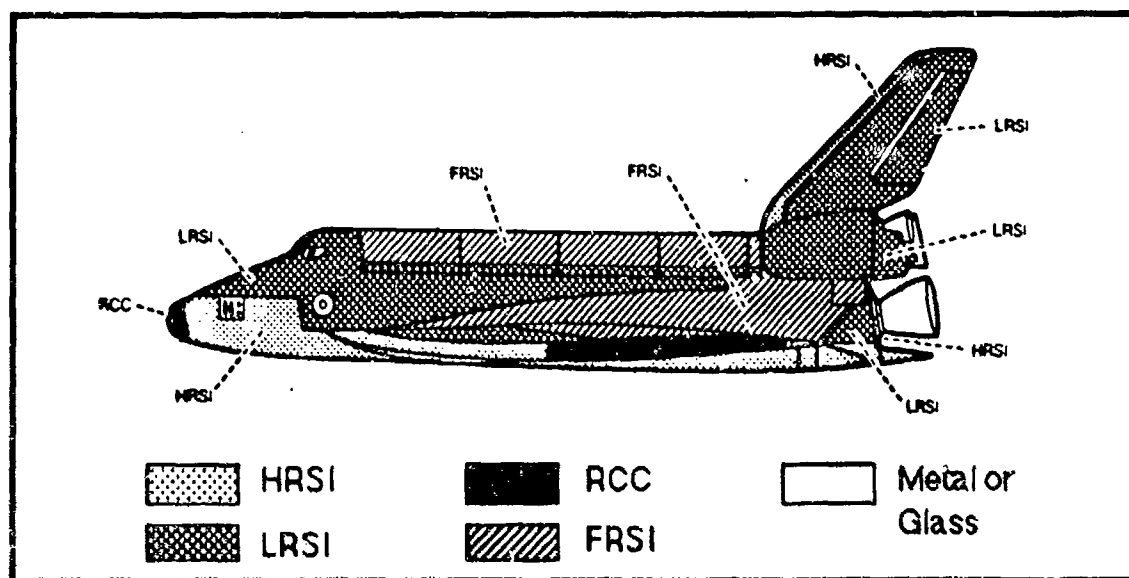


Figure 1. Thermal Protection System of the Orbiter. Side View.

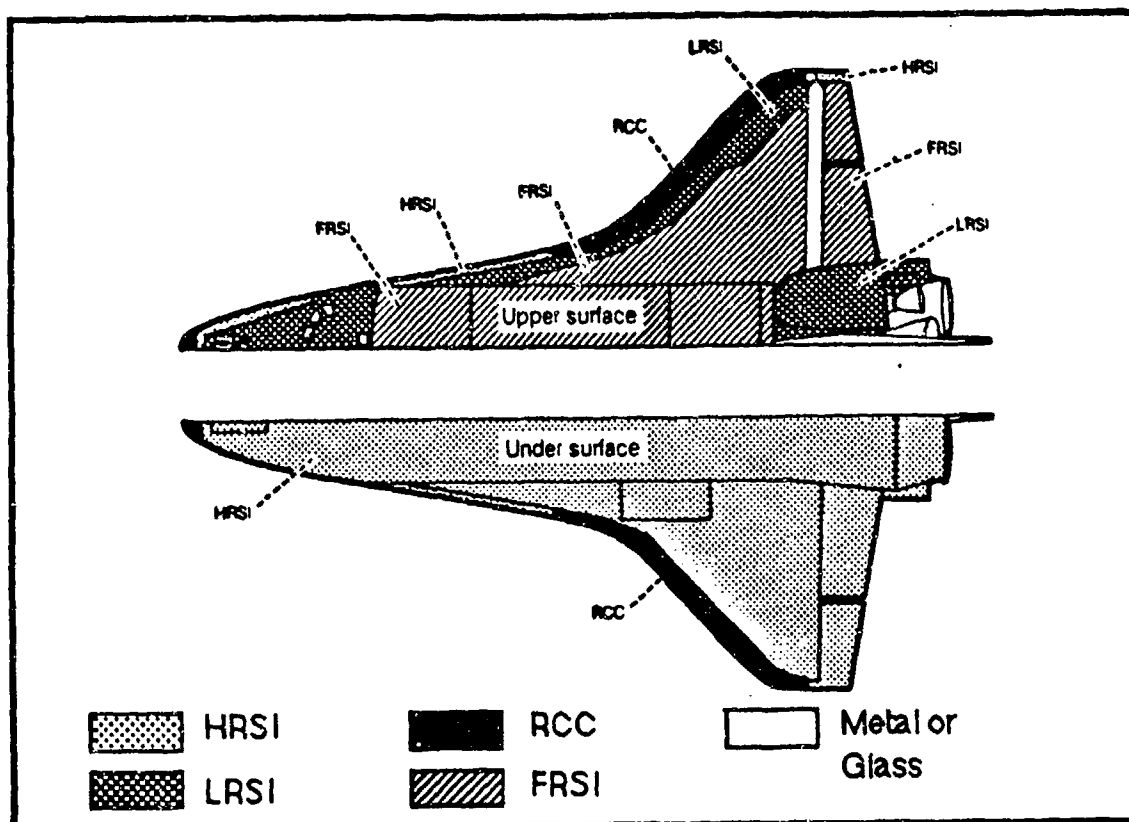


Figure 2. Thermal Protection System of the Orbiter. Upper and Under Surfaces.

Smith (77:575,576) stated that close to 70% of the Shuttle is thermally protected by approximately 24,000 silica-based, ceramic RSI tiles. Industrial silica can be obtained in two forms, fused or "96%" silica (77:580). Fused silica is 99.5% silicon dioxide (SiO_2), whereas 96% silica is 96.3% SiO_2 (77:582). Although Smith did not provide a specific silica percentage for the LRSI, he did say that HRSI "... is 99.7% pure silica" (77:576). However, NASA (55:48) reported that the difference between the HRSI and LRSI is in the coating of the silica for the different temperature regimes. The coating consists of ~4% boron-silicide (59:1). The type and size of RSI tiles,

their respective temperature range, coverage and location on the Orbiter are as follows (55:48,49):

Table 1

Thermal Protection System of the Orbiter

<u>Type</u>	<u>Size</u> (cm ²)	<u>Temp.</u> (K)	<u>Coverage</u> (m ²)	<u>Location</u>
LRSI	20	<925	281.7	Top
HRSI	15	<1500	475.4	Bottom and some leading edges.
FRSI	N/A	<645	302.4	Upper cargo bay door, lower aft fuselage sides, upper aft wing.
RCC	N/A	>1500	37.9	Nose and wing leading edges.

From this, the temperature range considered in this thesis (i.e., 300-2000K) spans the temperatures experienced by the Orbiter's TPS.

As pointed out in Chapter I, the heating to the tiles has increased by roughly 20% from STS-2 to STS-5, which points to a degradation of these tiles. This can impact the designed reuse capabilities of the Shuttle. Consequently, the cause(s) of the heating need to be addressed in order to preclude potentially serious problems due to the degradation. This thesis is concerned with atomic nitrogen recombination on uncoated silicon dioxide surfaces, thereby providing relatively ideal conditions which can serve as the basis for further research.

However, in the real world, ideal conditions rarely exist, particularly in the case of the Shuttle, where its natural operating environment is fluctuating temperature and pressure regimes as well as variations in the gaseous species it "sees" during launch and reentry. The gaseous species may be either atmospheric constituents (nitrogen atoms and molecules, oxygen atoms and molecules, and traces of some inert gases) or contaminants due to the thermal breakdown of the tile-to-surface adhesive. Both of these factors (gas species and contaminants) may alter the surface catalycity of the tiles and thus cause the heating of the tiles. Moreover, the heat generated during launch and reentry is taken up by the tiles which may alter their internal structure.

Green and others (21) investigated three issues relating to Shuttle flights STS-2 through STS-4: the gaseous envelope surrounding the Shuttle; particulates in orbit with the Shuttle; and the optical glow associated with the Shuttle (21:500). These missions occurred in the altitude range of 240-300 kilometers (km) with atmospheric kinetic temperatures between 800-2000K (21:501). Atomic oxygen is the dominant constituent in this region, but N_2 , O_2 , and He are also present in significant amounts (21:501). Green and others addressed each issue and concluded the following (21:510):

We now have an elementary understanding of the gaseous atmosphere that surrounds the Shuttle...Nonetheless,

much remains to be understood. The existence of a Shuttle-induced enhancement of the plasma density is still unclear. The vehicle glow is the most puzzling and intriguing phenomenon observed, and several possibilities have been put forth as an explanation. The particulate environment looks promising, with regard to cleanliness for most optical applications, yet there are disturbing hints from the video data and camera data on STS-4 that the particulates may pose a problem for some experiments.

In the same journal, Scott (71) reported the results of his investigations on the heat transfer to the Shuttle due to nonequilibrium conditions and wall catalysis at the tile surfaces. He postulated (71:491) that the change in surface catalycity and subsequent heating could be due to two primary agents: contaminants, in particular the adhesive used to bond the tiles to the Shuttle; and recombination of the gaseous species surrounding the Shuttle.

However, in a later report, Flowers and Stewart (15) examined the effect on the tiles' surface catalysis due to contaminants. The contaminants they considered were not only the adhesive itself, but also its thermally generated "degradation products" (15:2). They had thermocouples installed on certain tiles at strategic locations to monitor the temperatures. Based on their findings, they concluded (15:2)

... Tiles that were removed from the Orbiter after the STS-2 flight showed no increase in surface catalysis. Therefore, contaminants released from the sources investigated in this study were probably removed by the hot boundary-layer flow over the vehicle's surfaces during the second flight, or were not deposited in

sufficient quantity to change the surface catalytic efficiency.

Therefore, the heating of the Shuttle due to contaminants can be reasonably eliminated. Attention must be focused on the possibility of a changed internal tile structure and the other agent postulated by Scott (71); that of a recombination reaction between the Shuttle's tiled surfaces and the atmospheric species.

During Orbiter reentry, the energy created and released in the recombination of atmospheric species, primarily nitrogen and oxygen, is a key factor in the mission-to-mission reuse capability of the Orbiter (59:1). Under reentry conditions, some of the nitrogen molecules (N_2) and oxygen molecules (O_2) are dissociated behind the shock wave. Depending on the relative temperature and pressure (0.1 - 10 torr) conditions, an exothermic recombination forming molecular species will occur in the gas phase and/or on the surface (59:1). Consequently, a fraction of the recombination energy as heat is transferred to the surface, resulting in temperatures of about 1644K on certain areas of the Orbiter's underside (59:1).

According to Green (20:576), molecular nitrogen comprises 28% of the atmospheric air at an altitude of 240 km and 14% at 305 km. These are the operational altitudes of STS-3 and STS-5, respectively. Coupling the Shuttle's orbital velocity (8×10^5 cm/s) and the collision energy of nitrogen (9.3 ± 2 electron volts [eV]), Green postulated

that the nitrogen molecules could thus dissociate upon impact on the Shuttle since the dissociation energy of nitrogen (9.746 eV) is comparable to the collision energy (20:576). The dissociated atoms then adsorb to the surface. The interaction between the gas phase atoms and the surface is the subject of the next section.

Seward (72) addressed oxygen recombination on silicon dioxide in the temperature range 300-2000K. This thesis is concerned with nitrogen recombination on silicon dioxide in the same temperature range. Hence, from the above facts, the relationship between the Orbiter's Thermal Protection System and this thesis is clear. The TPS of the Orbiter, during launch and reentry, will experience temperatures within the range of temperatures considered in this thesis, 300-2000K. Furthermore, silica is the main constituent of the TPS RSI tiles, and silica is essentially silicon dioxide. Silicon dioxide is the solid of concern in this thesis. A follow-on study should be undertaken to investigate the role of the other atmospheric species (acting singly as well as in a competing or combined system) regarding recombination and heating effects.

This section presented a brief overview of the Shuttle's TPS. Of the three possible agents (contaminants, recombination, or an altered tile structure) that could contribute to the change in surface catalycity and increased heat flux, contamination could be safely ruled

out, leaving some type of recombination reaction and/or structure change as the remaining agents of concern.

Mechanisms of Heterogeneous Recombination

Introduction. The objective of this section is to present the most widely used mechanisms which describe the kinetics of gas phase atoms adsorbing, reacting, and subsequently recombining with the surface atoms. The events surrounding the gas/surface interaction are briefly presented first. Following this, attention focuses on two of these events: the adsorption of the gas on the surface, and the reaction leading to recombination.

The Langmuir isotherm is then derived, followed by a discussion of the different recombination mechanisms. The mechanisms addressed are the following:

1. The Langmuir-Hinshelwood (L-H) mechanism.
2. The Migration mechanism.
3. The Langmuir-Rideal (L-R) mechanism.
4. The mechanism used in this thesis, which is based on Langmuir-Rideal.

The definition of each mechanism as well as the associated theory will be given. Isobars and isotherms will not be covered. The Langmuir Adsorption Isotherm (hereafter termed the Langmuir isotherm) will be derived and applied to the first three mechanisms. The kinetic rate equations associated with the fourth mechanism (above) are then derived from first principles.

In the case of surface reaction kinetics, gaseous species interact with the solid surface and produce a product. To facilitate understanding of the interaction, it is customary to track the events in a gas/surface reaction. The sequence of events consists of the following (1:664; 41:265):

1. Diffusion of the gaseous reactants to the surface.
2. Adsorption of the reactants on the surface.
3. Reaction of the adsorbed reactants with or on the surface, resulting in recombination.
4. Desorption of the gaseous products.
5. Diffusion of the desorbed products into the volume of the gas.

Processes (1), (4), and (5) are beyond the scope of this paper. Attention will focus on process (2), adsorption, and process (3), the reaction at the gas/surface interface. Each process is discussed in turn below.

Adsorption. According to Hayward and Trapnell (25:5), adsorption occurs with a decrease in the surface free energy (ΔG) and a decrease in the surface entropy (ΔS). Thus, the standard equation, $\Delta G = \Delta H - T \Delta S$, shows that the enthalpy (ΔH) is decreasing (T is the temperature). Thus, adsorption, is, in general, exothermic. The heat liberated is termed the heat of adsorption (79:2).

Atoms that are in the bulk of solids are bound ionically or covalently and are surrounded by a full

complement of atoms. Hence, no net force due to charge imbalance exists. However, the situation at the surface is different; the surface atoms are lacking a full complement of neighbors. This creates a localized charge imbalance and the surface exerts an attractive force normal to the surface plane. This attractive force establishes a favorable condition for adsorption of the incoming gaseous particle (79:1).

Adsorption of a gaseous particle on a surface is of two types, physical adsorption (physisorption) and chemical adsorption (chemisorption). Each is discussed and contrasted below.

Physical Adsorption. Physisorption is the formation of a weakly interacting bond between the adsorbed gas particle (adsorbate) and the surface adsorbent. The bond is due to van der Waal's forces, which arise from fluctuating dipoles (79:3). Electron transfers do not occur in physisorption. The temperature range for physisorption is typically less than 300K.

Chemical Adsorption. Chemisorption, on the other hand, is the formation of a strong bond between the adsorbate and the surface atoms. According to Schwab (68:230), chemisorption can be defined as adsorption via

1. Complete transition of electrons and the formation of polar bonds.

2. Or, through the sharing of electrons and the formation of covalent bonds.

Chemisorption binding energies are typically on the same order of magnitude as those of the primary chemical bonds in molecules (79:3). The binding energy establishes short-range forces, thereby limiting the chemisorbed reactants to a monolayer coverage.

The differences between physisorption and chemisorption are as follows (25:5):

Table 2

Physisorption and Chemisorption Characteristics

	<u>Physisorption</u>	<u>Chemisorption</u>
Heat of Adsorption	(Low (-2-6kcal/mole)	High (>15-20kcal/mole)
Temperature (T) Range	T < 300K	T > 300K
Activation Energy	None required.	Usually required.
Surface Requirements	Can occur on all surfaces under correct conditions of temperature and pressure.	Surface must be clean. See Note 1.
Layer Coverage	No limit. Physisorbed layers several molecules thick can be obtained.	Monolayer. Chemisorption stops when the adsorbate is no longer in contact with the surface.

Notes:

1. Experimental observations show, however, that chemisorption can also occur on coated surfaces.

The potential energy of the adsorbate changes with distance from the surface. Graphic representations showing the potential energy change for physisorption and chemisorption are shown in Figure 3 (79:4).

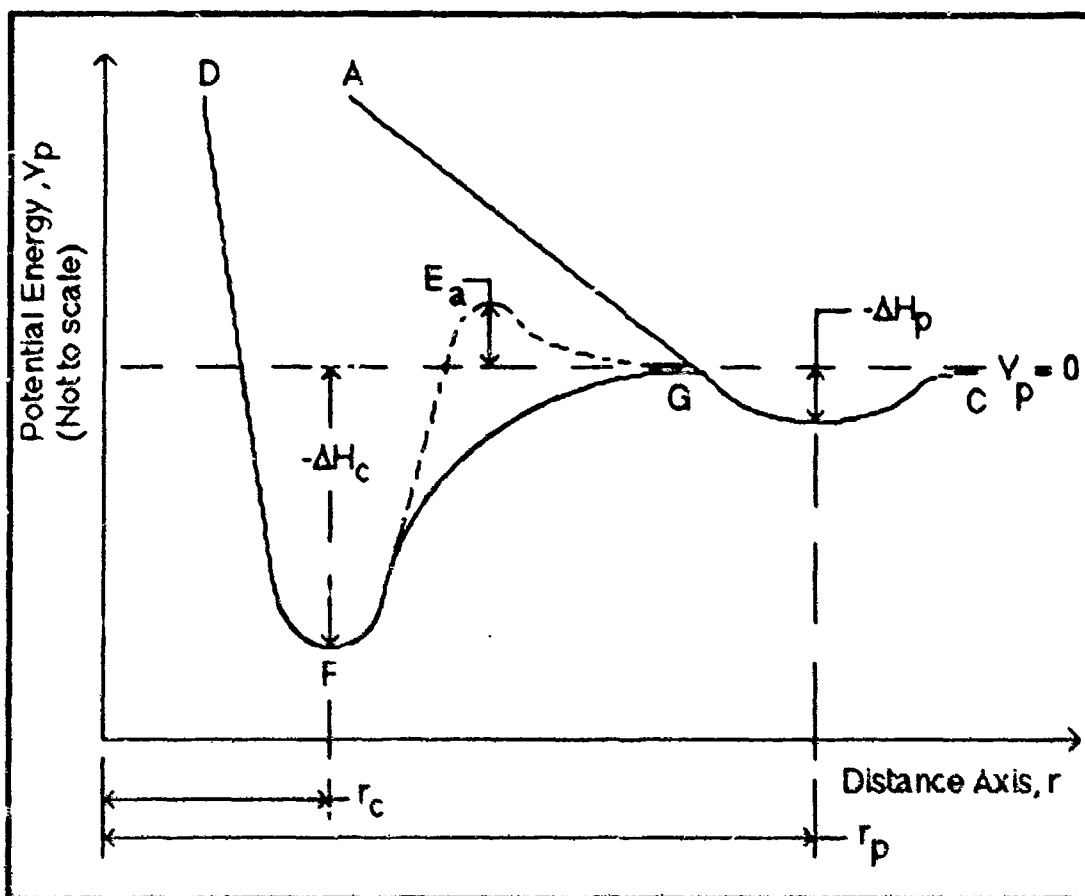


Figure 3. Potential Energy of a System as a Function of the Distance of the Adsorbate from the Surface Relative to Zero Potential Energy of the Adsorbate at an Infinite Distance.

The potential energy is plotted as a function of the distance of the adsorbate from the surface. The horizontal line ($V_p=0$) denotes zero potential energy for an adsorbate at infinite distance from the surface. The potential energy change associated with physisorption is shown via

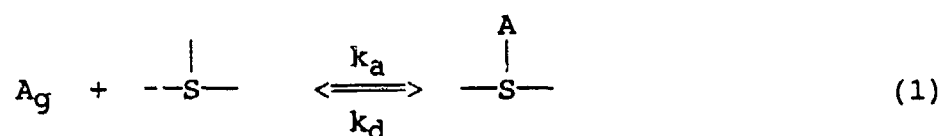
curve A-C; $-\Delta H_p$ is the heat of adsorption and r_p is the distance between the adsorbate and the surface at equilibrium. The potential energy change associated with chemisorption is shown via curve D-F-G with a heat of adsorption $-\Delta H_c$ at the equilibrium distance r_c . There is no activation energy associated with curve D-F-G. However, some systems require an activation energy before transitioning to the chemisorbed state. The curve D-dashed line-G shows this, where E_a is the activation energy.

Since physisorption is not within the temperature range of interest, the remainder of this paper concentrates on chemisorption.

To discuss the reaction leading to heterogeneous recombination, a relationship between the amount of gas adsorbed (surface coverage) and the pressure is required (30:182-183). An adsorption isotherm is used to describe the relationship when a gas and solid are in equilibrium at constant temperature (16:8). Several adsorption isotherms exist, among them are the Brunauer-Emmett-Teller, Freundlich, Temkin, and Langmuir isotherm (41:88). The Langmuir isotherm is important in adsorption theory in the same manner as the ideal gas laws are in kinetic theory (40:260). Consequently, the Langmuir isotherm is derived below, providing the functional relationship between the surface coverage and gas pressure. It will subsequently be

used to aid understanding of the mechanisms of heterogeneous recombination.

The Langmuir Isotherm. In order to derive the Langmuir isotherm, θ is defined as the fractional surface coverage. It assumes there are "n" vacant sites per unit area of surface and each site can only adsorb one gas phase particle. Under equilibrium conditions, the situation can be described as



where A_g is the gas phase adsorbate, $\begin{array}{c} | \\ \text{---S---} \end{array}$ is a vacant

site, $\begin{array}{c} A \\ | \\ \text{---S---} \end{array}$ is the chemisorbed product, k_a and k_d are the rate coefficients for adsorption and desorption, respectively.

From the law of mass action, the adsorption and desorption rates can be written in terms of the adsorption and desorption rate coefficients. That is,

$$\text{Rate of adsorption} = k_a[A_g][S] \quad (2)$$

$$\text{Rate of desorption} = k_d[AS] \quad (3)$$

where $[A_g]$ is the concentration of the gas phase adsorbate, $[S]$ is the concentration of vacant sites (the overstrike, leading, and trailing marks are deleted for ease of

presentation), and $[AS]$ is the concentration of the chemisorbed product (marks deleted as previously done).

But $[A_g]$ can also be expressed as the pressure, P_a , of species A_g at equilibrium, and $[S]$ can be replaced by $n(1-\theta)$, and $[AS]$ is equivalent to $n\theta$. Since, under the condition of equilibrium, the rate of adsorption must equal the rate of desorption, setting equations (2) and (3) equal, we obtain

$$k_a[A_g][S] = k_d[AS] \quad (4)$$

Or,

$$k_a P_a n(1-\theta) = k_d n\theta \quad (5)$$

Manipulating equation (5),

$$k_a P_a n - k_a P_a n\theta = k_d n\theta \quad (6)$$

$$-k_a P_a n\theta - k_d n\theta = -k_a P_a n \quad (7)$$

$$-\theta(k_a P_a n + k_d n) = -k_a P_a n \quad (8)$$

$$\theta = \frac{k_a P_a n}{k_a P_a n + k_d n} \quad (9)$$

$$\theta = \frac{k_a P_a}{k_a P_a + k_d} \quad (10)$$

Thus, the resulting expression is

$$\theta = \frac{k_a P_a}{k_d + k_a P_a} \quad (11)$$

Defining $\frac{k_a}{k_d} = K$, where K is the equilibrium constant,

then the final expression is the Langmuir isotherm.

$$\theta = \frac{K P_a}{1 + K P_a} \quad (12)$$

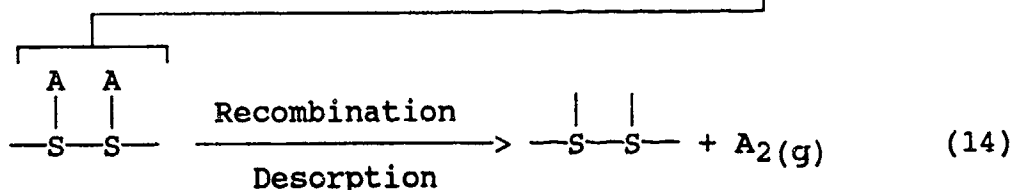
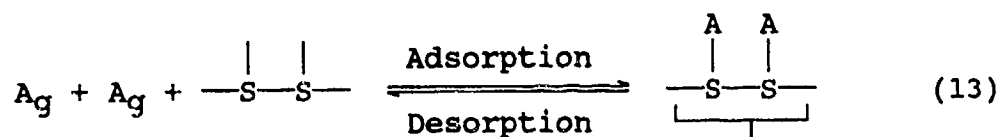
The Langmuir isotherm shows the relationship between the fractional surface concentration, θ , the equilibrium constant, K , and the pressure, P_a . The utility of "K" is realized by noting that if K is large (i.e., $k_a \gg k_d$), then equilibrium lies to the right. On the other hand, if K is small (i.e., $k_a \ll k_d$), then equilibrium lies to the left.

Using the Langmuir isotherm, equation (12), as the relationship between the amount of gas adsorbed on the surface and the gas pressure, a discussion of the reaction/recombination mechanism, process (3), can proceed.

Three such mechanisms have generally been used in the past. They are the Langmuir-Hinshelwood (L-H) mechanism, a Migration mechanism, and the Langmuir-Rideal (L-R) mechanism. Each is discussed below. Following this, details of the mechanism used in this thesis, based on L-R, will be discussed in detail since this mechanism provides a different way of viewing the surface and what could be occurring on the surface.

The Langmuir-Hinshelwood Mechanism. This mechanism views the heterogeneous recombination reaction as two gas phase atoms impinging and adsorbing to adjacent, vacant surface sites. The neighboring adsorbed atoms (adatoms) recombine and desorb as a molecule. (The desorption is not thermally generated. Rather, it occurs virtually

spontaneously following the impact and recombination because the excess energy of the recombination severs the bond to the surface.) The L-H mechanism can be schematically represented in the following way (40:266):



where $\begin{array}{c} | \quad | \\ \text{---S---S---} \end{array}$ are adjacent, vacant surface sites, $\begin{array}{c} A \quad A \\ | \quad | \\ \text{---S---S---} \end{array}$ depicts the atoms adsorbed to the surface, A_g is a gas phase reactant atom, and $A_2(g)$ is the product gas phase molecule.

It is instructive to see how the L-H mechanism predicts the dependence of the recombination desorption rate on pressure. The recombination desorption process involves the interaction of two neighboring adatoms (i.e., two atoms must come together to form a desorbing molecule). Therefore, the rate is proportional to the fraction of surface covered by each, or θ raised to the second power (30:195). That is,

$$\text{Rate} \propto \theta^2 \quad (15)$$

Or, using k_c as the proportionality constant,

$$\text{Rate} = k_c \theta^2 \quad (16)$$

Substituting for θ via equation (12),

$$\text{Rate} = k_C \left[\frac{K P_a}{1 + K P_a} \right] \left[\frac{K P_a}{1 + K P_a} \right] = \frac{k_C K^2 P_a^2}{1 + 2K P_a + K^2 P_a^2} \quad (17)$$

Consider the two limiting conditions of low and high temperatures. At low temperatures, the surface is essentially fully covered with adatoms (41:181), or $\theta \approx 1$. Consequently, $\theta \approx 1$ requires that the quantity $(K P_a / 1 + K P_a)$ also be ≈ 1 . This can happen when the magnitude of the product $(K P_a)$ is much larger than unity, that is, $(K P_a) \gg 1$. Thus,

$$\theta \approx \frac{K P_a}{K P_a} = 1 \quad (18)$$

Hence, the recombination desorption rate can be expressed as

$$\text{Rate} = k_C \theta^2 \approx k_C (1)^2 = k_C \quad (19)$$

From this, the recombination desorption process is zero order in pressure. In other words, the process is independent of pressure at low temperatures.

At the opposite extreme of high temperatures, the surface is sparsely covered with adatoms (41:181), and so $\theta \ll 1$. Consequently, $\theta \ll 1$ requires that

$$\frac{K P_a}{1 + K P_a} \ll 1 \quad (20)$$

This can happen when $(K P_a) \ll 1$, which leads to $\theta = K P_a$ and the following expression for the recombination desorption rate:

$$\text{Rate} = k_C \theta^2 = k_C (K P_a)^2 = k_C K^2 P_a^2 \quad (21)$$

Or, the recombination desorption rate is second order in gas pressure.

Thus, deriving and applying the Langmuir isotherm to the Langmuir-Hinshelwood mechanism results in the following conclusions:

1. At low temperatures, $\theta \approx 1$, $K P_a \gg 1$, and the heterogeneous recombination process is independent of the gas pressure (zero order).
2. At elevated temperatures, $\theta \ll 1$, $K P_a \ll 1$, and the process is second order dependent in gas pressure.

However, Laidler (41:180) observed that the surface recombination process of atoms is first order over a wide temperature and pressure range, with second order behavior at high temperatures. Attempting to explain this first-second order behavior, Laidler (41:180) applied the Langmuir-Hinshelwood mechanism (adsorption of atoms on adjacent sites). He concluded that the L-H mechanism could not explain the kinetics being first order over a wide temperature range. Laidler then considered another mechanism involving migration of the atoms on the surface. This mechanism is discussed next.

The Migration Mechanism. According to Laidler (41:180), this mechanism involves the following sequence of events:

1. Slow adsorption of the adatoms.

2. Rapid surface migration of the adatoms.
3. Recombination with other suitable adatoms, resulting in a molecule.
4. Desorption of the molecule.

In this situation, the rate of the reaction is determined by the adsorption rate (30:208). Moreover, since the adatoms recombine quickly and desorb as molecules, the adsorption rate is proportional to the gas pressure and the surface remains essentially bare of adatoms, i.e., $\theta \ll 1$.

Since the rate is proportional to the pressure, P_a , and the fraction of the surface that is bare ($1-\theta$), then

$$\text{Rate} = k_c P_a (1-\theta) \quad (22)$$

But, $\theta \ll 1$, so

$$\text{Rate} = k_c P_a \quad (23)$$

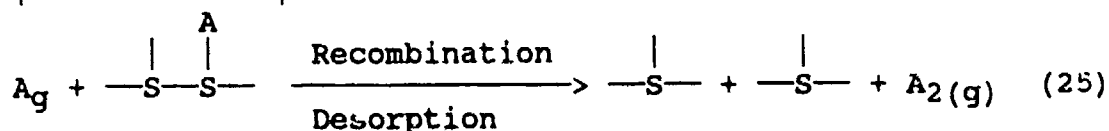
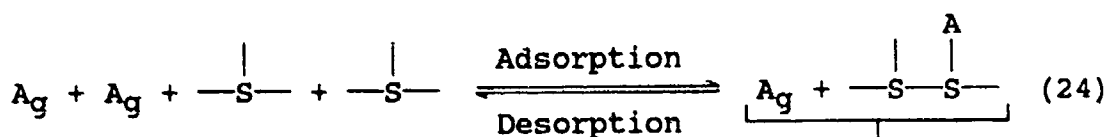
This means first order kinetics, which would remain invariant relative to changes in the temperature (41:181). Based on this, Laidler also dismissed this mechanism as one to adequately model surface recombination of atoms. Tompkins (79:7) came to a similar conclusion. Having examined and dismissed the L-H and Migration mechanisms, Laidler then concluded that the only other mechanism involved interaction between an adatom and a gas phase atom. This is the Langmuir-Rideal (L-R) mechanism.

The Langmuir-Rideal Mechanism. The Langmuir Rideal mechanism, also known as the Eley-Rideal mechanism

(7:2719), views the heterogeneous recombination reaction as follows:

1. A gas phase atom striking and adsorbing to a vacant site, forming an adatom.
2. Another gas phase atom strikes and recombines with the adatom, forming a molecule.
3. The molecule desorbs immediately following the recombination, leaving a vacant surface site.

Hence, the L-R mechanism can be schematically represented as the following (40:284):



where $\begin{array}{c} | \\ \text{---S---} \end{array} + \begin{array}{c} | \\ \text{---S---} \end{array}$ are vacant sites, $A_g + \begin{array}{c} | \quad A \\ \text{---S---S---} \end{array}$ depicts the atom adsorbed to the surface with an incoming gas phase reactant atom A_g , and $A_2(g)$ is the product gas phase molecule. In contrast to the L-H mechanism, the surface sites in the L-R mechanism do not necessarily have to be adjacent.

According to Hinshelwood (30:195), the rate can be expressed as

$$\text{Rate} = k_C P_a \theta \quad (26)$$

Substituting for θ via the Langmuir isotherm,

$$\text{Rate} = k_c P_a \frac{K P_a}{1 + K P_a} = k_c \frac{K P_a^2}{1 + K P_a} \quad (27)$$

As before, consider the two extreme cases of low and high temperature.

At low temperatures, the surface is essentially fully covered, $\theta \approx 1$. Following the same procedure as for Langmuir-Hinshelwood, $\theta \approx 1$ requires that $K P_a \gg 1$, and the rate is given by

$$\text{Rate} = k_c P_a \theta = k_c P_a \frac{K P_a}{1 + K P_a} = k_c P_a \frac{K P_a}{K P_a} = k_c P_a \quad (28)$$

Thus, the process is first order in pressure.

At elevated temperatures, the surface is sparsely covered with adatoms, $\theta \ll 1$. This requires $K P_a \ll 1$, so the rate can be written as

$$\text{Rate} = k_c P_a \theta = k_c P_a \frac{K P_a}{1 + \cancel{K P_a}^{\text{negligible}}} = k_c K P_a^2 \quad (29)$$

Thus, equation (29) shows that the rate is second order in pressure.

Hence, applying the Langmuir isotherm to the Langmuir-Rideal mechanism results in the following conclusions:

1. At low temperatures, $\theta \approx 1$, $K P_a \gg 1$, and the heterogeneous recombination process is first order in pressure.
2. At elevated temperatures, $\theta \ll 1$, $K P_a \ll 1$, and the process is second order in pressure.

Although a pure L-R mechanism yields first and second order behavior, some questions still remained in the minds of several investigators.

Campbell and Thrush (9:215), in a paper investigating nitrogen recombination, observed second order behavior and concluded it was due to heterogeneous recombination and not homogeneous recombination. In the discussion of their results, they stated that the second order behavior was (9:215)

Consistent with either the Hinshelwood mechanism or the Rideal mechanism provided the fraction of surface covered (θ) does not approach unity. If the Rideal mechanism operates, θ must be at least 10^{-4} .

In trying to assign a mechanism to explain their observations, Campbell and Thrush (9:215) were forced to exclude a pure L-R mechanism because the activation energy associated with the reaction reduced "... the number of reactive collisions with adsorbed atoms to an impossibly low value" (9:215).

The L-H mechanism also was inadequate to explain their observations. The only mechanism that seemed to fit their observations involved surface migration of the nitrogen adatoms. However, as pointed out previously, surface migration, in itself, is untenable. Hinshelwood (30:207) supports this position.

Hence, based on the literature, the three mechanisms (L-H, Migration, and L-R) fail to provide an adequate

explanation of the heterogeneous recombination of atoms on surfaces. The question of real significance remains: What process occurs, mechanistically, between the gas phase atoms and the surface to allow the progression from first to second order as the temperature increases?

Upon close inspection of each mechanism, however, the observation can be made that the investigators using these mechanisms paid slight attention to the chemical composition of the surface and its potential to actively participate in the recombination process. The realization of the importance of surface activity is not new, however. Hinshelwood (30:219, 228-229) suggested the surface atoms' lattice spacing should be considered in catalytic activity. Moreover, accounting for a changing surface structure, Hinshelwood stated (30:229)

The activity of many catalysts increases with the number of times that they have been used to bring about a given reaction...attributable to a change in the configuration of the surface.

In this regard, Seward (72), following an approach by Linnett and Marsden (43), used the L-R mechanism as a basis and extended it to account for surface catalycity.

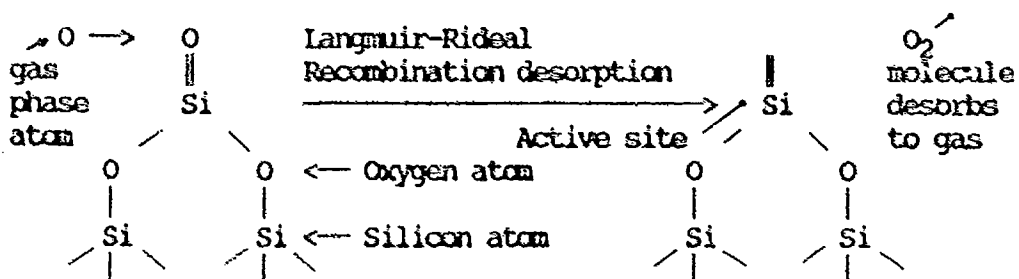
Details of the Model. Seward (72) modelled the heterogeneous recombination of atomic oxygen on a silicon dioxide surface in the temperature range 300-2000K. Accordingly, the gas phase oxygen atoms recombine directly with the atomic oxygen on the surface and desorb as oxygen

molecules. The vacancies created by this recombination are then filled by other gas phase oxygen atoms.

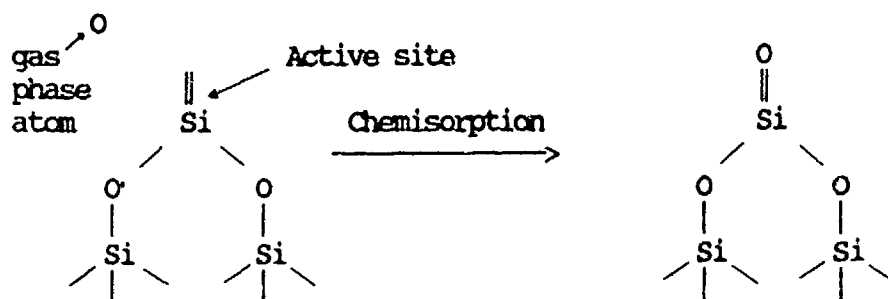
Viewed macroscopically, this is the Langmuir-Rideal mechanism. However, the underlying premise of the mechanism. However, the underlying premise of the adaptation differs considerably from the others. This new perspective views the surface as an actual participant in the recombination process in that the active adsorption sites are the silicon atoms instead of the oxygen atoms, which would be the case in a pure L-R recombination. Thus, the new mechanism views the sequence of events as the following:

1. The active surface sites are the silicon atoms rather than the oxygen atoms.
2. Gas phase oxygen atoms bond to these active sites forming the silicon dioxide surface.
3. Gas phase oxygen atoms could then collide and recombine with the oxygen atoms.
4. The atoms lost from the surface are then replaced by additional gas phase atoms.

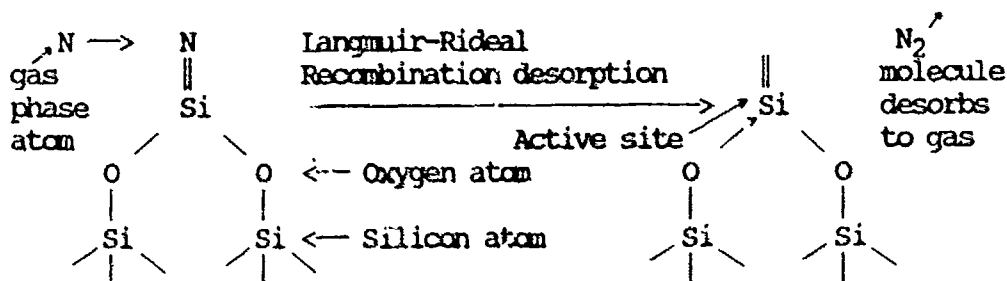
This sequence for oxygen is shown schematically below



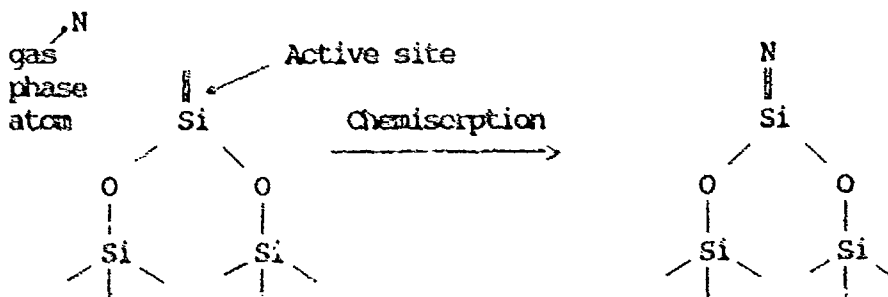
Another gas phase oxygen atom attaches to the silicon atom, which is the active surface site. This is shown via



The sequence of interest in this thesis, that of nitrogen recombining and chemisorbing onto silicon dioxide is



Another gas phase nitrogen atom attaches to the silicon atom, which is the active surface site. This is shown via



To allow the reader to grasp the essentials of this mechanism, the associated rate equations are derived from first principles in the following portion of the paper.

The Rate Equations from First Principles. Using arguments similar to those used in thermodynamic mass balance techniques, consider an atom number balance approach. That is, the time rate of change of the number of atoms per unit area, when atoms are chemisorbing, thermally desorbing, recombining via the L-R mechanism, and then desorbing as molecules can be written as shown

$$\left[\begin{array}{l} \text{Time rate of} \\ \text{change of atoms} \\ \text{per unit area} \end{array} \right] = \text{Number adsorbing} - \text{Number desorbing} \quad (30)$$

Or,

$$\left[\begin{array}{l} \text{Time rate of} \\ \text{change of atoms} \\ \text{per unit area} \end{array} \right] = \left[\begin{array}{l} \text{Number of atoms} \\ \text{chemisorbing to} \\ \text{the surface} \end{array} \right] - \left[\begin{array}{l} \text{Number of} \\ \text{atoms thermally} \\ \text{desorbing} \end{array} \right] - \left[\begin{array}{l} \text{Number of atoms} \\ \text{recombining via} \\ \text{L-R and thermally} \\ \text{desorbing as molecules} \end{array} \right] \quad (31)$$

Equation (31) can be expressed mathematically as

$$\frac{dn}{dt} = N S_0 (1-\theta) - \delta \theta - P N \theta \exp \left[\frac{-E_a}{kT} \right] \quad (32)$$

where N is the surface impingement rate per unit area and δ is the thermal desorption rate per unit of covered surface and is (72:11)

$$\delta = C_a \frac{k T}{h} \exp \left[\frac{-D}{k T} \right] \quad (33)$$

C_a is the number of adsorption sites per unit area.

k is the Boltzmann constant, Joules/K.

T is the temperature (Kelvin).

h is the Planck constant, Joule·sec.

D is the thermal desorption energy, Joule/atom.

S_0 is the initial or clean surface sticking coefficient, dimensionless.

θ is the fractional surface concentration (i.e., the fraction of the surface covered), dimensionless.

P is the steric factor, dimensionless.

E_a is the activation energy, Joules.

Before proceeding with the derivation, the terms that comprise the rate equation need to be clarified. A discussion of these components follows. The surface impingement rate per unit area, \dot{N} , is related to the gas pressure, P_a , in the following manner. From the kinetic theory of gases,

$$\dot{N} = \frac{n \bar{c}}{4} \quad (34)$$

where n is the number density (i.e., number per unit volume).

$$\bar{c} \text{ is the average velocity per particle} = \left[\frac{8 k T}{\pi m} \right]^{1/2} \quad (35)$$

m is the mass of the particle.

But, the pressure, P_a , can also be expressed as

$$P_a = nkT \quad (36)$$

Therefore, upon rearranging in terms of the number density, n , equation (36) becomes

$$n = \frac{P_a}{k T} \quad (37)$$

Substituting equation (37) into (34),

$$\dot{N} = \left[\frac{P_a}{k T} \right] \left[\frac{\bar{c}}{4} \right] \quad (38)$$

Thus, the surface impingement rate per unit area is directly proportional to the gas pressure.

"Sticking" implies adsorption into the strongly bonded chemisorbed state (16:41). The sticking coefficient, S , a function of the fraction of surface covered with adatoms, θ , and temperature, T , can be defined as the ratio of the rate of adsorption of the gas by a surface to the rate of collision (or impingement) with the surface (79:22). Thus, the adsorption rate is equal to the impingement rate times the sticking coefficient.

The fractional surface coverage, θ , is defined as the ratio of the number of particles adsorbed to the maximum uptake (16:40). The value of S as θ approaches zero is termed the initial, or clean surface sticking coefficient, S_0 . That is, $S = S_0$ when $\theta = \text{zero}$. According to Gasser (16:40), the results of investigating the temperature dependence of S_0 show that it varies little with

temperature or that it decreases with increasing temperature.

The sticking coefficient, S , is "...almost invariably less than unity" (79:34). To account for this, the adsorption rate must be less than the impingement rate. The adsorption rate can be lowered by one of several factors, including the following (25:87): the requirement for an activation energy (E_a); a steric factor (P); the relative efficiency of energy transfer; surface heterogeneity; or back-scatter into the gas phase due to collision with an occupied site.

Hinshelwood (30:41) defined the activation energy as "The energy which must be supplied to the reacting substances to make them capable of chemical transformation into the products". However, not every atom possessing the required activation energy will be chemisorbed. The steric factor, P , accounts for this in that it is a measure of the sufficiently energetic collisions with the surface that actually react and recombine (34:42). Having covered the essentials of the rate equation components, attention returns to the derivation.

Now, under steady state conditions, $dn/dt = 0$. Thus, equation (32) becomes

$$\frac{dn}{dt} = 0 = \dot{N} S_0 (1-\theta) - \delta\theta - P \dot{N} \theta \exp \left[\frac{-E_a}{kT} \right] \quad (39)$$

Expanding equation (39),

$$0 = \dot{N} S_O - \dot{N} S_O \theta - \delta \theta - P \dot{N} \theta \exp \left[\frac{-E_a}{kT} \right] \quad (40)$$

Or,

$$0 = \dot{N} S_O - \theta (\dot{N} S_O) - \theta \delta - \theta P \dot{N} \exp \left[\frac{-E_a}{kT} \right] \quad (41)$$

$$0 = \dot{N} S_O - \theta \left[\dot{N} S_O + \delta + P \dot{N} \exp \left[\frac{-E_a}{kT} \right] \right] \quad (42)$$

Rearranging equation (42),

$$\dot{N} S_O = \theta \left[\dot{N} S_O + \delta + P \dot{N} \exp \left[\frac{-E_a}{kT} \right] \right] \quad (43)$$

Solving for the fractional surface concentration, θ , yields

$$\theta = \frac{\dot{N} S_O}{\dot{N} S_O + \delta + P \dot{N} \exp \left[\frac{-E_a}{kT} \right]} \quad (44)$$

Equation (44) is expressed by the meaning of each term as follows:

$$\left[\text{Fraction of surface covered with atoms} \right] = \quad (45)$$

$$\frac{\left[\text{Number of incoming atoms that collide and stick} \right]}{\left[\text{Number of incoming atoms that collide and stick} \right] + \left[\text{Thermal desorption term} \right] + \dot{P}N \exp \left[\frac{E_a}{kT} \right]}$$

where $\dot{P}N \exp \left[\frac{-E_a}{kT} \right]$ is decomposed in a similar manner as

$$\dot{P}N \exp \left[\frac{-E_a}{kT} \right] =$$

$$\underbrace{\left[\text{Fraction of sufficiently energetic collisions that do react} \right]}_P \times \underbrace{\left[\text{Number of collisions with the surface} \right]}_{\dot{N}} \times \underbrace{\left[\text{Fraction of collisions that have sufficient energy (E}_a\text{) to result in a reaction} \right]}_{\exp \left[\frac{-E_a}{kT} \right]} \quad (46)$$

Next, defining the recombination coefficient, γ , which is the fraction of the collisions with the surface that recombine, as the following:

$$\gamma = \frac{2 \times \text{Recombination desorption rate}}{\text{Number of collisions with the surface}} \quad (47)$$

Or, since the number of collisions with the surface is the impingement rate, equation (47) can be written as

$$\gamma = \frac{2 \times \text{Recombination desorption rate}}{\dot{N}} \quad (48)$$

The factor of two arises because two atoms disappear from the gas phase; one in the recombination reaction and one to fill the vacancy at this location or elsewhere on the surface. Thus, constant surface concentration is maintained, in keeping with steady state conditions. From equation (32), the recombination desorption rate at steady-state is given by

$$\text{Recombination desorption rate} = P \dot{N} \theta \exp \left[\frac{-E_a}{kT} \right] \quad (49)$$

Substituting equation (47) into (49),

$$\gamma = \frac{2 P \dot{N} \theta \exp \left[\frac{-E_a}{kT} \right]}{\dot{N}} \quad (50)$$

Dividing out \dot{N} results in the following expression for the recombination coefficient, γ :

$$\gamma = 2 P \theta \exp \left[\frac{-E_a}{kT} \right] \quad (51)$$

Substituting equation (44), the fractional surface coverage, yields the following expression for the recombination coefficient:

$$\gamma = \frac{2 P \dot{N} S_O \exp \left[\frac{-E_a}{kT} \right]}{\dot{N} S_O + \delta + P \dot{N} \exp \left[\frac{-E_a}{kT} \right]} \quad (52)$$

Equations (44) and (48) are next used to analyze equation (52), the expression for the recombination coefficient. The procedure will be to examine the terms in the denominator of equation (52) and to determine the order of the recombination process.

Case 1. The chemisorption term, $\dot{N} S_O$, is the dominant term in equation (52). That is,

$$\left[\begin{array}{l} \text{Number of atoms} \\ \text{that collide} \\ \text{and stick to} \\ \text{the bare surface} \end{array} \right] \gg \left[\begin{array}{l} \text{Thermal} \\ \text{desorption rate} \\ \text{per unit area, } \delta \end{array} \right] \quad (53)$$

and

$$\left[\begin{array}{l} \text{Number of atoms} \\ \text{that collide} \\ \text{and stick to} \\ \text{the bare surface} \end{array} \right] \gg \dot{N} P \exp \left[\frac{-E_a}{kT} \right] \quad (54)$$

Then, the fractional surface coverage, θ , can be expressed as follows:

$$\theta = \frac{\dot{N} S_0}{\dot{N} S_0 + \delta + P \dot{N} \exp \left[\frac{-E_a}{kT} \right]} = \frac{\dot{N} S_0}{\dot{N} S_0} = \text{Unity} \quad (55)$$

Negligible for a large chemisorption term, $\dot{N} S_0$

Thus, from equation (55), $\theta = 1$, a fully covered surface. Moreover, equation (52) can be written as (for a large chemisorption term)

$$\gamma = \frac{2 P \dot{N} S_0 \exp \left[\frac{-E_a}{kT} \right]}{\dot{N} S_0 + \delta + P \dot{N} \exp \left[\frac{-E_a}{kT} \right]}$$

Negligible for a large chemisorption term, $\dot{N} S_0$

$$\gamma = \frac{2 P \dot{N} S_0}{\dot{N} S_0} \exp \left[\frac{-E_a}{kT} \right] \quad (56)$$

Therefore,

$$\gamma = 2 P \exp \left[\frac{-E_a}{kT} \right] \quad (57)$$

That is, the recombination coefficient, γ , does not depend on the impingement rate, as shown previously. Furthermore, since the impingement rate is directly proportional to the pressure via equation (38), the recombination coefficient is thus also independent of the pressure.

Examining the functionality of the recombination desorption rate on the pressure, since

$$\gamma = \frac{2 \times \text{Recombination desorption rate}}{\dot{N}} \quad (58)$$

Equating (57) and (58) results in,

$$\frac{2 \times \text{Recombination desorption rate}}{\dot{N}} = 2 P \exp \left[\frac{-E_a}{kT} \right] \quad (59)$$

Or,

$$2 \times \text{Recombination desorption rate} = 2 \dot{N} P \exp \left[\frac{-E_a}{kT} \right] \quad (60)$$

Rearranging to obtain the following functional dependence of the recombination coefficient, γ , on the impingement rate, we have

$$\text{Recombination desorption rate} = \dot{N} P \exp \left[\frac{-E_a}{kT} \right] \propto \dot{N}^{(1)} \quad (61)$$

Since the recombination desorption rate is proportional to the impingement rate to the first power, it is also

proportional to the pressure to the first power using equation (38). Thus, the recombination process obeys first order kinetics. Hence, for a high chemisorption rate, the results are the following:

1. The recombination coefficient, γ , is independent of the impingement rate, \dot{N} , and thus also the pressure.
2. The recombination process is first order in pressure.

To proceed in the term-by-term analysis of the denominator of equation (52), consider the situation (Case 2) where the exponential term is much larger than the other two terms.

Case 2. If $\dot{P}N \exp \left[\frac{-E_a}{kT} \right]$ dominates, i.e., $\dot{P}N \exp \left[\frac{-E_a}{kT} \right] \gg \delta$

and $\dot{N}S_0$, then

$$\theta = \frac{\dot{N} S_0}{\underbrace{\dot{N} S_0 + \delta + \dot{P} N \exp \left[\frac{-E_a}{kT} \right]}_{\text{Negligible for a large exponential term}}} = \left[\text{Large number} \right]^{-1} \quad (62)$$

From equation (62), θ is small, which means the surface is sparsely covered with adatoms.

Moreover, since the exponential term dominates, equation (52) can now be expressed as

$$\gamma = \frac{2 P \dot{N} S_0 \exp \left[\frac{-E_a}{kT} \right]}{\underbrace{\dot{N} S_0 + \delta + P \dot{N} \exp \left[\frac{-E_a}{kT} \right]}_{\text{Negligible}}} \quad (63)$$

Or,

$$\gamma = \frac{2 P \dot{N} S_0 \exp \left[\frac{-E_a}{kT} \right]}{P \dot{N} \exp \left[\frac{-E_a}{kT} \right]} \quad (64)$$

Thus, equation (64) results in

$$\gamma = 2 S_0 \quad (65)$$

Equation (65) shows that the recombination coefficient is independent of the impingement rate, and so also the pressure. Now, since the recombination coefficient was given by

$$\gamma = \frac{2 \times \text{Recombination desorption rate}}{\dot{N}} \quad (66)$$

Setting equations (65) and (66) equal to each other and cancelling terms, the functional dependence of the recombination process is obtained. That is,

$$2 \times \text{Recombination desorption rate} = 2\dot{N}S_0 \quad (67)$$

Thus,

$$\text{Recombination desorption rate} = \dot{N}S_0 \quad (68)$$

Therefore, the recombination desorption rate $\propto \dot{N}^{[1]}$, again first order in pressure. Hence, for a large

$\dot{N} \exp \left[\frac{-E_a}{kT} \right]$ term, the conclusions are as follows:

1. The recombination coefficient, γ , is independent of the impingement rate, \dot{N} , and the pressure.
2. The overall recombination process is again first order, but is controlled by the chemisorption rate through the initial sticking coefficient, S_0 .

The final case involves a large thermal desorption rate per unit area, δ .

Case 3. If δ dominates, i.e., $\delta \gg \dot{N}S_0$ and $\delta \gg \dot{N} \exp \left[\frac{-E_a}{kT} \right]$,

then rewriting equation (44) with δ being the dominant term,

$$\theta = \frac{\dot{N}S_0}{\delta} = [\text{Large number}]^{-1} \Rightarrow \theta = \text{A small number} \quad (69)$$

Hence, from equation (69), the surface is sparsely covered with adatoms. Proceeding to examine the effect of a high thermal desorption term on the expression for the recombination coefficient, and using equation (33), we have

$$\gamma = \frac{2 P \dot{N} S_0 \exp \left[\frac{-E_a}{kT} \right]}{C_a \frac{kT}{h} \exp \left[\frac{-D}{kT} \right]} \quad (70)$$

From equation (70), the functional dependence of the recombination coefficient is first order. That is,

$$\alpha \dot{N}^{[1]} \quad (71)$$

Since the recombination desorption rate is given by equation (48) as

$$\gamma = \frac{2 \times \text{Recombination desorption rate}}{\dot{N}} \quad (72)$$

Then, setting equation (70) equal to equation (72) and rearranging, the result is

$$2 \times \text{Recombination desorption rate} = \frac{2 P \dot{N} \dot{N} S_0 \exp \left[\frac{-E_a}{kT} \right]}{\delta} \quad (73)$$

Cancelling the factor of two and rewriting equation (73)

results in the following expression for the recombination desorption rate.

$$\text{Recombination desorption rate} = \frac{p \dot{N}[2] S_0 \exp\left[\frac{-E_a}{kT}\right]}{\delta} \quad (74)$$

From equation (74), the dependence of the recombination desorption rate is

$$\text{Recombination desorption rate} \propto \dot{N}[2] \quad (75)$$

Thus, the recombination desorption rate is second order dependent with respect to the impingement rate; or, second order kinetics. Hence, for a high thermal desorption rate, the results are as follows:

1. The recombination coefficient, γ , is dependent on the impingement rate, \dot{N} .
2. The overall recombination process is second order.

Incorporating the observations from the previous discussion on the mechanisms of recombination, conclusions from the above analysis follow:

1. For the fractional surface coverage to be large at low temperatures, the chemisorption term must also be large under the same temperature condition.
2. At higher temperatures, the recombination process is first order and the exponential term dominates.
3. On the other hand, for a second order recombination

process to occur at high temperatures, then thermal desorption is taking place at a high rate.

One key term used throughout the preceding analysis was the recombination coefficient, γ . The next section reviews the literature and sheds some light on this term and others.

Review of the Literature

Introduction. Developing a model for heterogeneous recombination of atomic nitrogen on a silicon dioxide surface should include a determination of the recombination coefficient as a function of temperature. In addition, due to the complex nature of the reaction, the model should also include a determination of the surface as well.

This literature review provides a summary of the information regarding heterogeneous recombination of atomic nitrogen on a silicon dioxide surface in the temperature range 300-2000K from several books, refereed journals, and Department of Defense documents. The review covers three main topics: definitions given for the recombination coefficient; values of the recombination coefficient of gas phase nitrogen on silicon dioxide surfaces and pyrex; and the effect of surface coatings or "poisons" which were used by some of the experimentalists. Along with the recombination coefficient values, this review will present the maximum values of the recombination coefficient and the order of the recombination process. Knowing how the

recombination coefficient varies with temperature, its maximum value, and the order of the reaction facilitate the development of an accurate mechanism to describe the recombination reaction.

Discussion of the Literature. Two techniques are used to present the results of heterogeneous recombination. One technique can be thought of as "static" and holds the influencing parameters (temperature, pressure, and atomic surface coverage) constant (16). Consequently, this method places limiting constraints on the model development and was not used in this thesis. The other technique is "dynamic" in the sense that it considers the recombination coefficient as a function of temperature as well as pressure (5;24;29-35). This method thereby allows the temperature and pressure to vary. Furthermore, it can also account for a changing surface and hence a changing surface coverage by the adsorbing gaseous species. This method is not constrained via constant parameters and the dynamics of the reaction can be realized. This latter technique was used in this thesis.

The need to develop a model for heterogeneous recombination on silicon dioxide is underscored due to the existing lack of understanding of the overall recombination reaction. Several authors, among them Golde and Thrush (18:1297), Kofsky and Barrett (38:151), Marshall (51:1-3), Rosner and Cibrian (65:429-430), Scott (70:5), and Shuman

and Brennen (75:4083), explicitly state that the precise details of the heterogeneous recombination are not known. For example, in a paper on atomic recombination and its application to reentry vehicles, Scott concluded (70:5):

The significance of nitrogen recombination is much greater for future spacecraft such as orbit transfer vehicles...It is therefore important to know the temperature-dependent nitrogen recombination accurately for the materials of interest.

Furthermore, the character, precise structure, and adsorbed atom bonding mechanism are not clearly known. In a recent article, Himpsel (29) reviewed the state of the current understanding of the electronic structure of semiconductor surfaces. He reported (29:205)

There is an increasing urge to understand chemical reactions at semiconductor surfaces...However, there is no knowledge of microscopic mechanisms...

A similar conclusion regarding the need to determine the properties of silica and other TPS surfaces was emphasized by Marinelli (46:5-1).

A consistent terminology for the recombination coefficient also is lacking. For instance, it has been termed the surface constant (50), surface efficiency (39), surface catalytic efficiency (45), and recombination efficiency (2). Some examples of the various terms and definitions of the recombination coefficient are as follows:

1. "The surface constant γ is defined as the probability that an atom hitting the surface from the gas phase will recombine with the adsorbed atom" (50:1658).

2. "...A surface efficiency of 6.5×10^{-6} , i.e., that fraction of collisions of nitrogen atoms with the wall effective in causing recombination" (39:1773).
3. "The surface catalytic efficiency γ for wall recombination (and thus removal) of nitrogen atoms is defined as the fraction of atoms incident to the walls which are lost there" (45:110).
4. "The recombination coefficient is defined as the ratio of atoms which recombine on the surface to the total number of atoms striking the surface" (67:860).
5. "The constant γ is defined as the probability that a nitrogen atom will recombine upon striking the quartz surface" (49:2501).
6. "The recombination coefficient, γ , defined as two times the ratio of the number of fluorine atom wall collisions resulting in a recombination to the total number of fluorine atom wall collisions" (34:43).
7. "Therefore, the recombination coefficient is equal to two times the recombination desorption rate divided by the atom impingement rate" (72:20).
3. "... γ , the recombination efficiency...the fraction of collisions with the surface leading to combination..." (2:2059).

Thus, although lacking consistent wording, the various terms and definitions can be summarized as follows: the recombination coefficient, γ , is the number of atoms that collide with the surface and ultimately recombine divided by the total number of atoms that collide with the surface.

Table 3, shown on the following page, contains the recombination data obtained from the literature. Following Table 3, explanatory notes are given, including a discussion of "apparent" temperature, recorded by Breen and others (5). The effect of the surface coatings on the value of the recombination coefficient is then addressed.

Table 3

Recombination Coefficient Data for
Atomic Nitrogen on Silicon Dioxide and Pyrex Surfaces

<u>Recombination</u> <u>Coefficient (γ)</u>	<u>Surface</u> <u>Temperature (K)</u>	<u>Surface</u>	<u>Surface</u> <u>Coating</u>	<u>Source</u>
3.5×10^{-4}	973	Glass*	$Mg_3(PO_4)_2$	(2:2062)
4.4×10^{-4}	973	Glass*	$AlPO_4$	(2:2062)
1.5×10^{-4}	300	Quartz	Clean	(5:29)
1.8×10^{-4}	300	Quartz	Clean	(5:29)
2.3×10^{-4}	300	Quartz	Clean	(5:29)
2.6×10^{-4}	300	Quartz	Clean	(5:29)
3×10^{-4}	300	Quartz	Clean	(5:29)
3.5×10^{-4}	300	Quartz	Clean	(5:29)
3.8×10^{-4}	300	Quartz	Clean	(5:29)
1×10^{-2}	1000**	Quartz	Clean	(5:29)
1.1×10^{-2}	1123**	Quartz	Clean	(5:29)
1.3×10^{-2}	1250**	Quartz	Clean	(5:29)
9×10^{-3}	See Note 3.	Quartz	Clean	(5:29)
7.9×10^{-3}	See Note 3.	Quartz	Clean	(5:29)
6×10^{-3}	1355**	Quartz	Clean	(5:29)
4×10^{-3}	See Note 3.	Quartz	Clean	(5:29)
2×10^{-2}	1078	Silica	Clean	(5:37)
2.8×10^{-2}	1176	Silica	Clean	(5:37)
5×10^{-2}	1290	Silica	Clean	(5:37)
3.7×10^{-2}	1311	Silica	Clean	(5:37)
3.4×10^{-2}	1384	Silica	Clean	(5:37)
$<0.1 \times 10^{-5}$	298	Pyrex	Clean	(10:3072)
$<0.1 \times 10^{-5}$	298	Pyrex	HPO_3	(10:3072)
1.2×10^{-5}	611	Pyrex	Clean	(10:3072)
55×10^{-5}	300	Quartz	Clean	(13:2457)
0.7×10^{-5}	300	Quartz	Clean	(13:2457)
3.2×10^{-3}	300*	Pyrex	Clean*	(17:767)
1.6×10^{-5}	195-450	Glass	H_2O	(27:879)
2.65×10^{-4}	328	Glass*	Na_2HPO_4	(35:73)
2.86×10^{-4}	673	Glass*	Na_2HPO_4	(35:73)
$1.9(\pm 0.4) \times 10^{-4}$	300	RCG	Clean	(46:3-36)
2.3×10^{-4}	300	Pyrex	Clean	(51:90)
0.63×10^{-3}	300	Quartz	Clean	(51:90)
0.53×10^{-3}	600	Quartz	Clean	(51:90)
0.72×10^{-3}	800	Quartz	Clean	(51:90)
1.05×10^{-3}	1000	Quartz	Clean	(51:90)
1.5×10^{-3}	1200	Quartz	Clean	(51:90)
$<2.5 \times 10^{-3}$	-2300	Quartz	Clean	(51:90)
$1.1(\pm 0.1) \times 10^{-5}$	300	Pyrex	Clean	(58:403)
6×10^{-4}	300	Pyrex	Clean	(64:176)
3.5×10^{-6}	300	Pyrex	Clean	(64:176)
3.4×10^{-5}	300	Pyrex	Clean	(64:176)

Table 3 (continued)

Recombination Coefficient Data for
Atomic Nitrogen on Silicon Dioxide and Pyrex Surfaces

<u>Recombination</u> <u>Coefficient(γ)</u>	<u>Surface</u> <u>Temperature(K)</u>	<u>Surface</u>	<u>Surface</u> <u>Coating</u>	<u>Source</u>
2.7×10^{-5}	300	Pyrex	Clean	(64:176)
$5(\pm 3) \times 10^{-5}$	300	Pyrex	Clean	(67:863)
4×10^{-6}	300	Pyrex	Clean	(75:4081)
3×10^{-5}	300	Pyrex	Clean	(83:231)
3.2×10^{-6}	300	Pyrex	Clean	(85:4252)
1.7×10^{-5}	300	Glass	Na ₂ HPO ₄	(86:1294)

Notes:

1. * Data or information inferred from article.
2. ** Apparent temperature. See discussion following these Notes.
3. The temperatures for these recombination coefficients could not be determined from the plot in Breen and others' report (5:29).
4. The value 1.3×10^{-2} at 1250K for γ was reported by Breen and others (5:29) as a maximum value. Marshall's value of $\gamma < 2.5 \times 10^{-3}$ at -2300K (51:90) was obtained via extrapolation, but Marshall extrapolated beyond the range of his observations. RCG is reaction cured glass.

Next, the order of the reaction and the corresponding temperature and pressure conditions are considered.

Finally, the "quality" of the data for use in this thesis will be addressed.

Figure 4 shows the empirical data plotted versus the reciprocal temperature. The key provides the source, surface, and surface condition. For example, Back-Q-C represents the source Back (2), a quartz (Q) surface, which is coated (C). Upper case (U) stands for the uncoated or clean surface. Silica and pyrex are designated by S and P, respectively.

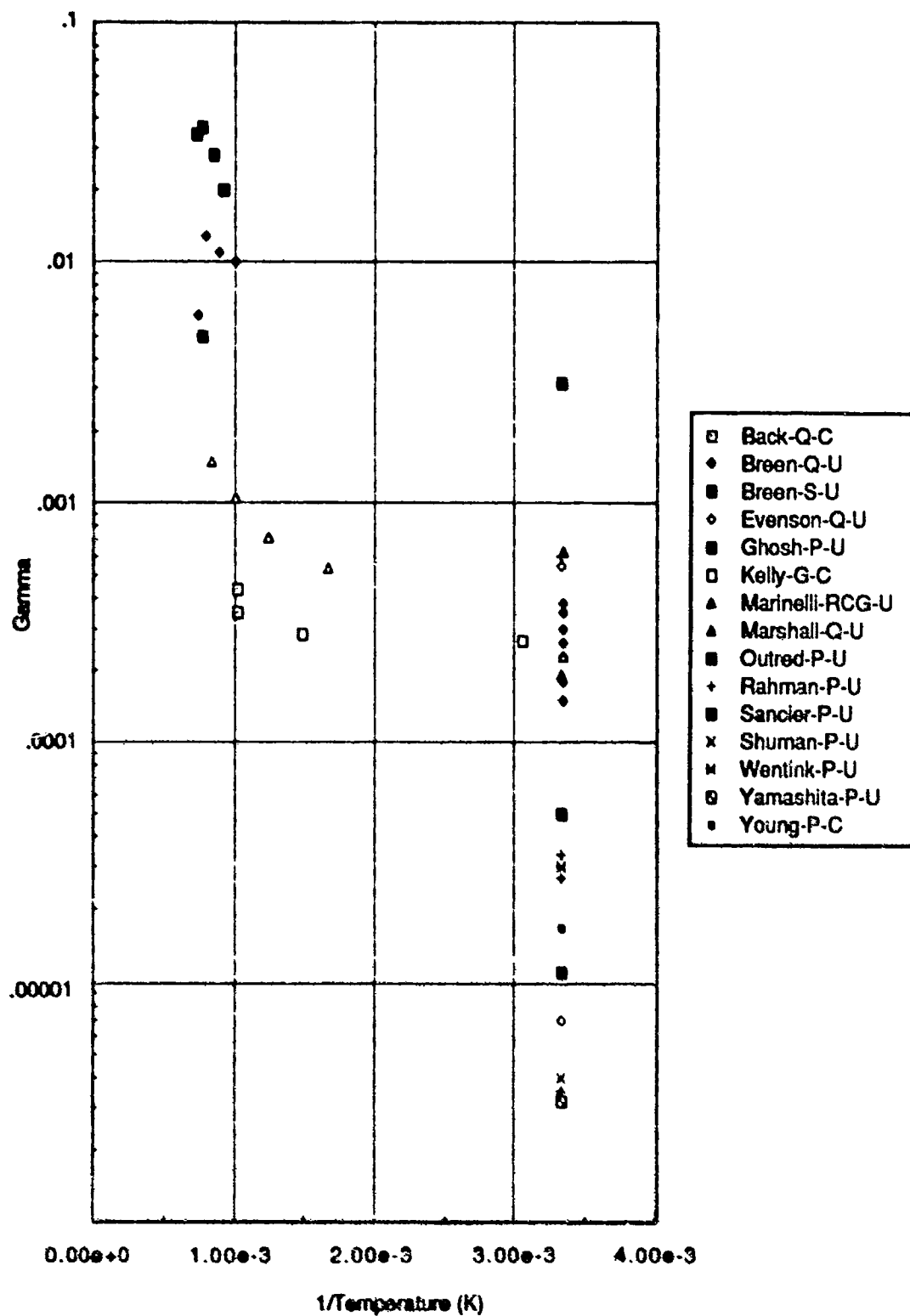


Figure 4. Recombination Coefficients of Atomic Nitrogen on Silica Surfaces.

The following provides a brief background and a discussion of "apparent" temperature. Breen and others reported (5:28)

It is apparent from our data that γ has a maximum value (occurring at an apparent temperature of 1250K) of about 1.3×10^{-2} and then decreases rapidly to a value of approximately 6×10^{-3} at 1355K.

The values given by Breen and others (5:28,29) were based on temperatures of an "...outer graphite susceptor and not those of the quartz wall" (5:28). In other words, their values of the recombination coefficient were reported at the temperatures of an outer tube assembly, not the internal quartz surface in contact with the nitrogen gas. Consequently, they termed their temperature readings as "apparent" temperatures and should be regarded as approximate values.

Although this thesis is concerned with clean, uncoated surfaces, a brief discussion of the effects of the surface coatings is warranted since, as a catalyst, a coating may inhibit or promote the reaction. However, according to Bond (4:43)

A poison is therefore a substance which is much more strongly adsorbed than the reactants, and therefore denies them access to the surface for reaction.

Bond's definition of a poison was in reference to recombination on metallic surfaces. However, silicon dioxide and pyrex are nonmetallic and from Table 3, it is clear that a difference exists between the values of the

recombination coefficient for coated surfaces and those for clean surfaces.

From Table 3, Kelly and Winkler's data (35:73) shows that γ increases from 2.65×10^{-4} to 2.86×10^{-4} as the temperature increased from 328K to 673K. However, their surface was coated and thus their results are not indicative of nitrogen recombination on clean silicon dioxide.

Rather, their results, as well as those of other workers using coated surfaces may reflect a chemical reaction of some sort between the coating and the nitrogen atoms. The behavior of this reaction is shown via the scatter among the values of the recombination coefficient at 300K.

Kretschmer and Petersen (39:1772), in their experiment on nitrogen recombination, used phosphoric acid as a coating and observed "The rate of surface recombination was reduced to a very small value by coating the walls of the flow tube with phosphoric acid..." Marshall (47:128) also stated that metaphosphoric acid (Na_2HPO_4), water vapor, and sulfuric acid (H_2SO_4) significantly reduce the value of the recombination coefficient. He postulated that the coating forced the recombination process "...back into the volume phase for nearly every experimental condition" (47:128).

Although recombination coefficient values on coated surfaces are not quantitatively useful for this thesis,

close examination of these values yields an important qualitative conclusion: at 300K, the recombination of nitrogen atoms on quartz and pyrex surfaces coated with Na_2HPO_4 , AlPO_4 , H_2O , or $\text{Mg}_3(\text{PO}_4)_2$ is markedly lower than that of uncoated quartz or pyrex. This finding agrees with Marshall (47:128). Furthermore, the lower values of the recombination coefficient with coated surfaces appear to also occur at the elevated temperatures. For example, consider Back and others' (2) data, repeated below:

<u>Recombination</u> <u>Coefficient</u> (γ)	<u>Surface</u> <u>Temperature</u> (K)	<u>Surface</u>	<u>Surface</u> <u>Coating</u>	<u>Source</u>
3.5×10^{-4}	973	Glass*	$\text{Mg}_3(\text{PO}_4)_2$	(2:2062)
4.4×10^{-4}	973	Glass*	AlPO_4	(2:2062)

From Marshall's data, who used a clean surface, the recombination coefficient is approximately 1×10^{-3} at about 973K. Comparing to the above data, this is roughly an order of magnitude difference between the coated and clean surface recombination coefficients. The data in Table 3 and Figure 4 clearly show that the recombination coefficient is lowered for coated surfaces at 300K and at the elevated temperatures. It is reasonable to conclude then, that the recombination process is also affected by the coatings.

The order of the recombination process can be deduced from the recombination coefficient's functionality relative to the pressure, as shown in Chapter II. The results showing this correlation are detailed in Table 4. Note

that the data were taken from the same set of sources as in Table 3. Taken together, both tabulations provide a

Table 4

Order of the Recombination

<u>Order Information/Commentary</u>	<u>Source</u>
Four nearly equal slopes were obtained at pressures from 3 to 27 torr and yielded a value of 55×10^{-5} for the recombination coefficient.	(13:2453)
Data for nitrogen atom recombination on quartz were taken over the pressure range of 3-13 torr with no variation in the recombination coefficient. For nitrogen on Pyrex, the concentration of nitrogen atoms at various locations on the wall was independent of gas pressure in the range of 0.5-2.0 torr.	(51:82 ⁺)
The recombination coefficient equalled 3×10^{-4} at 300K on clean Pyrex and was independent of pressure in the range 0.5-2.0 torr.	(50:753)
The recombination process is first order at 0.08 torr and is almost entirely first order at 0.094 torr. At about 0.9 torr, a second order behavior contributed to the process.	(64:176)
It was experimentally shown that the recombination coefficient was independent of pressure.	(67:860,864)
The recombination of nitrogen on clean Pyrex was constant at 3×10^{-5} . Above 0.5 torr, the rate coefficients were much less pressure dependent and in some cases independent of pressure.	(83:231)
For clean glass, the recombination coefficient was constant in the pressure range of 1-2 torr. For a glass surface coated with metaphosphoric acid, the recombination coefficient was also constant in the same pressure range.	(86:1292)

concise collection of the available data regarding heterogeneous recombination of atomic nitrogen on silicon dioxide and pyrex surfaces.

The majority of investigations give first order kinetics, except the observations of Rahman and Linnett (64:176). In their paper, they examined the question of "order" and their result of a first order behavior at 0.1 torr and a second order contribution at higher pressures. However, they were forced to conclude that "...no definite answer is possible" for the second order kinetics (64:176). They postulated a mechanism by which the first order behavior might have involved the nitrogen atoms adsorbed onto the pyrex. On the other hand, they stated that the second order behavior might have involved "...nitrogen atoms adsorbed as a second layer on the first" (64:176). (Note that as pointed out in Chapter II, chemical adsorption is limited to a monolayer.) Hence, based on Rahman and Linnett's own statement, the reason for the second order behavior remains in doubt. However, the second order behavior at the high temperatures could be due to some intermediate interaction involving the chemisorption rate and/or thermal desorption rate acting singly or in combination which could account for the second order process.

However, based on the majority of the empirical data presented in Table 4, the recombination coefficient is

independent of pressure which means the overall recombination process obeys first order kinetics. Furthermore, a significant observation can be made: the recombination process obeys first order behavior for clean quartz and clean pyrex as well as for coated quartz and coated pyrex surfaces. It should be noted that the definition of order used in this thesis is that given by Hinshelwood (30:195):

The chance that r molecules (or atoms) shall occupy positions on the surface to render interaction possible depends on the r th power of the surface concentration, and this in its turn depends on the r th power of the pressure.

To conclude this section, a discussion of the "quality" or accuracy of certain data is presented. The presentation focuses on the values of the recombination coefficients given by Marshall in 1962 (49:2501), which were later found to be incorrect.

Evenson and Burch, in their paper on atomic nitrogen recombination, stated the following regarding the data by Marshall (13:2460):

Marshall, the only other worker reporting values of k_1 using ESR techniques identical to ours and employing a quartz flow tube, reported a value of $1.5 \times 10^{-32} \text{ cm}^6 \text{ sec}^{-1}$ for k_1 ; however, he used an incorrect calibration formula due to a typographical error in a previous paper. Marshall also calculated an average velocity by integrating over the radius, rather than the area of the flow tube, thus adding an additional error to the determination of k_1 .

Marshall's mathematical errors thus placed his published values of the recombination coefficient in serious doubt.

However, since Marshall's original paper in 1962, two sources have provided corrections to his data. The first was by Marshall himself in 1964 (51:88) and the second by Wright and Winkler in 1968 (84:168). In his 1964 report, Marshall explicitly concluded the following (51:88):

Some of the material in this report has been previously published, and it has been found since then that the published values of the recombination coefficients were in error...The values in this report have been so corrected.

The corrected recombination coefficient data given by Marshall in 1964 (51:88) are in Table 3 and Figure 4.

Summary. This literature review presented the results of obtaining the following recombination data:

1. The recombination coefficient as a function of temperature and surface conditions (relative to coating).
2. The maximum values of the recombination coefficient.
3. The order of the recombination process.
4. Discussions of the terminology for the recombination coefficient, "apparent" temperature and order.
5. A discussion on the validity of Marshall's 1962 data (49).

It was found that the recombination coefficient was independent of pressure and thus the recombination process obeys first order kinetics. Also, from 300K to higher

temperatures, the values of the recombination coefficient are lowered if the surface is coated with Na_2HPO_4 , AlPO_4 , H_2O , or $\text{Mg}_3(\text{PO}_4)_2$. Coupling this result to Bond's observation (4:43) that nitrogen recombination is inhibited on coated metal surfaces, it is reasonable to conclude that coating metallic and nonmetallic quartz or pyrex surfaces inhibits the heterogeneous recombination of atomic nitrogen.

The remaining issue to examine is the surface upon which the atoms strike and recombine. The final section in this chapter, which follows, addresses this issue with a discussion of the silicon dioxide surfaces and structures of concern in this thesis.

Silica Surface Structure

Introduction. This section provides a brief description of the various silica based solids which are of concern in this thesis. The properties of quartz and its phase transitions are shown along with photographs of each crystal structure, Figures 6-17. Furthermore, two species of nitrated silicon are discussed: silicon nitride and silicon oxynitride. The properties and photographs of the crystal structure of silicon nitride are also provided in the figures.

Silicon Dioxide. Silicon dioxide (SiO_2) is also known as silica. The silicon-oxygen separation is 1.60Å (36:143). The predominant crystalline phases of silica are

quartz, tridymite, and cristobalite, with each phase transitioning at a certain temperature. The alpha (α) phase is the low temperature phase, whereas the beta (β) phase is the high temperature phase. Each phase has its own unique crystal structure and accompanying set of characteristics, such as temperature range, crystal system, and density. These properties are shown below in Table 5 (53:5.4.6-1).

Table 5

Properties of the Phases of Silica

<u>Phase</u>	<u>Temp. Range(K)</u>	<u>Crystal Structure</u>	<u>Density (gm/cm³)</u>	<u>Melting Point(K)</u>
α -Quartz	To 845	Trigonal	2.65	-
β -Quartz	845-1140	Hexagonal	2.52	1743
Tridymite*	1140-1743	Orthorhombic	2.32	1933
α -Cristobalite	To 545	Tetragonal	2.32	-
β -Cristobalite*	545-1998	Cubic	2.27	1998

*Notes:

- Kingery (36:123) listed the following temperature ranges (K):
 β -Tridymite 1140 < T < 1743.
 β -Cristobalite 1743 < T < 1983.
- According to Norton (57:174), pyrex consists of 80.5% silicon dioxide.

As shown in Table 5, the density decreases with increasing temperature. Thus, there is an accompanying change in the volume of each phase. Figure 5, shown below, depicts the relative volume expansions of crystalline (pure) and

amorphous silica (53:5.4.6-11). The phases are denoted by the following: C = cristobalite; Q = quartz; T = tridymite; and FS = fused silica. Fused silica is essentially pure silica (53:5.4.6-1). The volume-expansion ratio is $V_2:V_1$, where V_2 is the volume at the elevated temperature and V_1 is the volume referenced to 273 K.

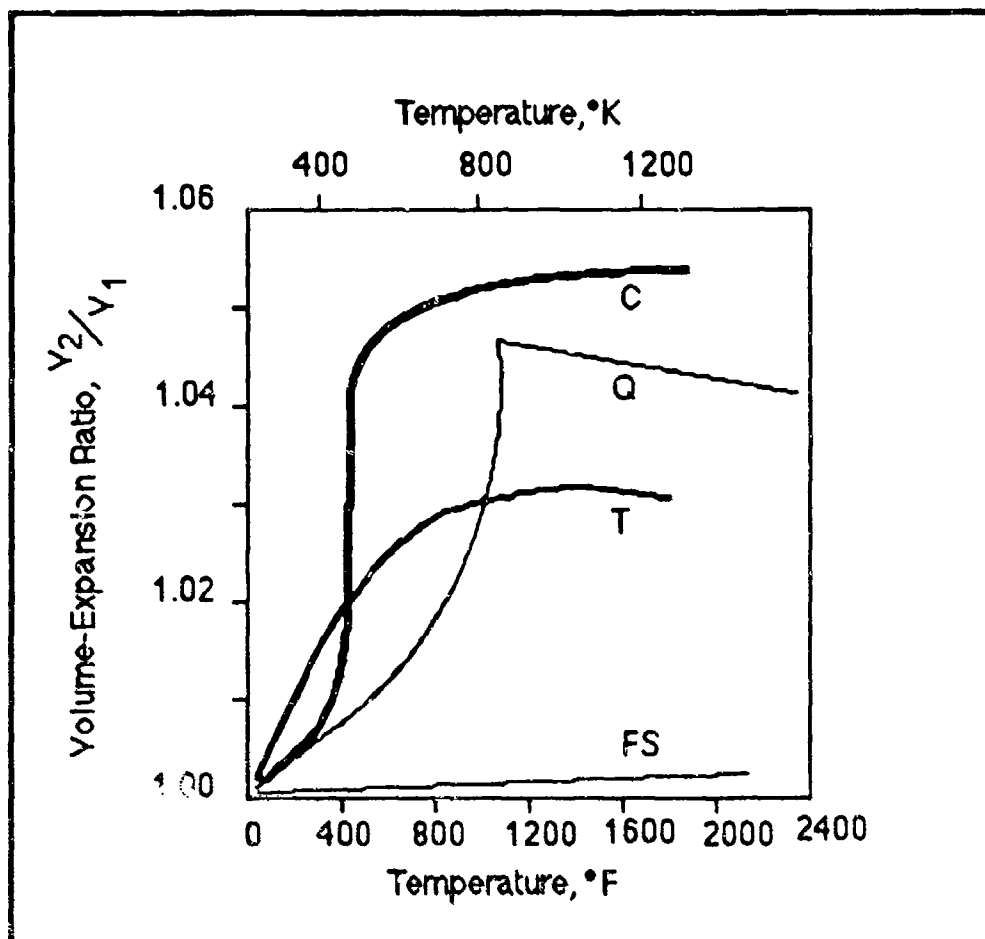


Figure 5. Relative Volume Expansions of Crystalline and Amorphous Phases of Silica.

Photographs of the phases of silica (Figures 6-11, 15-17) are shown following the discussion of silicon nitride and silicon oxynitride.

Nitriding of silica surfaces was observed by Breen and others (5:74). After passing dissociated nitrogen gas over a silica sample, they observed that the nitrogen was incorporated into the silicon dioxide at temperatures above 1720K as either silicon nitride or silicon oxynitride, Si_3N_4 or Si_2ON_2 , respectively (5:74).

However, in contrast to the amount of precise information known about silica and its phases, details of these two forms are less clear. The available data relative to each is presented below.

Silicon Nitride. According to Popper and Ruddelsen (63:621), silicon nitride occurs in two phases, alpha and beta, depending on the temperature. Alpha-silicon nitride is the low temperature form and transitions to the high temperature form, β -silicon nitride, between 1673-1873K (63:615). Their respective properties are given below in Table 6 (63:621).

Table 6

Properties of the Phases of Silicon Nitride

<u>Phase</u>	<u>Crystal Structure</u>	<u>Lattice Parameters</u> (Å)	<u>Density</u> (gm/cm ³)
α -Silicon Nitride	Hexagonal	a = 7.748 c = 5.617	3.184
β -Silicon Nitride	Hexagonal	a = 7.608 c = 2.911	3.187

Two points of qualitative significance were included in their paper: the presence of oxygen can reduce the

nitriding rate (63:603); and, the nitriding reaction is highly exothermic (63:607). No hard data were given, however, as to how much the rate was reduced nor as to the amount of heat released in the exothermic reaction.

Regarding the atomic arrangement of silicon nitride, Parr (61:11) stated that each silicon atom forms four covalent bonds with the neighboring nitrogen atoms. Hu (33:694) provided the Si-N bond length of 1.72-1.75Å. Hu also reported that the Si-N is triply bonded, owing to the trivalent nature of nitrogen. Photographs of silicon nitride, and α - and β -silicon nitride are shown in Figures 12, 13, and 14, respectively.

Silicon Oxynitride. Much less is quantitatively known about silicon oxynitride. For example, Popper and Ruddelsen (63:615) gave its stoichiometry as Si_2ON , whereas Loehman (44:10) reported that oxynitride glasses contain Si, O, N, and one other cation, which could be another N atom. Loehman (44:36) listed $\text{Si}_2\text{N}_2\text{O}$ as the stoichiometric relation.

Regarding the crystal structure of silicon oxynitride, Loehman stated (44:36)

Very little direct evidence of oxynitride glass structure has been reported. Most structural models, which are only very rudimentary at present, are plausibility arguments based on analogous crystalline structures and on glass properties data. The existence of SiN_4 and SiON_3 in tetrahedral structural units in crystalline Si_3N_4 and $\text{Si}_2\text{N}_2\text{O}$ leads one to postulate that oxynitride glasses containing oxygen are built up of $\text{Si}(\text{O},\text{N})_4$ tetrahedra.

Loehman observed that $\text{Si}_2\text{N}_2\text{O}$ formed upon heating above 1573K (44:32).

Summary. This chapter provided the background information regarding the heterogeneous recombination of atoms on surfaces, particularly silicon dioxide. The Shuttle's TPS was discussed first, followed by the details of the heterogeneous recombination reaction. In this connection, the most widely accepted mechanisms used to describe the reaction were covered, focusing on the Langmuir-Rideal mechanism.

Seward (72) modelled atomic oxygen recombination on silicon dioxide and assumed the number of active sites did not vary with temperature, but was constant at $5 \times 10^{14} \text{ cm}^{-2}$ (72:50). However, as shown above, for increasing temperature, the structure of silicon dioxide changes, resulting in volume and density changes. Moreover, it is reasonable to postulate that the structural change is also accompanied by a changed number of active surface sites.

One of the primary assumptions made in this thesis was that the number of sites is not constant and depends on the particular phase of the silicon dioxide (i.e., quartz, tridymite, or cristobalite). Consequently, the number of sites was calculated and shown in the next chapter. This value was used in the software routine, the output of which was used to compare to the empirical data from the literature.

The various silicon dioxide phases are shown in Figures 6-17.

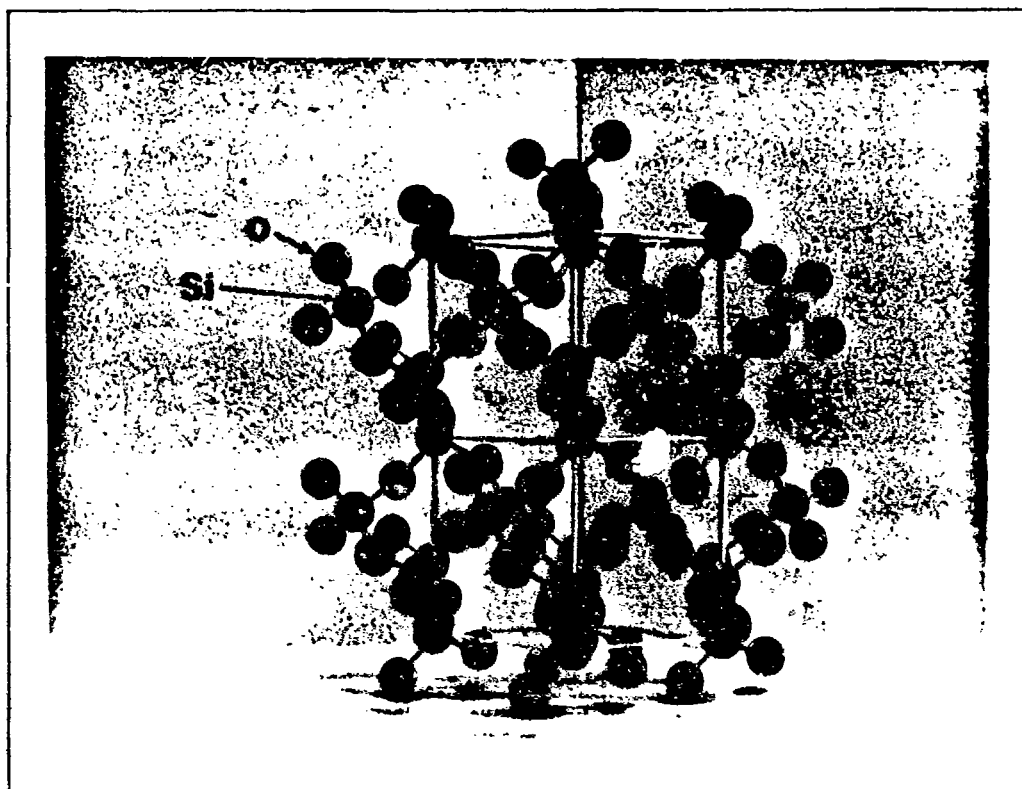


Figure 6. Alpha-Quartz (Two Cells), SiO₂. Low Temperature Phase.

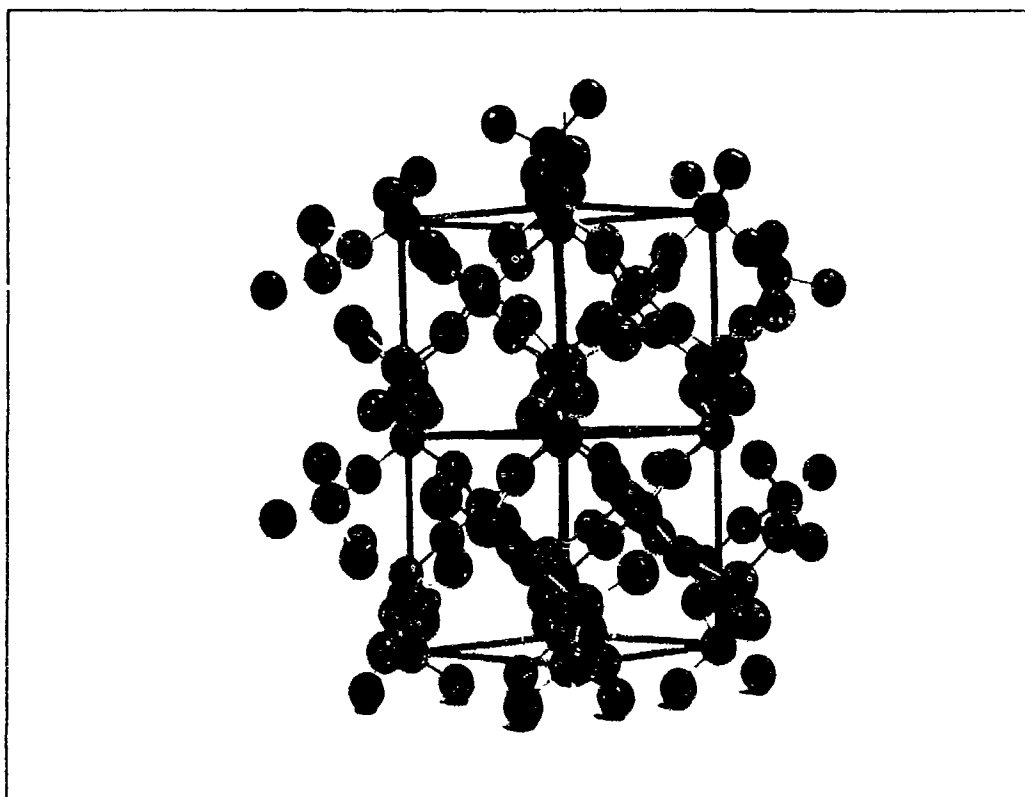


Figure 7. Beta-Quartz (Two Cells), SiO_2 . High Temperature Phase.

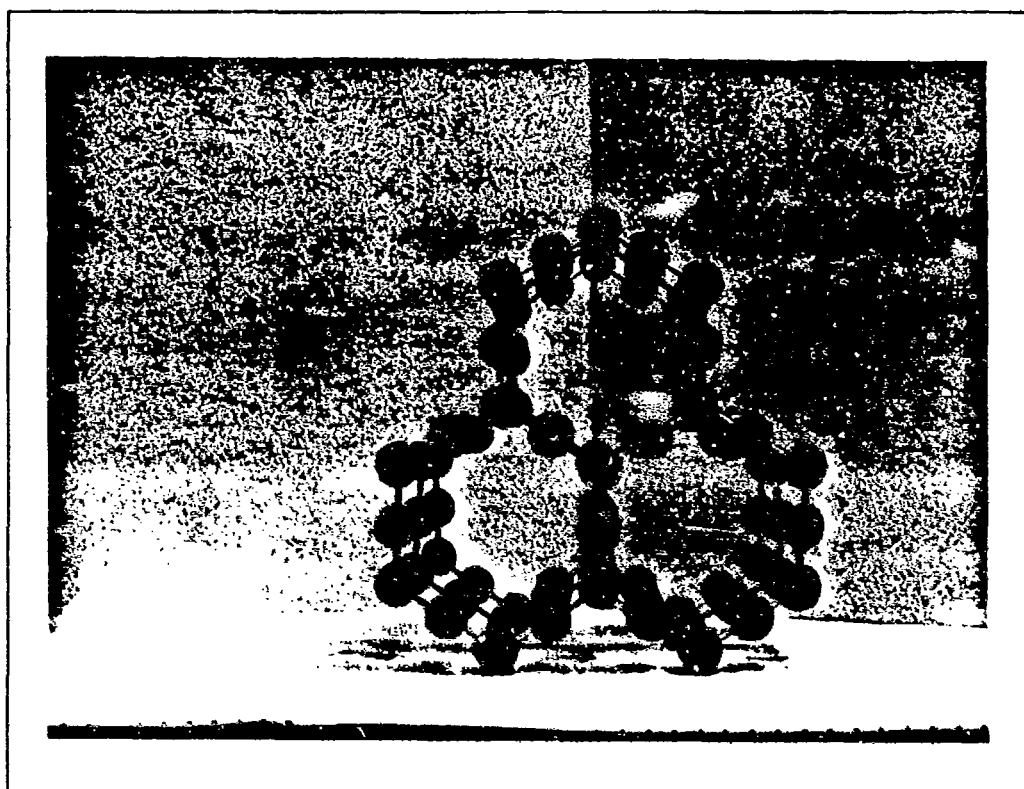


Figure 8. Tridymite, SiO_2 . Viewed Along $\langle 110 \rangle$ Direction.

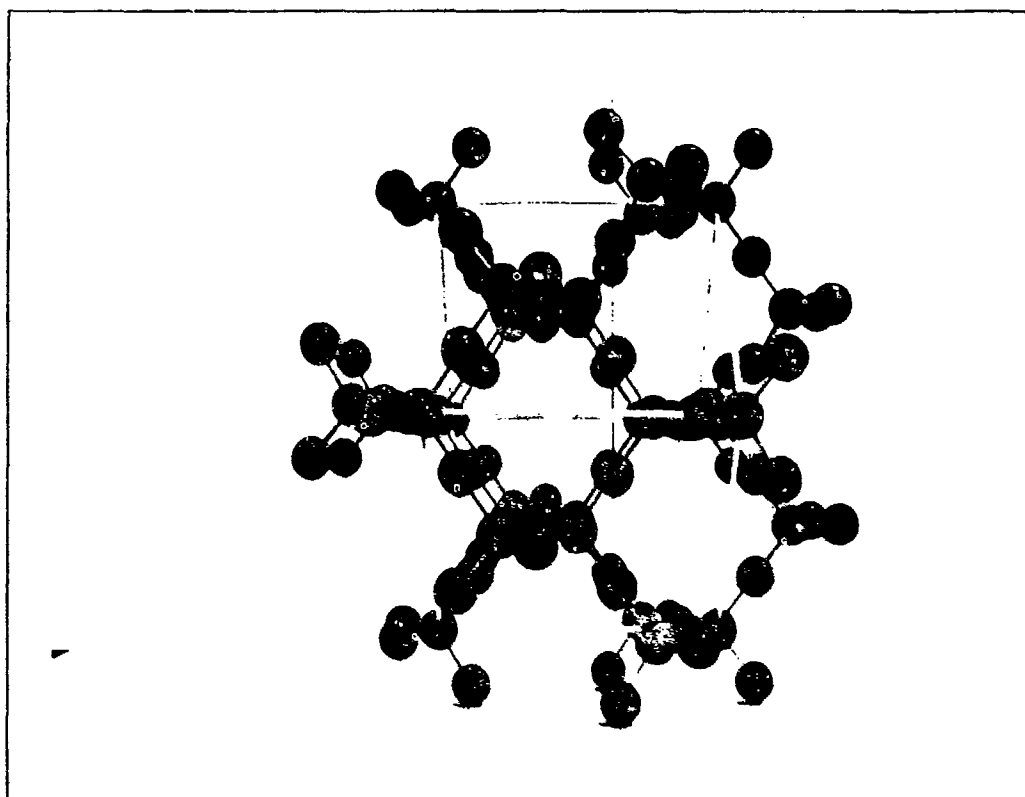


Figure 9. Alpha-Cristobalite, SiO₂. Low Temperature Phase.

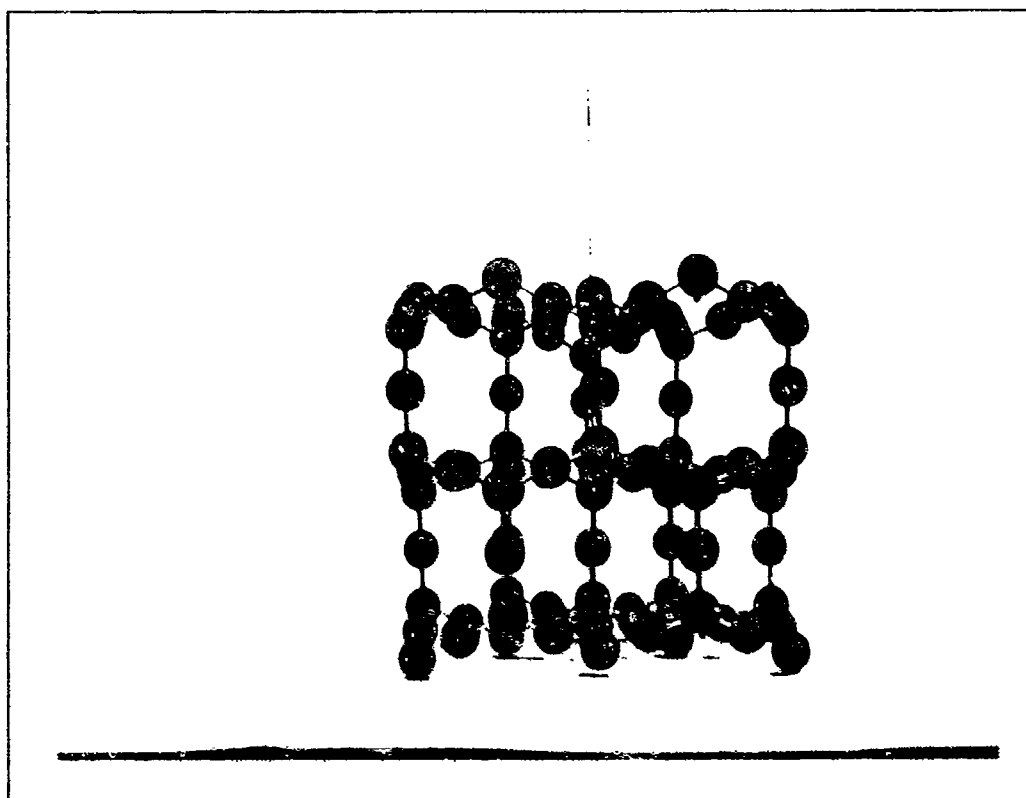


Figure 10. Beta-Cristobalite, SiO₂. High Temperature Phase.

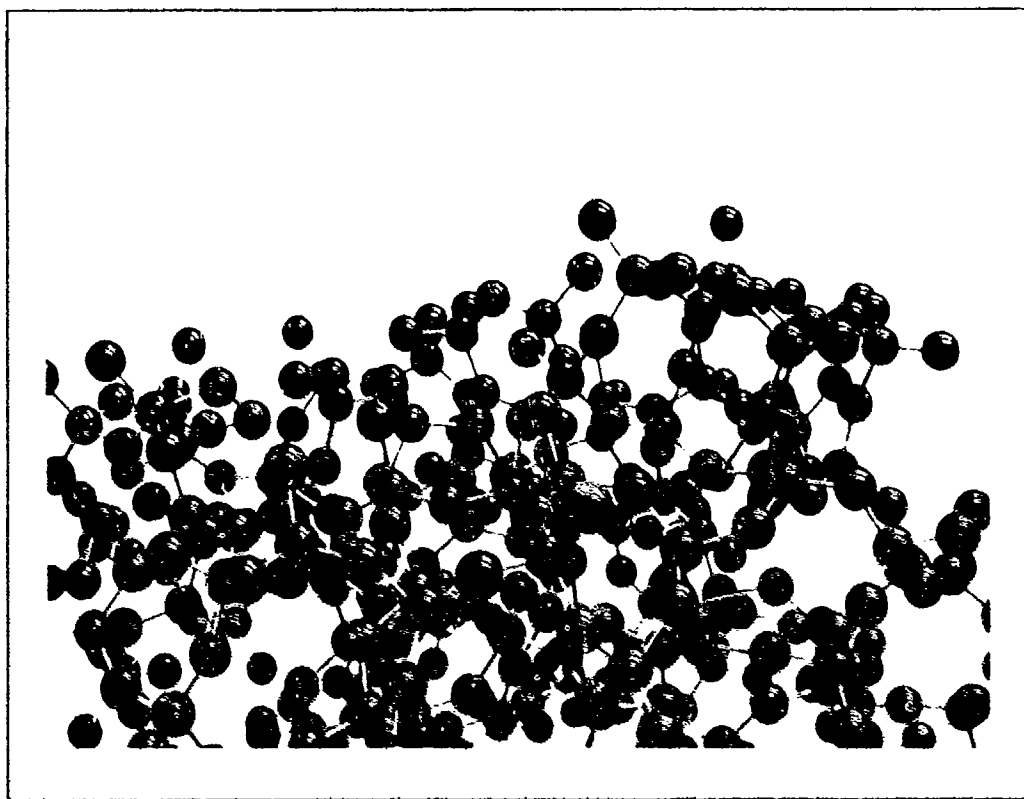


Figure 11. Silica Glass, SiO_2 .

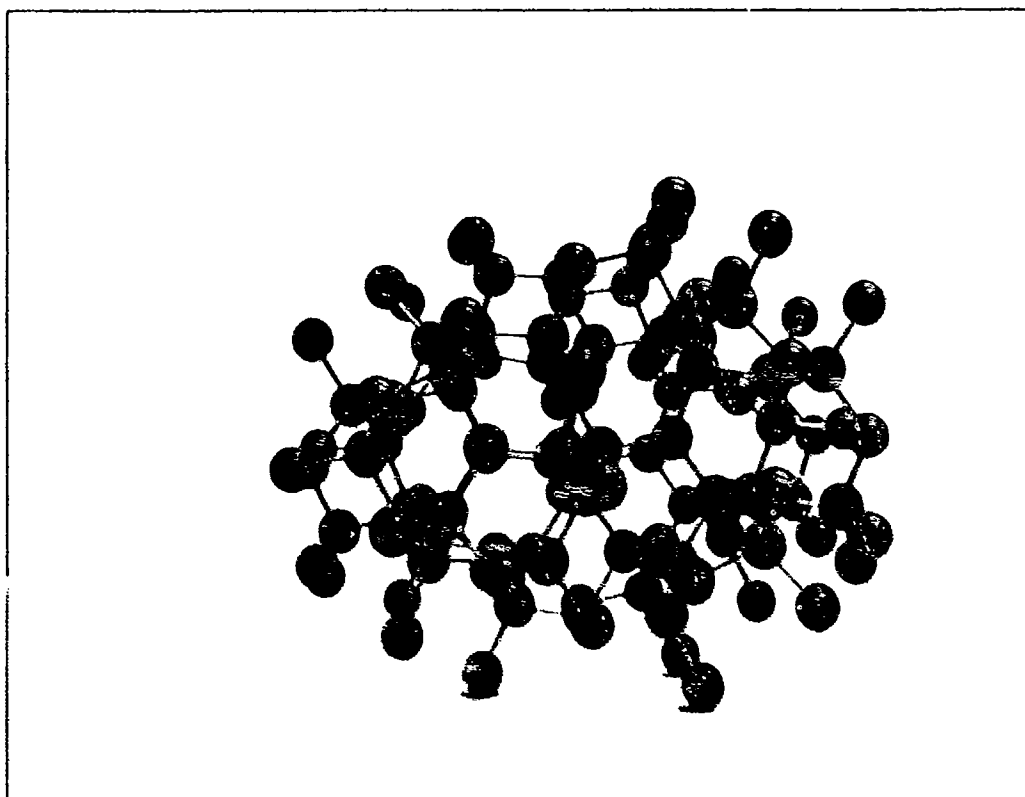


Figure 12. Silicon Nitride, Si_3N_4 .

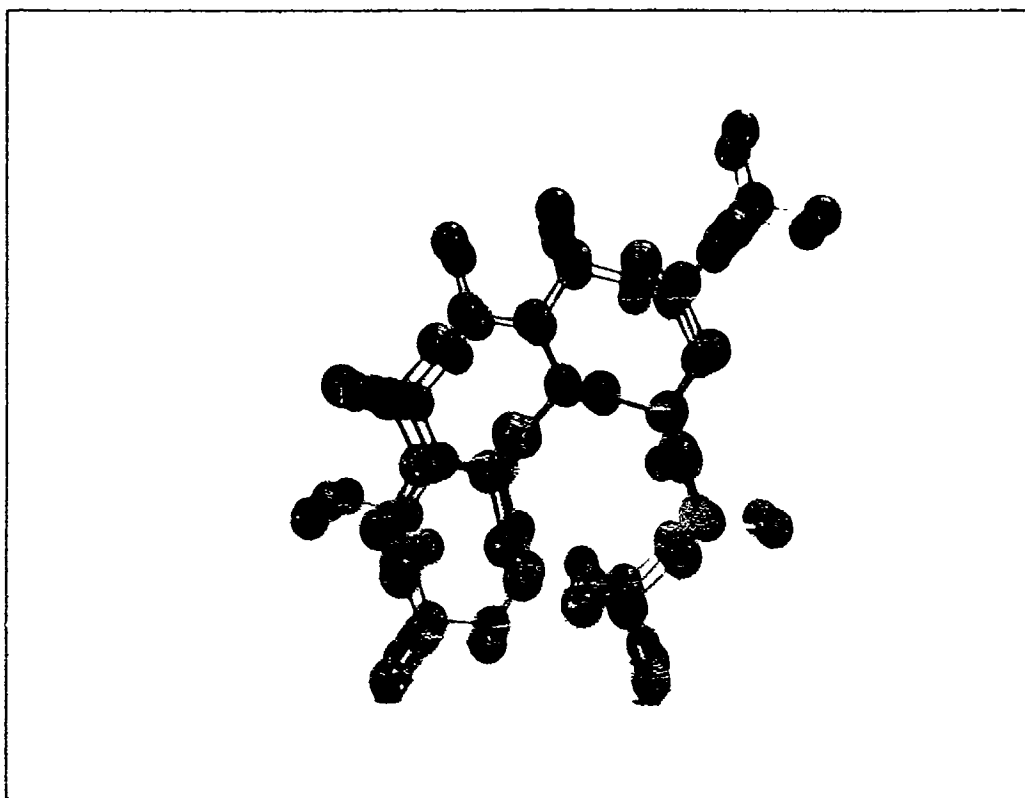


Figure 13. Alpha-Silicon Nitride, α - Si_3N_4 . Low Temperature Phase.

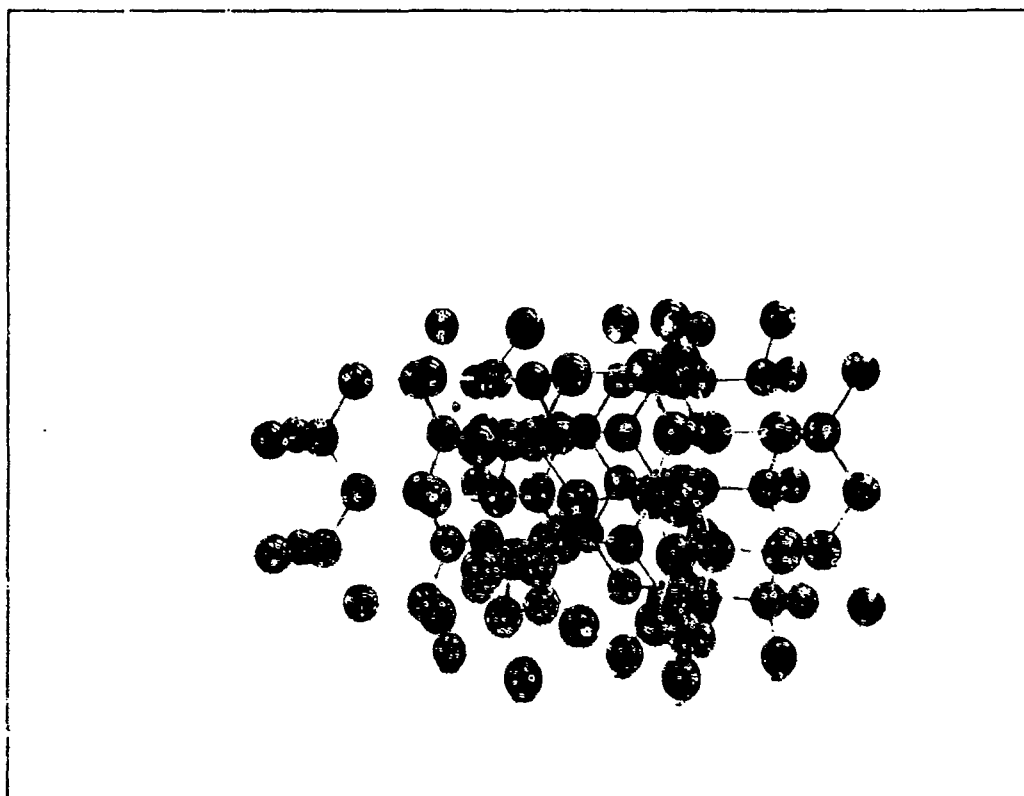


Figure 14. Beta-Silicon Nitride, β - Si_3N_4 . High Temperature Phase.

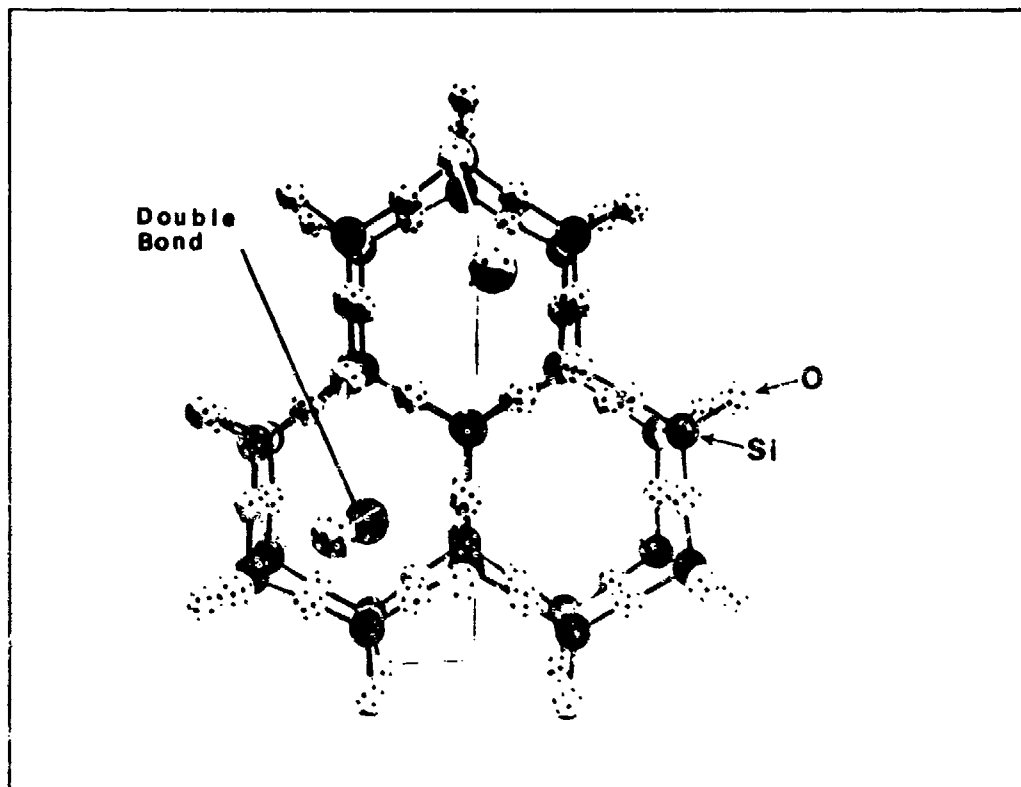


Figure 15. Silicon Dioxide Model Showing Double Bonds at the Surface. Top View, $\langle 110 \rangle$ Direction.

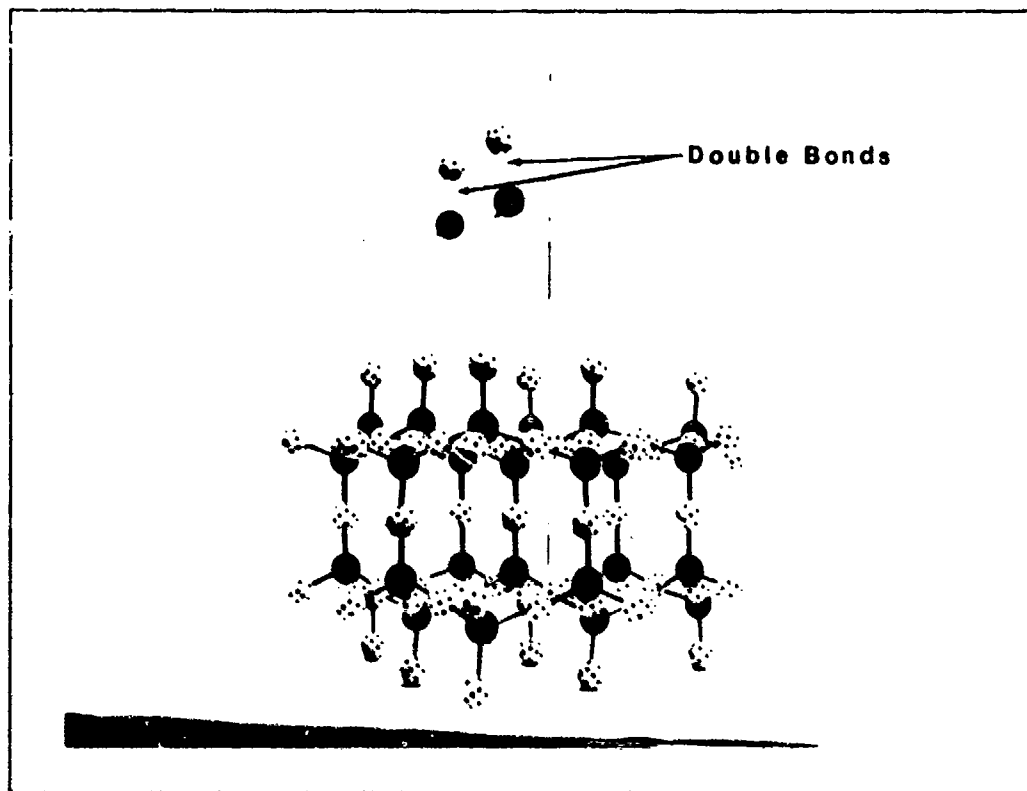


Figure 16. Silicon Dioxide Model Showing Double Bonds at the Surface. Side View.

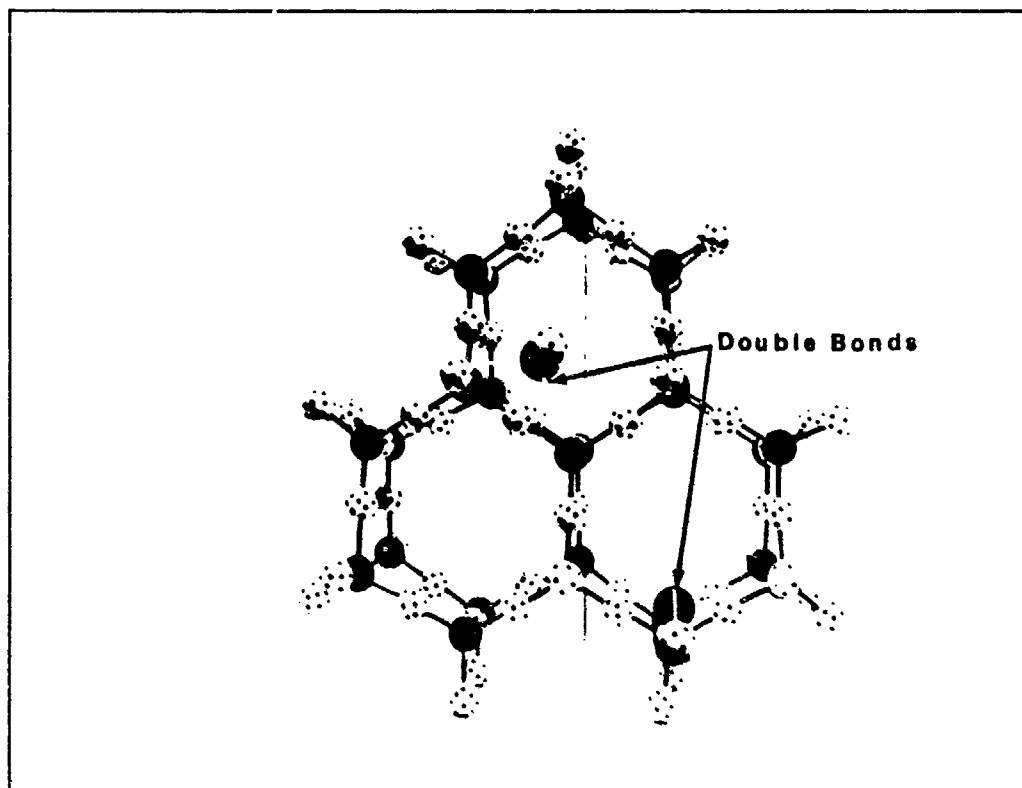


Figure 17. Silicon Dioxide Model Showing Rearrangement of the Double Bonds at the Surface. Stoichiometry is Maintained. Top View, $\langle 110 \rangle$ Direction.

III. Analytical

Introduction

The goal of this thesis was to develop a model which described the steady-state heterogeneous recombination of atomic nitrogen on a silicon dioxide surface in the temperature range 300-2000K. To this end, the kinetic rate equations corresponding to a Langmuir-Rideal recombination mechanism were developed. Moreover, a literature search yielded empirical values of the recombination coefficient of nitrogen on silicon dioxide as well as a dissertation (72) for atomic oxygen recombination on silicon dioxide.

In this dissertation, the recombination coefficient, γ , was calculated based on rate equations corresponding to a Langmuir-Rideal recombination mechanism. Some of the recombination parameters such as the steric factor, dissociation energy, and an expression for the initial sticking coefficient were available from the literature as empirical data. Other parameters (the activation energy and pressure) were calculated.

On the other hand, another parameter, the number of surface sites available for recombination, was assumed to be the number in the bulk, $5 \times 10^{14} \text{ cm}^{-2}$ (72:50). Now, because the same recombination mechanism (Langmuir-Rideal) was used in this thesis, a computer routine was developed

for nitrogen recombining on silicon dioxide in the temperature range 300-2000K. From Chapter I, recall that an underlying assumption was that nitrogen is doubly bonded to the silicon atoms.

The computer routine for this thesis was developed directly from the kinetic rate equations in Chapter II and is presented in Appendix A. The essence of the routine is as follows:

- a. Declare the input parameters (listed below), variables, or constants.
- b. Calculate the values of the recombination coefficient, γ ; surface coverage, θ ; sorption rates; and the impingement rate, N . The terms appearing in the denominator of Equation (52) were also calculated since these affect the behavior of the recombination in the higher temperature regime. Each of the above values was calculated over the temperature range 300-2000K.

- c. Output the results in numerical and graphic form. To maintain a coherent flow, the sequence of presentation begins with the calculations of the parameters which are then used as inputs to the program. These parameters are as follows:

- a. The calculation of the surface area.
- b. The calculation of the number of surface sites per unit area.

- c. The calculation of the nitrogen gas pressure used by Marshall (51).
- d. The calculation of the activation energy and steric factor.
- e. The determination of the dissociation energy.
- f. The value selected for the initial sticking coefficient.

The computer routine, based on the rate equations and these parameters, calculates the recombination coefficient as a function of temperature (300-2000K). The calculated values of the recombination coefficient are then plotted and compared to the empirical data.

Calculation of the Surface Area

The objective of this section is to calculate a firm value for the number of surface sites per unit area for silicon dioxide. The need for such a determination exists because throughout the literature, the number of sites per unit area has been estimated at approximately 10^{15} cm^{-2} (16:182; 24:357; 79:27). Indeed, as pointed out in Chapter I, Seward (72:50) used a value of $5.4 \cdot 10^{14} \text{ cm}^{-2}$ as the number of surface sites, even though this was the number in the bulk. The number of sites per unit area will be determined for the phases of quartz, i.e., quartz, tridymite, and cristobalite. The surface area is calculated first, followed by the calculation of the number of possible sites.

Figures 15 and 17 (Chapter II) show the silicon dioxide surface viewed along the $\langle 110 \rangle$ axis and served as the initial crystal model for the associated phases of quartz. This structure was built using two Ball and Spoke Kits, Part Number KS7999, from Klinger Educational Products (37). White balls represent oxygen atoms and black balls represent silicon atoms. The final configuration shown in Figures 15, 16, and 17 was based on photographs of Wells (82:808). The following is a short discussion of the phases of silica since these phase transitions provided the rationale and motivation for examining the specific crystal structures with regard to areas and possible sites.

The phases and temperature ranges of stability were presented in Chapter II and shown below to facilitate the discussion.

Quartz \rightarrow 1143K \leftarrow Tridymite \rightarrow 1743K \leftarrow Cristobalite \rightarrow 1983K (Melting Point)

Recall that each has its own low temperature (alpha) phase and high temperature (beta) phase. These three phases each consist of linked SiO_4 tetrahedra so that every oxygen atom is bound to two silicon atoms, resulting in the overall stoichiometry, SiO_2 .

However, the structural configuration of each phase is different due to the manner the tetrahedra are connected. For instance, the cristobalite-tridymite difference is akin to the difference between the wurtzite and zincblende crystal structures (82:785). On the other hand, the alpha

and beta forms of each phase differ due to "slight rotations of the tetrahedra relative to one another without any alteration in the general way in which they are linked" (82:785).

The phase transition from quartz to tridymite to cristobalite involves breaking the oxygen-silicon-oxygen (O-Si-O) bonds and connecting the tetrahedra in the new structural arrangement. From Table 5 (Chapter II), the density (gm/cm^3) of each phase was alpha quartz = 2.65; beta quartz = 2.52; tridymite = 2.32; alpha cristobalite = 2.32; and beta cristobalite = 2.27. According to Wells (82:786), the lower density results in the tridymite and cristobalite phases having more amorphicity than the quartz phase in that they are more "open" structurally.

In its unit configuration, the SiO_4 tetrahedron in alpha quartz conforms to the following dimensions (78:344): Si-O bond angle = 109.48° ; Si-O bond distance = 1.60\AA ; O-O bond distance = 2.27\AA . The Si-O bond distance for alpha cristobalite is 1.59\AA and that for beta cristobalite is 1.63\AA (82:786). A bond distance for tridymite was not available from the literature. From these bond distance values, it should be clear that as bond distance decreases, the density either increases or decreases and thus no distinct correlation can be drawn between the density and bond distance, substantiating the amorphous character of silica.

Note that the method of determining the number of possible sites per unit area was an assumed technique since no published techniques were found in the literature. Thus, to arrive at the number of active sites, a hexagonal region of the surface was chosen to depict the surface area (A). Figure 18 shows the hexagonal arrangement of atoms

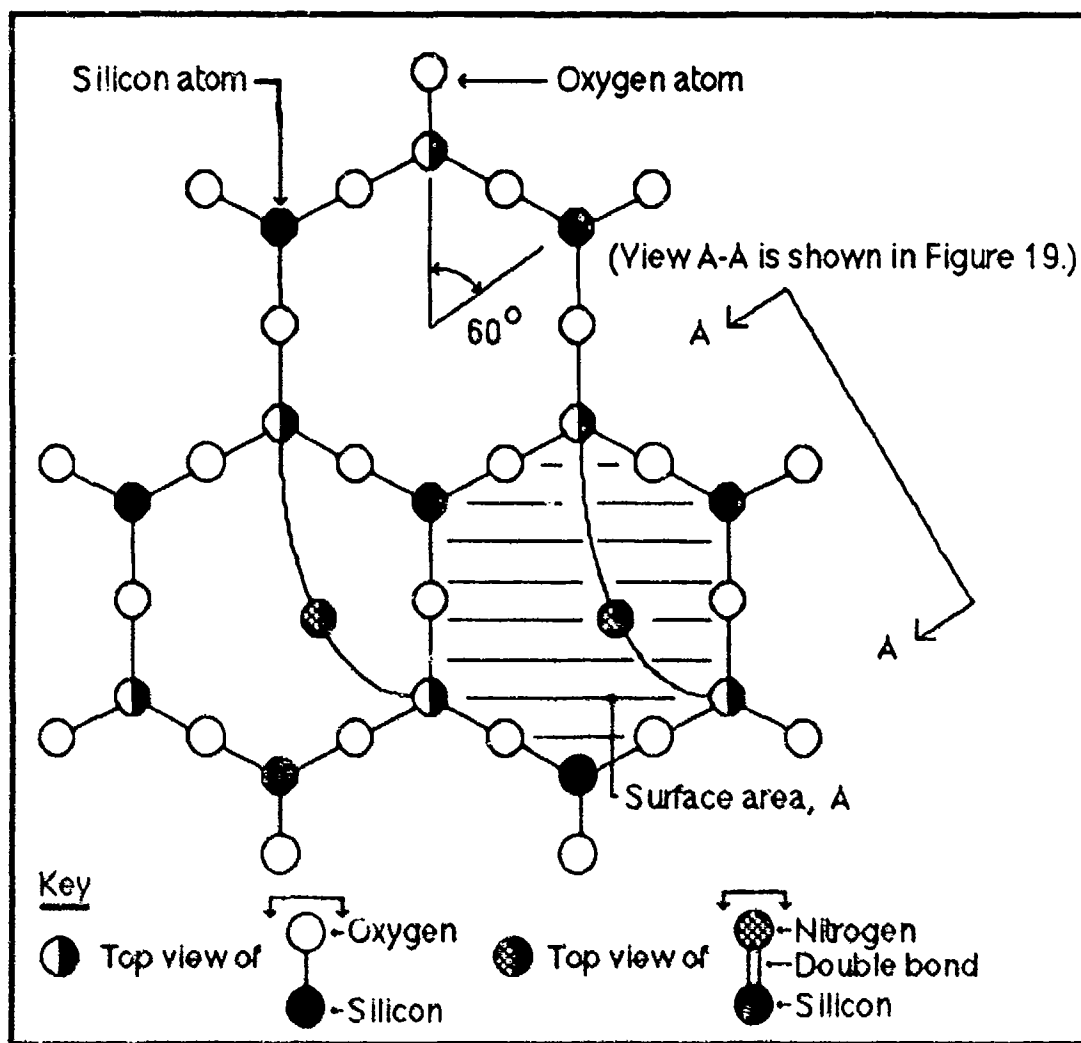


Figure 18. Top View of Quartz Surface.

chosen to depict the number of possible sites per unit area and the hexagonal region of the surface, A. Each site is

shown via the nitrogen atom ("checkerboard" pattern) doubly bonded to a silicon atom directly beneath the nitrogen atom, which in turn is bonded to the two oxygen atoms.

Figure 19 presents View A-A. For clarity, complete tetrahedra from the surface into the bulk were omitted. This view depicts a side view of the quartz configuration in order to identify the double bond, the associated atomic species, and the surface A, which was used for the subsequent surface area calculation. This value of area then enters as the denominator term in the expression for the number of sites per unit area.

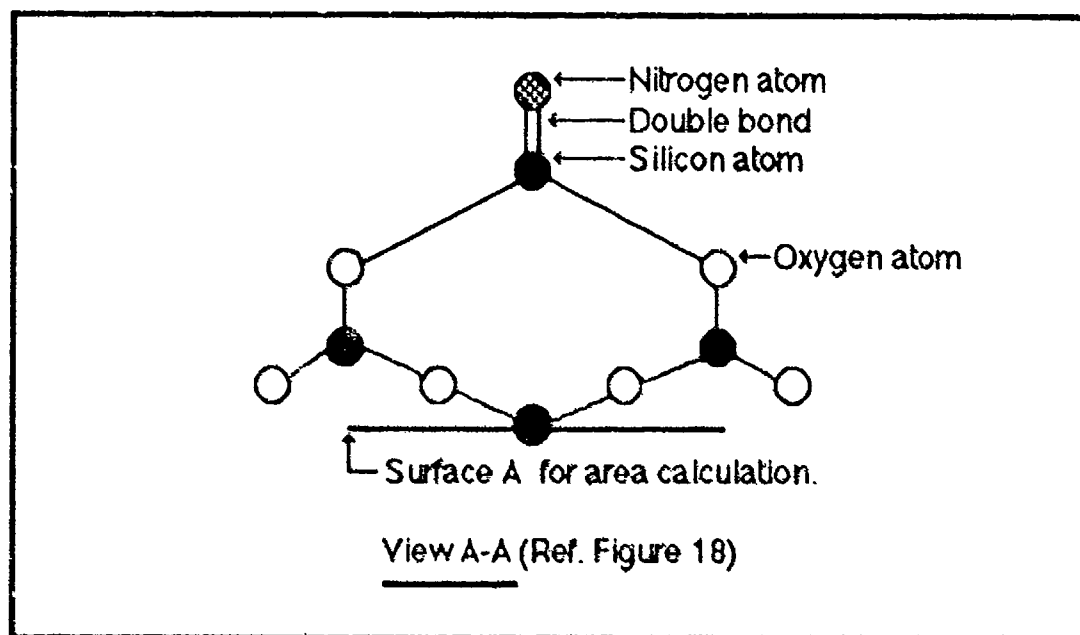


Figure 19. Side View of the Quartz Surface (View A-A).

The surface area to be calculated is that resulting from a projection onto a horizontal plane. An end view, corresponding to View A-A in Figures 18 and 19, shown in

Figure 20, provides the relative locations and displacements of the atoms as well as the projected plane of interest, denoted by A. Dimensions are from Sze (78:344).

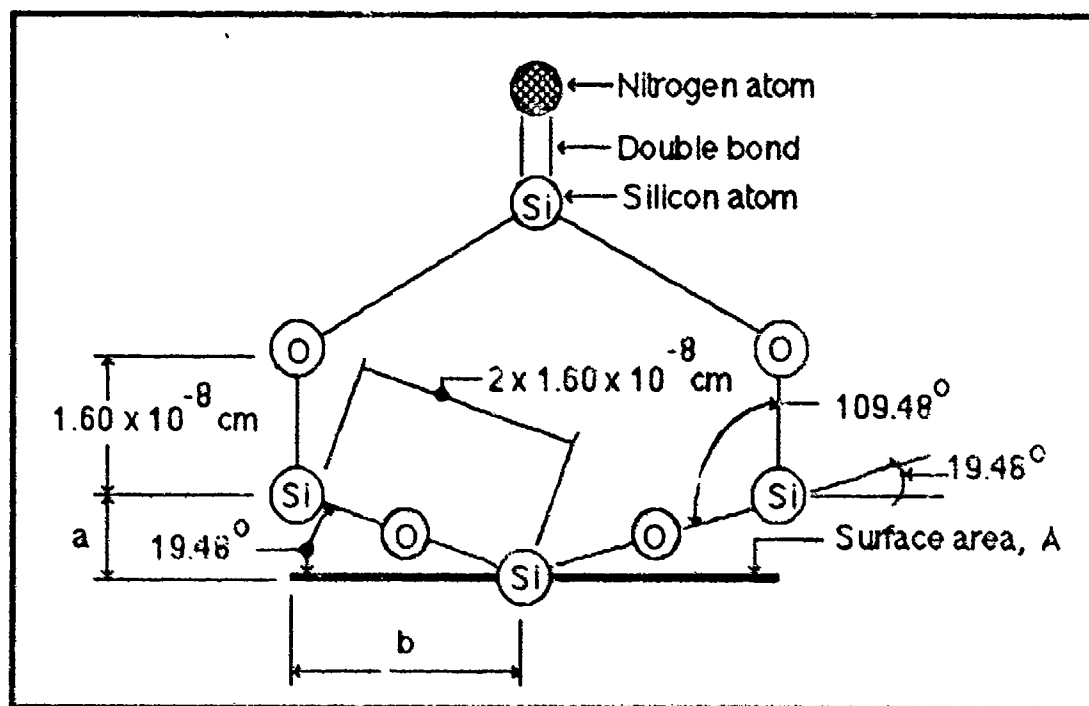


Figure 20. Calculation of the Surface Area, A.

The dimensions corresponding to "a" and "b" were calculated as follows:

$$\sin 19.48^\circ = \frac{a}{3.20 \times 10^{-8} \text{ cm}} \quad (76)$$

From which,

$$a = 1.07 \times 10^{-8} \text{ cm} \quad (77)$$

Similarly,

$$\cos 19.48^\circ = \frac{b}{3.20 \times 10^{-8} \text{ cm}} \quad (79)$$

Giving,

$$b = 3.02 \times 10^{-8} \text{ cm} \quad (79)$$

Figure 21 shows "b" as one side of a planar hexagon, from which the surface area can be calculated.

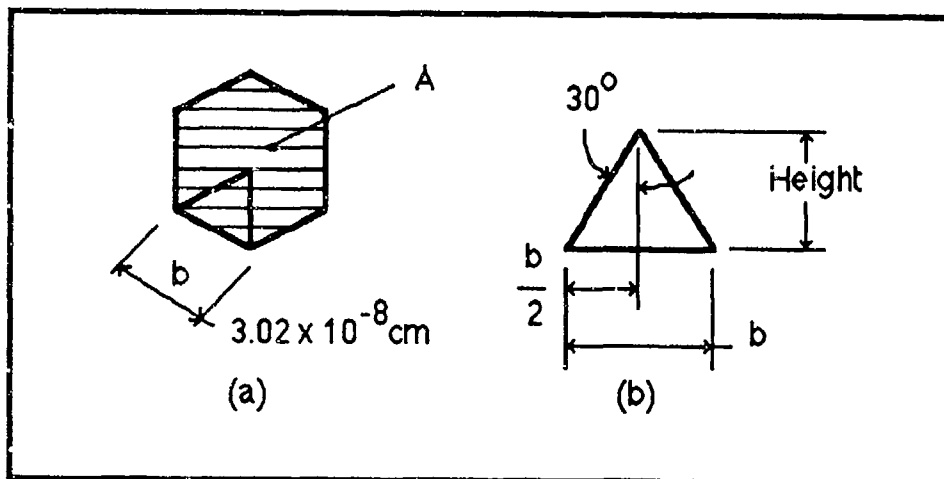


Figure 21. Dimensions Used to Determine the Surface Area, A.

The area of a regular hexagon can be given by six times the area of each equilateral triangle, as shown in Figure 21(a). The surface area of the hexagon is designated by A. That is,

$$A = 6 \times \frac{1}{2} \times \text{Base} \times \text{Height} \quad (80)$$

From the geometry associated with Figure 21(b)

$$\tan 30^\circ = \frac{3.02 \times 10^{-8}}{2} \times \text{Height} \quad (81)$$

Resulting in

$$\text{Height} = 2.61 \times 10^{-8} \text{ cm} \quad (82)$$

So that the surface area is

$$\begin{aligned} A &= 6 \times 0.5 \times 3.02 \times 10^{-8} \times 2.61 \times 10^{-8} \\ &= 2.36 \times 10^{-8} \text{ cm}^2 \end{aligned} \quad (83)$$

The solution to obtaining the number of sites per unit area is half complete at this point, since the surface area is known. The remaining term to determine is the number of possible sites per unit area.

Calculation of the Number of Surface Sites Per Unit Area

It was initially assumed that one bond site existed for each hexagon. However, stoichiometric considerations dictated otherwise. This fact is illustrated via the three-hexagon quartz configuration shown in Figure 18. The 3-hexagon pattern of Figure 18 was simplified to a schematic representation to aid visualization.

Figure 22 shows the configuration (in heavy black line) prior to being simplified to a corresponding schematic. The schematic is presented in Figure 23. Note that the simplification involved deleting the intermediate oxygen atoms and showing only the oxygen and silicon atoms at the vertices as reference points. (This deletion was accounted for in the calculations.)

Figure 23 gives the simplified version of the quartz configuration of Figure 22 in terms of a three-hexagon network.

Each open circle at alternate vertices corresponds exactly to an oxygen atom to which the active silicon atom bonds, in turn leading to the doubly bonded nitrogen atom, as shown in Figures 18 and 19, and View C-C (Fig. 23). The

O-Si-O bond provides the active silicon atom to which the nitrogen doubly bonds.

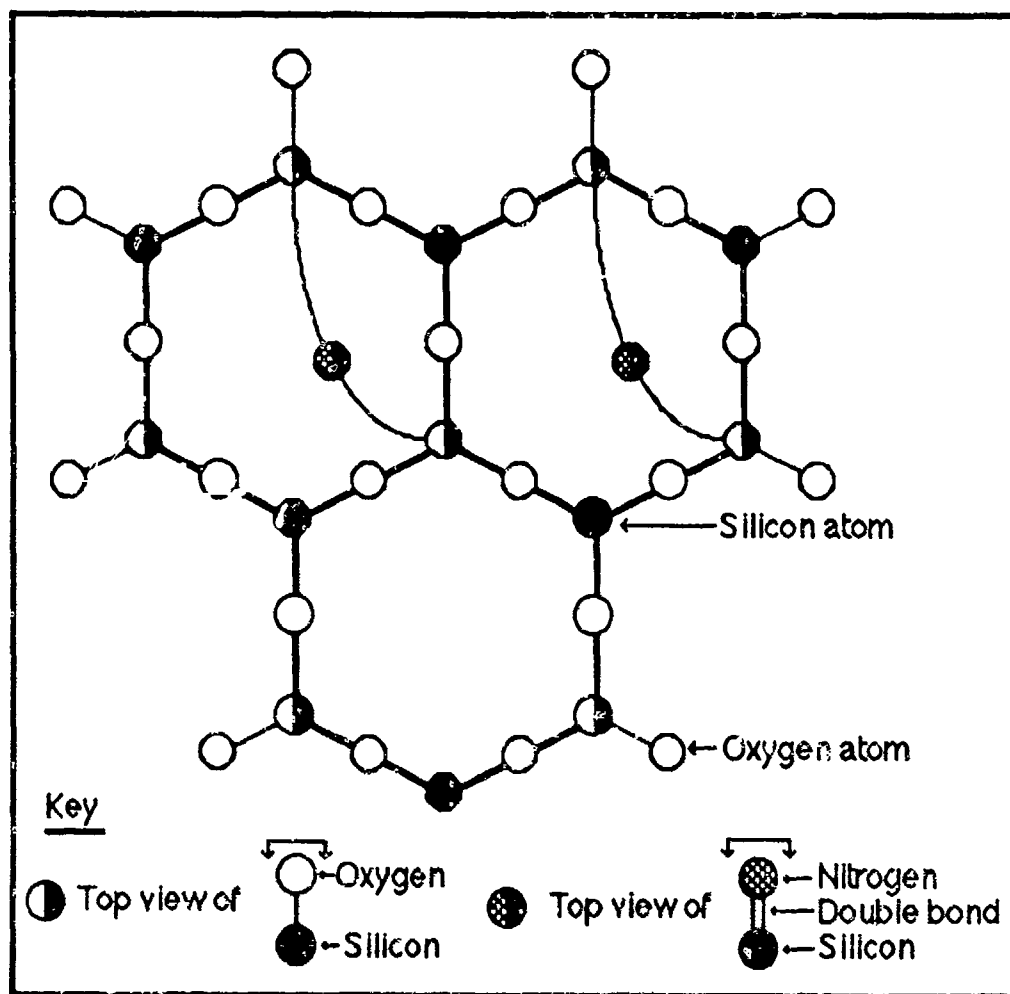


Figure 22. The Quartz Configuration Before Simplification.

Following the simplification to a schematic representation, the three-hexagon network was expanded to a larger hexagon pattern and connections to points were made to show the bond sites. Assuming the silicon atoms (Figure 23) bond at the surface in a random order, the connections were thus made arbitrarily.

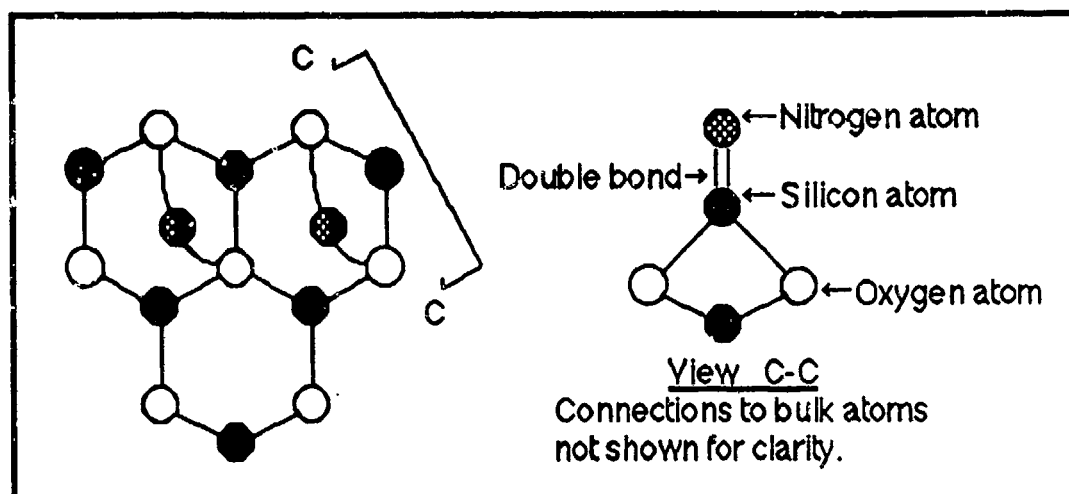


Figure 23. The Quartz Configuration After Simplification.

Since there are three oxygen atoms per hexagon to support an O-Si-O bond, once the O-Si-O bond is formed on one hexagon, then only one oxygen atom remains. This lone oxygen atom, however, is shared by adjacent hexagons, so an O-Si-O bond could form with this lone atom if the adjacent hexagons do not already have two of their available oxygen atoms bonded via O-Si-O. This latter bond could occur on the adjacent hexagon or over its neighbors. In any case, if the bond exists, the lone atom will remain unbonded. A larger hexagon network is shown in Figure 24 and illustrates this approach. This diagram shows a possible configuration of the double bond sides. Also shown in Figure 24 are the areas attributed to each oxygen atom which participates in the O-Si-O bond. These are shown via the hatched areas and can be thought of as primitive cells, which, by repeated translation, cover all space.

As shown in Figure 24, each participant oxygen atom is surrounded by three adjacent hexagons. Each adjacent hexagon thereby attributes one third of its area to each oxygen atom. Thus, each participant oxygen atom effectively occupies one hexagon and therefore, since there exists two oxygen atoms per O-Si-O bond, each bond site covers two hexagons, resulting in a bond:hexagon ratio of 1:2.

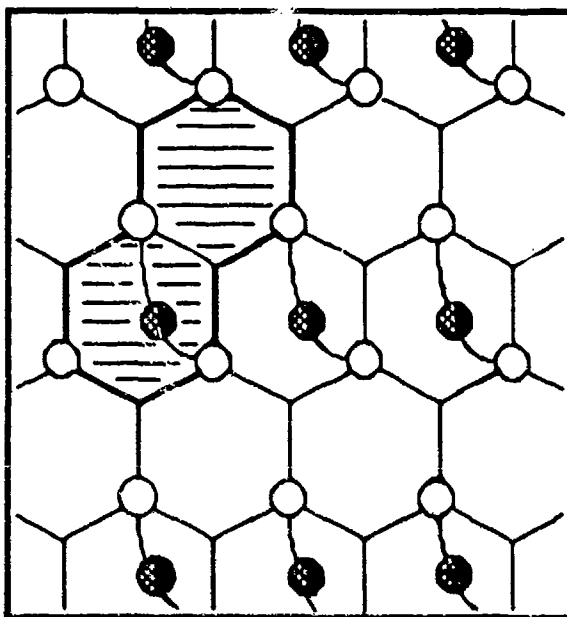


Figure 24. A Hexagon Pattern Used to Determine the Number of Sites.

Therefore, since one bond accommodates one active site, then there are 0.50 active sites per hexagon of area $2.36 \times 10^{-15} \text{ cm}^2$. In other words, using C_a to denote the number of surface sites per unit area,

$$C_a = \frac{0.50 \text{ sites}}{2.36 \times 10^{-15} \text{ cm}^2} = 2.12 \times 10^{14} \text{ sites per cm}^2 \quad (84)$$

Hence, in contrast to the estimated number of sites (i.e., $\sim 10^{15} \text{ cm}^{-2}$), the above calculation gives a value of 2.12×10^{14} sites per square cm, which is within one order of magnitude of the estimates and close to that in the bulk, $5 \times 10^{14} \text{ cm}^{-2}$ (72:50). In the following, the phase transitions of quartz are considered in the calculation of the number of surface sites.

Wells (82:786) provided the following Si-O bond distances for alpha-quartz, and alpha- and beta-cristobalite. (No bond distances were available for tridymite.)

Alpha-quartz:	Si-O bond distance = $1.61 \pm 0.03 \text{ \AA}$
Alpha-cristobalite	Si-O bond distance = 1.59 \AA
Beta-cristobalite	Si-O bond distance = 1.63 \AA

The number of possible sites was determined using two methods; both were assumed techniques as noted previously. The first was identical to the previous method except the bond distances of cristobalite were used. The second involved the densities of the quartz phases, since according to Wells (82:786), as the temperature increases, the quartz phase transitions yield more open structures. This could possibly mean a lower number of sites due to the openness or the direction of the structure. (With amorphous materials such as quartz, however, specific crystal directions are difficult to define, except over small regions of relative periodicity.)

In the first case, using Wells' Si-O bond distance in alpha-cristobalite, 1.59Å, the planar hexagonal surface area $A = 2.34 \times 10^{-15} \text{ cm}^2$. Next assuming the same fraction of bond sites per hexagon network, i.e., 0.50, the number of sites was found to be 2.14×10^{14} sites per square cm. Although this value is close to the previous case, it is greater which is in contradiction to the observed fact that tridymite and cristobalite have more "open" structures, leading to the supposition that the number of sites went as the density. Therefore, the number of sites was again calculated using the densities of quartz.

Thus, a ratio of the densities of tridymite to quartz is 2.3:2.7 or 0.8519. Multiplying this by 2.12×10^{14} sites per square cm yielded 1.80×10^{14} sites per square cm. Admittedly, these are rough calculations and yield crude approximations at best; only future experimental work will precisely determine the actual number of sites.

This section detailed the procedures used to quantify, rather than estimate, the number of active surface sites per unit area. The surface area of each hexagonal bonding arrangement, viewed along the $\langle 110 \rangle$ -direction, was calculated to be $2.36 \times 10^{-15} \text{ cm}^2$.

It was found that only a fraction, namely 0.50, of the surface could stoichiometrically accommodate the O-Si-O bond and an active surface site. Coupling these two values, the number of active surface sites was calculated

to be in the range of $1.80-2.12 \times 10^{14}$ sites per square cm. Since this value has influence in the rate equations, one must be willing to accept the fact that the densities and the structural transformations may play a much larger role in accounting for the number of sites and the observed discrepancies between various experimentalist's determinations of the recombination coefficient of nitrogen on quartz. Again, experimental work would go far in addressing this issue.

As stated in the introduction to this chapter, this range of values for the number of sites will be used as an input parameter to a software program to calculate the recombination coefficient as a function of temperature. These activities are discussed after the calculation of the remaining input parameters (pressure, activation energy, steric factor, and the dissociation energy).

Calculation of the Pressure

As shown in equation (38), the atomic nitrogen gas pressure governs the impingement rate, \dot{N} , of the nitrogen atoms on the surface, hence the need to obtain this value. However, the sources in the literature did not state the atomic nitrogen gas pressure, except Marshall (47:128), who gave a value of gas pressure <1 torr. Even in this case, it was not clear if this value was that of molecular or atomic nitrogen. Thus, the atomic nitrogen gas pressure was determined as outlined below.

In his experimental discussion, Marshall (51:84) gave the value of the number density of atomic nitrogen as $<5 \times 10^{13}$ atoms/cm³. Therefore, assuming ideal gas law behavior.

$$P_a V = NRT \quad (85)$$

where P_a = gas pressure, V = volume, N = number of particles, R = universal gas constant, and T = temperature, Kelvin. Upon rearranging equation (85), the pressure is

$$P_a = \frac{NRT}{V} \quad (86)$$

But, since the Boltzmann constant (k) is equal to the gas constant divided by Avogadro's number, and $\frac{N}{V} = n$ is the number density of particles (atoms), equation (86) can be cast in the more familiar form

$$P_a = nkT \quad (87)$$

Or,

$$P_a = n \frac{\text{atoms}}{\text{cm}^3} \times \frac{1 \text{ torr}}{1333.2 \frac{\text{gm}}{\text{cm sec}^3}} \times \frac{\text{gm cm}^2}{\text{sec}^2} \times \frac{1 \text{ erg}}{1 \times 10^{-7} \text{ J}} \times 1.38054 \times 10^{-23} \frac{\text{J}}{\text{K}} \times T \quad (88)$$

Resulting in an atomic gas pressure, as a function of temperature, of

$$P_a = 5.18 \times 10^{-6} \times T, \text{ torr} \quad (89)$$

For instance, at 300K, the atomic nitrogen gas pressure is

0.00155 torr and at 2000K, the atomic gas pressure is 0.01 torr.

Since Marshall (51) did not state whether the number density varied or if the atomic pressure varied, it was assumed that the atomic pressure increased as the temperature increased, for a constant number density. Hence, this value of pressure, as a function of the temperature, was used as another input parameter to the software program to calculate the recombination coefficient.

Calculation of the Activation Energy and Steric Factor

The recombination reaction is concerned with the rate at which the atoms in the gas phase recombine with those on the surface. For this reaction to proceed from the unreacted (i.e., gas) state to the reacted (i.e., recombined) state, the reactant atoms must have sufficient energy to overcome an activation energy barrier. This additional energy required above the average energy of the atoms is called the true activation energy, denoted by E_a , and is typically measured in joules per mole or calories per mole.

There is a distinction between the "true" activation energy and a so-called "apparent" activation energy; the true activation energy is that energy that must be supplied to the reacting species, by collisions or some other means, before reaction can occur. However, the apparent

activation energy is so termed because at the high temperature regimes, the added thermal energy serves to "trigger" other mechanisms by which the reaction can occur. This point is addressed later following Table 8. It should be clear from the temperature region whether the true or apparent activation energy is being discussed.

To determine the effect of temperature on chemical reaction rates, an equation was experimentally arrived at by Arrhenius, which also can be derived via kinetic theory and given as

$$\text{Rate of reaction} = C \exp \left[\frac{-E_a}{RT} \right] \quad (90)$$

where C = the rate constant, independent of temperature

E_a = the activation energy, joules (J)/mole or calories (cal)/mole.

R = the universal gas constant = 8.314 J/(mol-K) or 1.987 cal/(mol-K).

T = the temperature, Kelvin.

Hence, the Arrhenius equation (90) implies that the reaction rate among atoms or molecules in many cases depends on the number of reacting atoms or molecules that have activation energies of E_a or greater.

The Arrhenius rate law is usually rewritten in natural logarithmic form as

$$\ln \text{Rate} = \ln \text{Constant} - \frac{E_a}{RT} \quad (91)$$

Or, in the base ten form as

$$\text{Log Rate} = \text{Log Constant} - \frac{E_a}{2.303 RT} \quad (92)$$

Equation (92) was used in the subsequent calculations and took the form

$$\text{Log } \gamma = \text{Log } 2P - \frac{E_a}{2.303 RT} \quad (93)$$

which corresponds to equation (57) developed in Chapter II. (Recall from Chapter II that P is the steric factor which accounts for orientationa^l effects of the reacting species as well as other deviations from "ideal" collisional behavior.) Thus, a plot of $\text{Log } \gamma$ versus $1/T$ on log scale produces a straight line of slope $- E_a/(2.303R)$.

In the analysis, if a plot of experimental Log (reaction rate) versus $1/T$ data produces a straight line, the activation energy for the process of interest (that is, heterogeneous atomic recombination) can be calculated from the slope of the line. The Arrhenius equation (93) was used in the following to determine the activation energy (E_a) and steric factor (P).

Table 7 gives the values of the recombination coefficient versus temperature and $(\text{temperature})^{-1}$ from Marshall (51:90) and Breen and others (5:29). The data are presented in the order of increasing temperature. These sources were chosen because the surface used in their experiments was uncoated quartz. Moreover, both data sets

provide a range of empirical data from 300K to over 1300K, including an empirical maximum value for the recombination coefficient. Recall that at low temperatures, via equation (57), the recombination coefficient is independent of the impingement rate and depends mainly on the steric factor and activation energy.

As a prefatory note, since many values of the recombination coefficient exist at 300K (see Table 7), the

Table 7

Recombination Coefficient Versus Temperature

<u>Recombination Coefficient</u>	<u>Temperature(K)</u>	<u>(Temperature, K)⁻¹</u>	<u>Source</u>
0.00015	300	0.00334	(5:29)
0.00018	300	0.00334	(5:29)
0.00023	300	0.00334	(5:29)
0.00026	300	0.00334	(5:29)
0.00030	300	0.00334	(5:29)
0.00035	300	0.00334	(5:29)
0.00038	300	0.00334	(5:29)
0.00063	300	0.00334	(51:90)
0.00053	600	0.00167	(51:90)
0.00072	800	0.00125	(51:90)
0.00105	1000	0.00100	(51:90)
0.00150	1250	0.00080	(51:90)
0.01000	1000*	0.00100	(5:29)
0.01100	1123*	0.00089	(5:29)
0.01300 (Maximum)	1250*	0.00080	(5:29)
0.00600	1355*	0.00074	(5:29)

*Note: As specified in Chapter II, these values are those corresponding to an "apparent" temperature (5:24).

average value of these was taken to yield one value with which to evaluate the activation energy (E_a) and the steric factor (P). The average of the values at 300K resulted in

0.00031. Using this value at 300K, the approximate activation energy in the range 300-600K was found to be 640 cal/mole. Using equation (93), the associated steric factor in this range is 0.000453.

In the higher temperature region, say between 1000-1200K, the activation energy was approximately 4260 cal/mole. The associated steric factor is 0.00447, again via equation (93). These values are summarized in Table 8.

Table 8

Activation Energies and Steric Factors

<u>Temperature Range (K)</u>	<u>Activation Energy (cal/mole)</u>	<u>Steric Factor (Unitless)</u>	<u>Empirical Value of Activation Energy (cal/mole)</u>
300-600	640	0.000453	620±50 (9:201)
1000-1200	4260 *	0.00447	4600 (51:84)

*Note: The true activation energy is that energy that must be supplied to the reacting species, by collisions or some other means, before reaction can occur. Thus, the true activation energy for the recombination of nitrogen on silicon dioxide is 640 cal/mole for the entire temperature range 300-2000K. At the higher temperatures, say beyond 800K, the activation energy was -4260 cal/mole. However, at these higher temperatures, other factors such as the chemisorption term and thermal desorption term may begin to have an appreciable influence on the behavior of the recombination. These denominator terms appear in equation (52). Thus, the activation energy of 4260 cal/mole is what is usually termed in the literature as the "apparent" activation energy; i.e., "apparent," since other factors now influence the overall reaction.

Although the steric factor was determined above, after inputting these values into the routine, it was found that the curve did not match the data within reasonable limits. To obtain workable values, several iterations were

accomplished using different values for the steric factor. The resulting steric factors yielding a reasonable fit to the empirical data and therefore those used in this thesis are shown in Table 9. Note that the possibility of temperature dependence of the steric factor can be due to "added complexity of the surface" (34:42).

Table 9

Steric Factors

<u>Temperature Range(K)</u>	<u>Steric Factor</u>
300-900	0.000453
900-1000	0.0008
1000-2000	0.01

Determination of the Dissociation Energy

The dissociation energy, also known as the well-depth, is a measure of the strength of the well in terms of binding the particle. The dissociation energy of nitrogen in the silicon nitride, silicon oxynitride, or the more general form $\text{Si}_x\text{O}_y\text{N}_z$ molecule is not available from the literature.

However, the dissociation energy (D) of SiN is listed by several sources (11:279; 78:45) as approximately 105 kcal/mole. Furthermore, the fact whether a single, double, or triple bond forms between the nitrogen atom and the silicon atom is not known. Hu(33:695), in a paper on the properties of amorphous silicon nitride, observed sharp peaks in the infrared spectrum of silicon nitride films and

stated that the peaks were probably due to triply bonded $\text{Si} \equiv \text{N}$, but provided no definition of the triple bond. The issue here is whether the nitrogen atom can form double bonds to the silicon atom.

According to Pauling (62:343-345), the following oxynitrides are doubly bonded: nitric oxide (NO); dinitrogen dioxide (N_2O_2); nitrogen dioxide (NO_2); nitrosylfluoride (ONF), nitrosyl chloride (ONCl), and nitrosylbromide (ONBr); and nitrosyl-metal complexes such as nitrosyl iron ($\text{Fe}(\text{NO})_3\text{Cl}$), in which the nitrogen is doubly bonded to the iron atom. Although no information is available for nitrogen double bonding to silicon, from the preceding, it is clear that nitrogen can form double bonds to other species, gaseous as well as metallic. Now, from the electronic configurations of nitrogen and silicon, Lewis structures (19:62) can be formed. As presented in Figure 25, the Lewis structure for $\text{Si}_x\text{O}_y\text{N}_z$ clearly shows

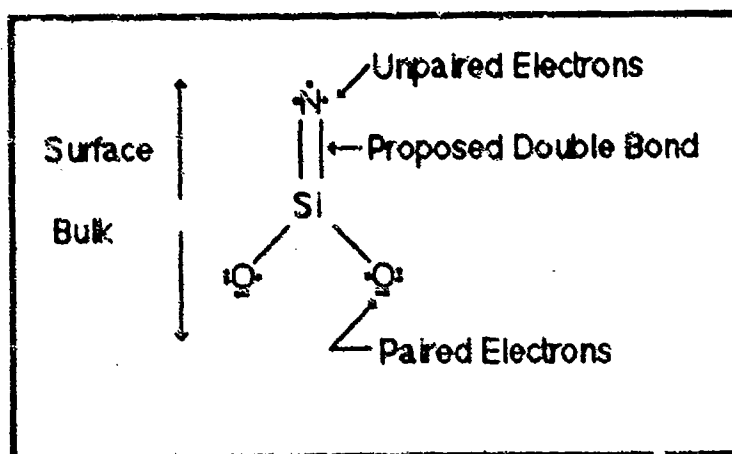


Figure 25. A Lewis Structure for the $\text{Si}_x\text{O}_y\text{N}_z$ Molecule.

the proposed double bond of the nitrogen atom to the surface silicon atom.

According to Wells, "Any atom in which there are unpaired electrons possesses a permanent magnetic moment and exhibits paramagnetism" (82:242). As depicted in Figure 25, the unpaired electrons of nitrogen may contribute to the magnetic character of the molecule and so, if the $\text{Si}_x\text{O}_y\text{N}_z$ molecule is experimentally shown to be paramagnetic, then the Lewis structure in Figure 25 depicting the doubly bonded nitrogen is feasible. To date, no data have shown whether or not the $\text{Si}_x\text{O}_y\text{N}_z$ molecule is paramagnetic. Moreover, Marshall (48:743), Green (20:576-577), and others have observed that nitrified quartz surfaces possess highly reactive atomic nitrogen. The unpaired electrons for the nitrogen atom (Figure 25) could be a possible explanation of this phenomenon. Future experiments are thus needed to determine the order, strength, and stoichiometric composition of the $\text{Si}_x\text{O}_y\text{N}_z$ bond at the surface.

Now, assuming that the nitrogen atoms are doubly bound to the surface matrix, and following an approach similar to Seward (72:44), then with $D(\text{SiN}) = 105$ kcal/mole, the double bond strength is roughly $(105/2) \times 1.5 = 78.75$ kcal/mole = $D(\text{Si=N})$. A similar "semi-empirical scheme" was given by Hirschfelder (31:645) for approximating the activation energy (E_a) in terms of the dissociation energy (D) as

$$E_a = 0.055 D \quad (94)$$

It is important to realize that Hirschfelder's rule in equation (94) is by no means a definitive relation. However, it can be used to obtain the order of magnitude of the activation or dissociation energy, say 100 kcal/mole as opposed to 1000 kcal/mole. Thus, the order of magnitude of the dissociation energy can be obtained via

$$D = \frac{E_a}{0.055} \quad (95)$$

Inserting the value of $E_a = 0.640$ kcal/mole into equation (95) resulted in a dissociation energy of 11.65 kcal/mole.

Thus, the dissociation energy of nitrogen in the nitrated silicon dioxide surface, lacking of quantitative, experimental data indicating otherwise, appears to be -12 - 78 kcal/mole. These values were substituted into the computer routine to see their impact on the plot of the recombination coefficient versus the empirical data points. As will be shown in Chapter IV, a dissociation energy of 79 kcal/mole provided an excellent match to the empirical data. This value was used for the dissociation energy.

Values Selected for the Initial Sticking Coefficient

The sticking probability, S , also termed the sticking coefficient, is the ratio of the rate of adsorption of a gas to the rate of collision with the surface, i.e., the number of atoms that stick to the surface out of the total

number that strike the surface. The value of the sticking coefficient as the surface coverage approaches zero is termed the initial sticking coefficient, S_0 .

Since no value for the initial sticking coefficient of atomic nitrogen on quartz was available in the literature, as pointed out in Chapter I the assumption was made that the initial sticking coefficient for nitrogen on silicon dioxide behaved in a similar manner as that for oxygen on silicon dioxide (72:50). Thus, the initial sticking coefficient took the form, $B \times \exp(-0.002 \times T)$, where B is a constant and T is the temperature (K). Specifically, the initial sticking coefficient used was

$$S_0 = 0.95 \exp (-0.002 \times T) \quad (96)$$

where T is the temperature in Kelvin. The pre-exponential value of 0.95 was selected since this yielded a plot of the recombination coefficient whose maximum value coincided with that of the source data. For example, any values less than 0.95 gave the maximum recombination coefficient as much less than the source data.

The input parameters used to calculate the recombination of nitrogen on silicon dioxide are summarized in Table 10.

Having determined the necessary input parameters to the code, the program was written based on the rate equations and input parameters and executed. The program was written in Fortran 77 on a Macintosh Plus, using the MicrosoftTM

Table 10

Input Parameters to Calculate the Recombination Coefficient

Activation Energy	= 0.640 kcal/mole
Pressure	= 0.00155 to 0.01 torr
Initial Sticking Coefficient	= $0.95 \times \exp(-0.002 \times T)$
Number of Surface Sites	= $2.12 \times 10^{14} \text{ cm}^{-2}$ ($T \leq 900\text{K}$) $1.80 \times 10^{14} \text{ cm}^{-2}$ ($T > 900\text{K}$)
Steric Factor	= See above, Table 9.
Dissociation Energy	= 79 kcal/mole

Fortran 77 compiler and is presented in Appendix A.

Referring to Appendix A, the steric factors are "imbedded" in a series of "if" statements. This was accomplished for the sole purpose of providing a smooth transition between temperature break-points, rather than sharp discontinuities at these break-points.

Summary

This chapter presented the calculations and accompanying discussion regarding the kinetic parameters for nitrogen recombination on silicon dioxide. The parameters, some of which were obtained by analysis of the empirical data, included the number of surface sites, activation and dissociation energies, the atomic gas pressure, the initial sticking coefficient, and the steric factor. Having these as input variables to the program (Appendix A) to determine the recombination coefficient of

atomic nitrogen on silicon dioxide, it remains to show whether the calculated values of the recombination coefficient match those determined experimentally.

IV. Results and Discussion

Introduction

The activities thus far in this research effort have been to develop a mechanism for nitrogen recombination on a silicon dioxide surface, obtain empirical recombination data, generate the associated rate equations, and to assume or calculate the kinetic rate parameters such as activation and dissociation energies, steric factor, and pressure of the atomic nitrogen. These activities, along with a computer routine (Appendix A) based on the rate equations and parameters were dealt with in the preceding chapters. The ongoing objective, as a result of these activities, was to determine whether or not the data set generated by the routine matched that in the literature.

The topic in this chapter is to present the results of the research effort as well as to interpret the results through discussion. It will be shown that a reasonable match exists between the empirical data and the results of the model.

The presentation will follow a pattern of showing the results in graphic form, followed by the numerical data in tabular format, and closing with the discussion. The topics to be addressed are as follows:

- a. The recombination coefficient of nitrogen on silicon dioxide as a function of temperature for a dissociation energy of 79 kcal/mole.
- b. The effect of varying the dissociation energy on the recombination reaction.
- c. The sorption rates of nitrogen on silicon dioxide.
- d. The effect of certain terms, such as the chemisorption rate, on the recombination reaction.
- e. The effect of varying the sticking coefficient on the recombination reaction.
- f. The effect of holding the pressure constant as opposed to allowing the pressure to be a function of the temperature.
- g. The fractional surface coverage of nitrogen on silicon dioxide. In this particular section, the fractional surface coverage of oxygen will be compared to that of nitrogen.

The Recombination Coefficient of Nitrogen on Silicon Dioxide

The empirical data and the resulting plot of the calculated recombination coefficient, γ as a function of temperature and for a dissociation energy of 79 kcal/mole is shown below in Figure 26.

The computer routine calculated the values of the recombination coefficient which are shown in Table 11. To facilitate the presentation, the symbology "0.309E-03"

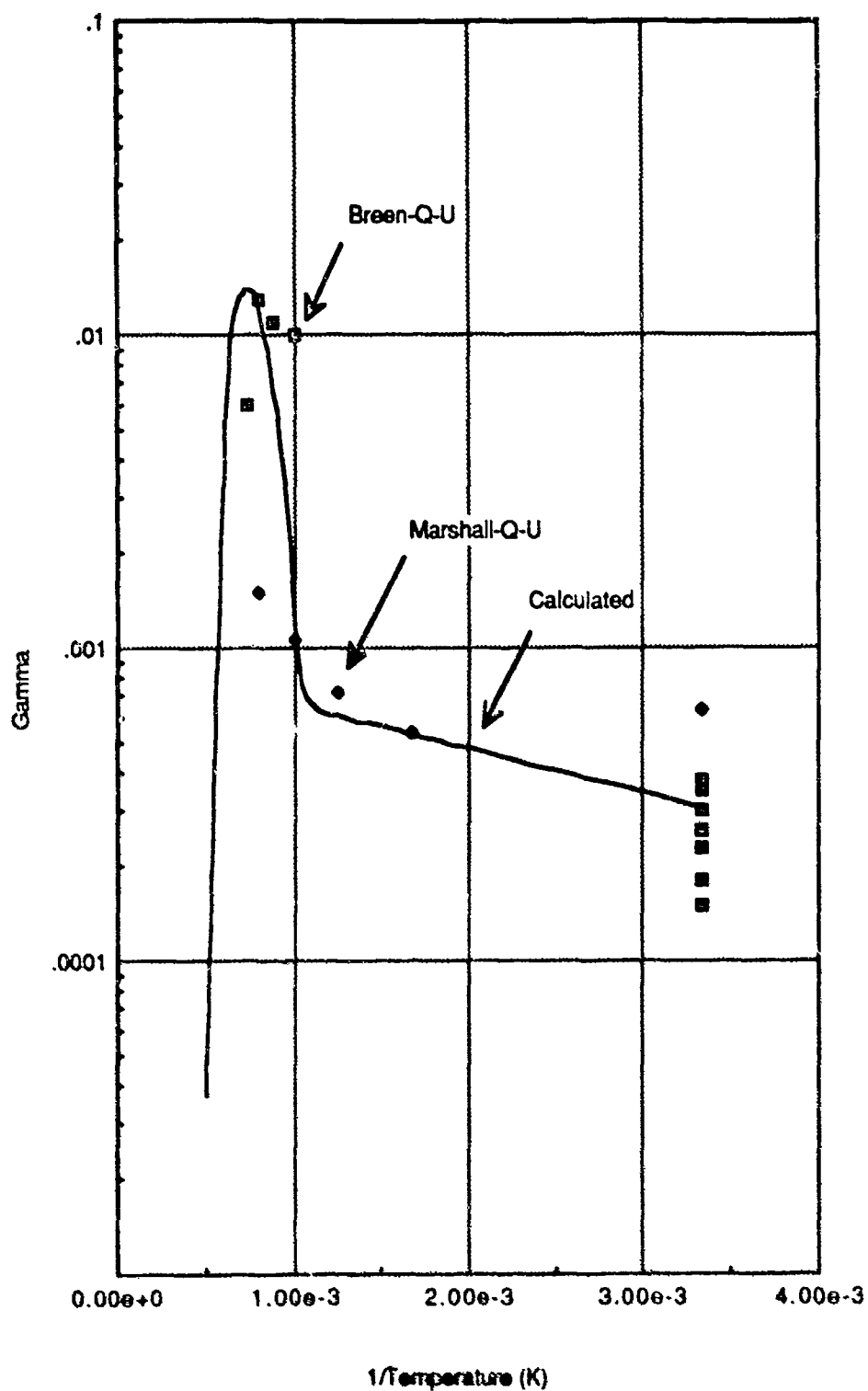


Figure 26. The Recombination Coefficient of Nitrogen on Silicon Dioxide as a Function of Temperature and a Dissociation Energy of 79 Kcal/Mole.

represents 0.309×10^{-3} in all of the tables to follow. The maximum value of the recombination coefficient is 0.014. Comparison with the maximum value provided by Breen and others (5:29) of 0.013 at 1250K, Table 7 (Chapter III) shows a close match.

Table 11

Calculated Values of the Recombination Coefficient,
Gamma, for a Dissociation Energy of 79 Kcal/Mole

<u>Temperature(K)</u>	<u>(Temperature, K)⁻¹</u>	<u>Gamma</u>
300	0.00334	0.310E-03
400	0.00250	0.405E-03
500	0.00200	0.475E-03
600	0.00167	0.529E-03
700	0.00143	0.571E-03
800	0.00125	0.605E-03
900	0.00111	0.632E-03
1000	0.00100	0.115E-02
1100	0.00091	0.562E-02
1200	0.00083	0.999E-01
1300	0.00077	0.140E-01
1400	0.00071	0.137E-01
1500	0.00067	0.118E-01
1600	0.00063	0.656E-02
1700	0.00059	0.201E-02
1800	0.00055	0.500E-03
1900	0.00053	0.130E-03
2000	0.00050	0.369E-04

Figure 27, below, illustrates the effect of changing the dissociation energy (D) to a larger value of 105 kcal/mole. The plot for the recombination coefficient at D = 105 kcal/mole was superimposed on that of Figure 26 (D = 79 kcal/mole). As shown, the two calculated values of the recombination coefficient are identical up to about 1300K,

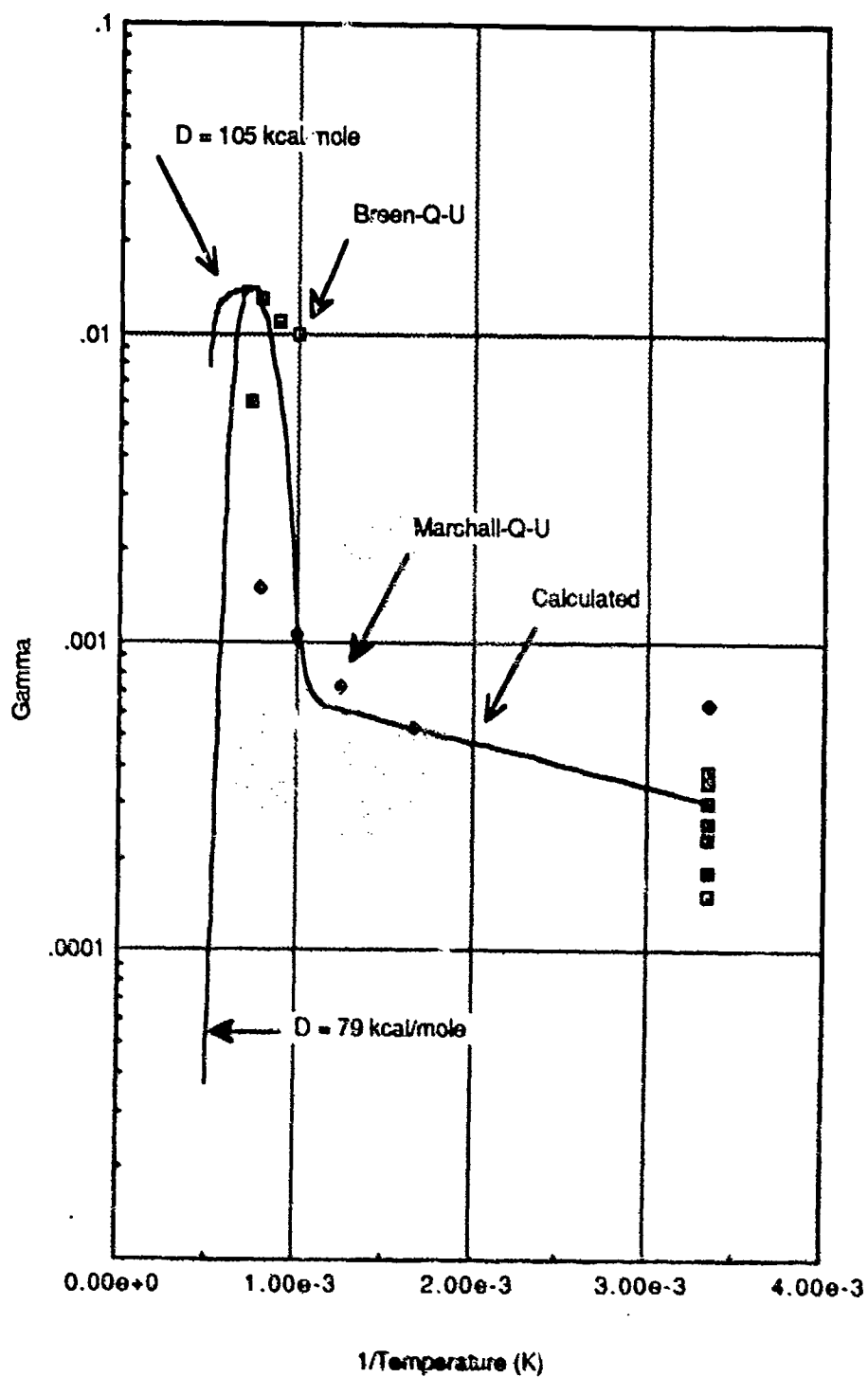


Figure 27. The Recombination Coefficient as a Function of Temperature for Dissociation Energies of 79 and 105 Kcal/Mole.

at which point, due to the larger dissociation energy, the recombination coefficient for $D = 105$ kcal/mole is greater than that for $D = 79$ kcal/mole from 1300-2000K since the atoms are more tightly bound in their positions.

The computer routine calculated the values of the recombination coefficient, γ , for a dissociation energy of 105 kcal/mole are shown in Table 12. The maximum value of the recombination coefficient is 0.0141, essentially the same as that for a dissociation energy of 79 kcal/mole. Comparison with the maximum value provided by Breen and others (5:29) of 0.013 at 1250K, Table 7 (Chapter III) again shows a close match.

Table 12

Calculated Values of the Recombination Coefficient, Gamma, for a Dissociation Energy of 105 Kcal/Mole

<u>Temperature(K)</u>	<u>(Temperature, K)⁻¹</u>	<u>Gamma</u>
300	0.00334	0.310E-03
400	0.00250	0.405E-03
500	0.00200	0.475E-03
600	0.00167	0.529E-03
700	0.00143	0.571E-03
800	0.00125	0.605E-03
900	0.00111	0.632E-03
1000	0.00100	0.115E-02
1100	0.00091	0.562E-02
1200	0.00083	0.999E-02
1300	0.00077	0.141E-01
1400	0.00071	0.140E-01
1500	0.00067	0.138E-01
1600	0.00063	0.135E-01
1700	0.00059	0.131E-01
1800	0.00055	0.124E-01
1900	0.00053	0.110E-01
2000	0.00050	0.792E-02

Comparing the plotted empirical data and the calculated values of the recombination coefficient of either Figure 26 or Figure 27 shows a close match between the empirical and calculated values. Regardless of the dissociation energy, both plots exhibit the same behavior from 300-2000K; beginning from the low temperature regime, transitioning through the intermediate regimes, obtaining a maximum value of the recombination coefficient, and finally decreasing as temperature increases.

From the calculated values of γ shown accompanying each figure (Tables 11 and 12), the recombination coefficients are equal up to and including about 1200K and at 1300K the maxima are reached: $\gamma_{\max}(\text{for } D = 79 \text{ kcal/mole}) = 0.0140$; $\gamma_{\max}(\text{for } D = 105 \text{ kcal/mole}) = 0.0141$. The gas kinetics can account for the recombination coefficient obtaining a maximum value in that at the high temperatures the increased thermal energy goes to increase the apparent activation energy, thereby increasing the surface recombination reaction. At the same time, however, more particles are thermally desorbing due to the higher temperatures and thus the surface concentration decreases. Taken in tandem, the increasing surface reaction coupled with the necessarily decreasing surface coverage yield the observed maximum value for the recombination coefficient. As the temperature continues to increase, more particles

thermally desorb and thus declines since there are very few particles on the surface with which to recombine.

Although the curves for the recombination coefficient are similar in overall behavior, they do show dissimilarity after about 1300K. This is mainly due to the value of the dissociation energy, or well-depth. For the lower value of the well-depth, 79 kcal/mole, the atoms are less tightly bound within the well. Now, as an incoming gas phase atom strikes and recombines with a surface atom, the mechanical energy of the collision, coupled with the thermal energy in the system, provide some of the recombined species with sufficient energy to surmount the energy barrier and desorb as a molecule.

On the other hand, for a larger well-depth, the well-bound particles have a larger potential barrier to overcome and thus more energy is required before desorption can occur. Since the particles remain on the surface longer, the fractional surface concentration and recombination coefficient are larger over a broader range of temperature than that for a smaller value of the well-depth. This was illustrated in Figure 27. For example, as will be shown in a later section, the fractional surface concentrations at 2000K are 0.00217 atoms per square cm and 0.465 atoms per square cm for $D = 79$ and 105 kcal/mole, respectively. The recombination coefficients at 2000K are 0.0000369 and 0.00792 for $D = 79$ and 105 kcal/mole, respectively.

The main application of nitrogen recombination on silicon dioxide was stated in Chapter I and centers on the Space Shuttle as well as other earth orbiting reentry vehicles. Specifically, since the external skin of these crafts consists of silica based tiles and the launch and reentry conditions expose the tiles to atmospheric gases such as nitrogen, it is of interest to consider more closely the reaction of atomic nitrogen on the surface of the Shuttle.

Since a fraction of the atmospheric nitrogen molecules dissociate and recombine on certain areas of the Shuttle's surface, then an issue to examine is the energetic state(s) of the newly formed molecules following recombination. Specifically, do the new species leave in a highly activated state? What percentage are activated? Hence, how is the energy partitioned among the various states? How much of the exothermic heat is removed via the desorbed molecules? How exothermic is the recombination of atomic nitrogen on the silica tile? Moreover, if there is a significant percentage that adsorb and are in an activated state, is there a mechanism by which this additional energy can be utilized?

If we consider atomic nitrogen recombination in a more general sense on silicon dioxide rather than as an application to the tiles, Figures 26 and 27 illustrated the effect of the dissociation energy on the recombination. In

addition, to gain the best possible explanation of the recombination reaction and the mechanism of recombining, efforts should begin to determine the bond between nitrogen and silicon at a surface (i.e., is the Si-N bond a single, double, or triple bond?) Furthermore, what is the bond strength, % ionic character, or % covalent character? Does the newly recombined species exhibit paramagnetism? Answers to these last questions would provide information applicable to determining the electronic state of the recombined species at the surface and possibly shed some light on the near-surface layer in the bulk of the sample.

From Marshall's empirical data (51:84) plotted in Figure 26, γ is 0.00063 at 300K, 0.00053 at 600K, 0.00072 at 800K, 0.00105 at 1000K, and 0.0015 at 1200K. The decrease in γ at 600K raises some questions, since one usually sees γ behaving uniformly over a given temperature range. One possible explanation is that it is due to the alpha-quartz preparing to undergo its transition to beta-quartz and thereby severely decreasing the number of available surface sites. Recall that the transition occurs at 848K. Contaminants could also be responsible, even though in his report, Marshall stated the surface was clean (51). In this same vein, what are the effects of coatings or contaminants on silicon dioxide in the temperature range 300-2000K?

The Sorption Rates of Nitrogen on Silicon Dioxide

The resulting plot of the calculated sorption terms for a dissociation energy of 79 kcal/mole is shown below in Figure 28. Each term is discussed below.

The computer routine calculated the values of the sorption rates, which are presented below in Table 13.

Table 13

Calculated Values of the Sorption Rates for a Dissociation Energy of 79 Kcal/Mole

<u>Temperature(K)</u>	<u>Adsorption Rate</u>	<u>Thermal Desorption Rate</u>	<u>Recombination Desorption Rate</u>
300	0.130E+15	0.000E+00	0.130E+15
400	0.197E+15	0.000E+00	0.197E+15
500	0.258E+15	0.636E-07	0.258E+15
600	0.315E+15	0.436E-01	0.315E+15
700	0.367E+15	0.657E+03	0.367E+15
800	0.416E+15	0.911E+06	0.416E+15
900	0.461E+15	0.256E+09	0.461E+15
1000	0.887E+15	0.201E+11	0.887E+15
1100	0.453E+16	0.802E+12	0.453E+16
1200	0.843E+16	0.172E+14	0.841E+16
1300	0.125E+17	0.228E+15	0.123E+17
1400	0.145E+17	0.209E+16	0.125E+17
1500	0.238E+17	0.127E+17	0.111E+17
1600	0.451E+17	0.387E+17	0.638E+16
1700	0.558E+17	0.538E+17	0.202E+16
1800	0.520E+17	0.514E+17	0.516E+15
1900	0.447E+17	0.446E+17	0.137E+15
2000	0.378E+17	0.377E+17	0.401E+14

The resulting plot of the calculated sorption rates for a dissociation energy of 105 kcal/mole is shown below in Figure 29.

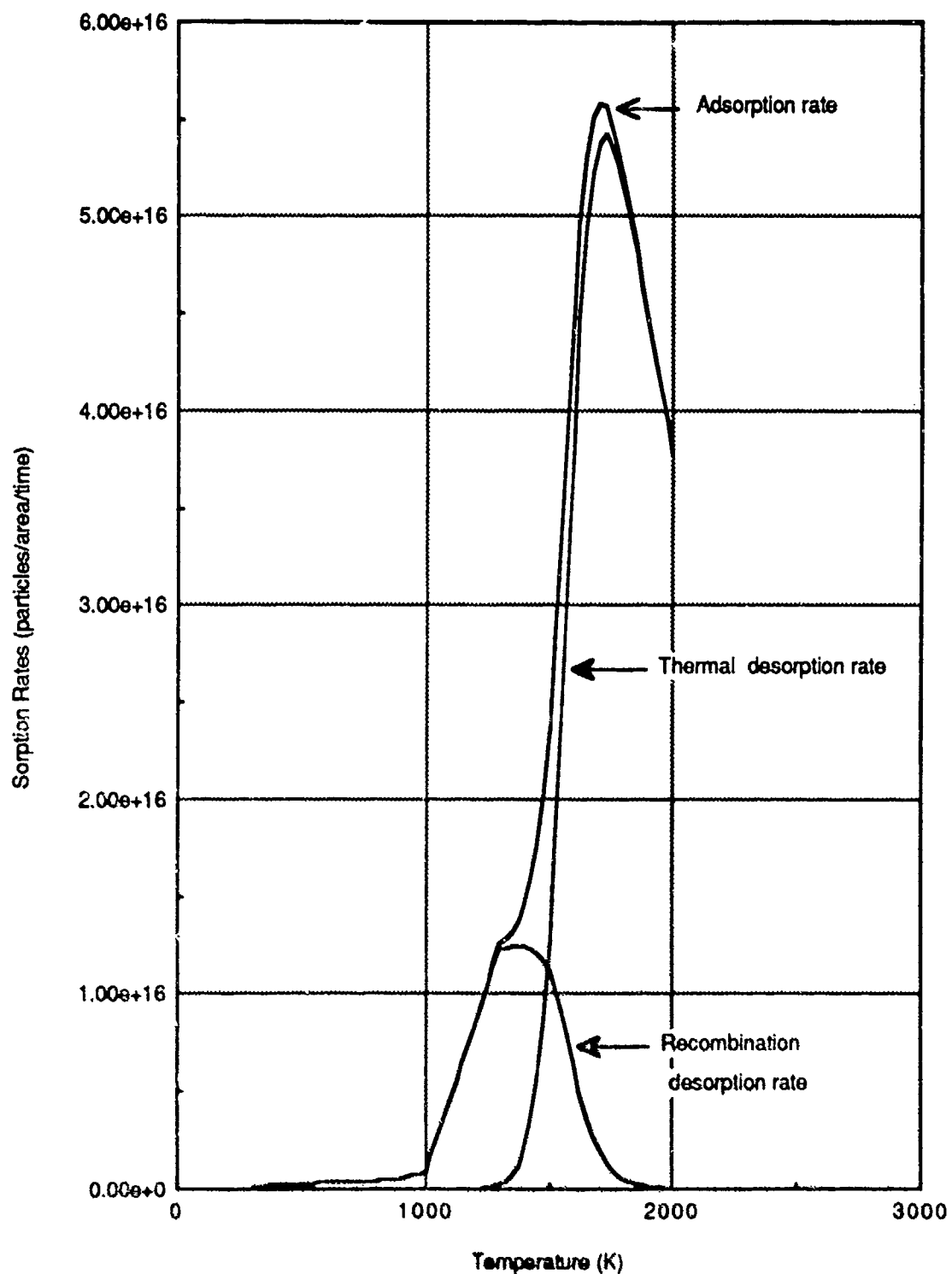


Figure 28. The Sorption Rates vs. Temperature for Nitrogen on Silicon Dioxide at a Dissociation Energy of 79 Kcal/Mole.

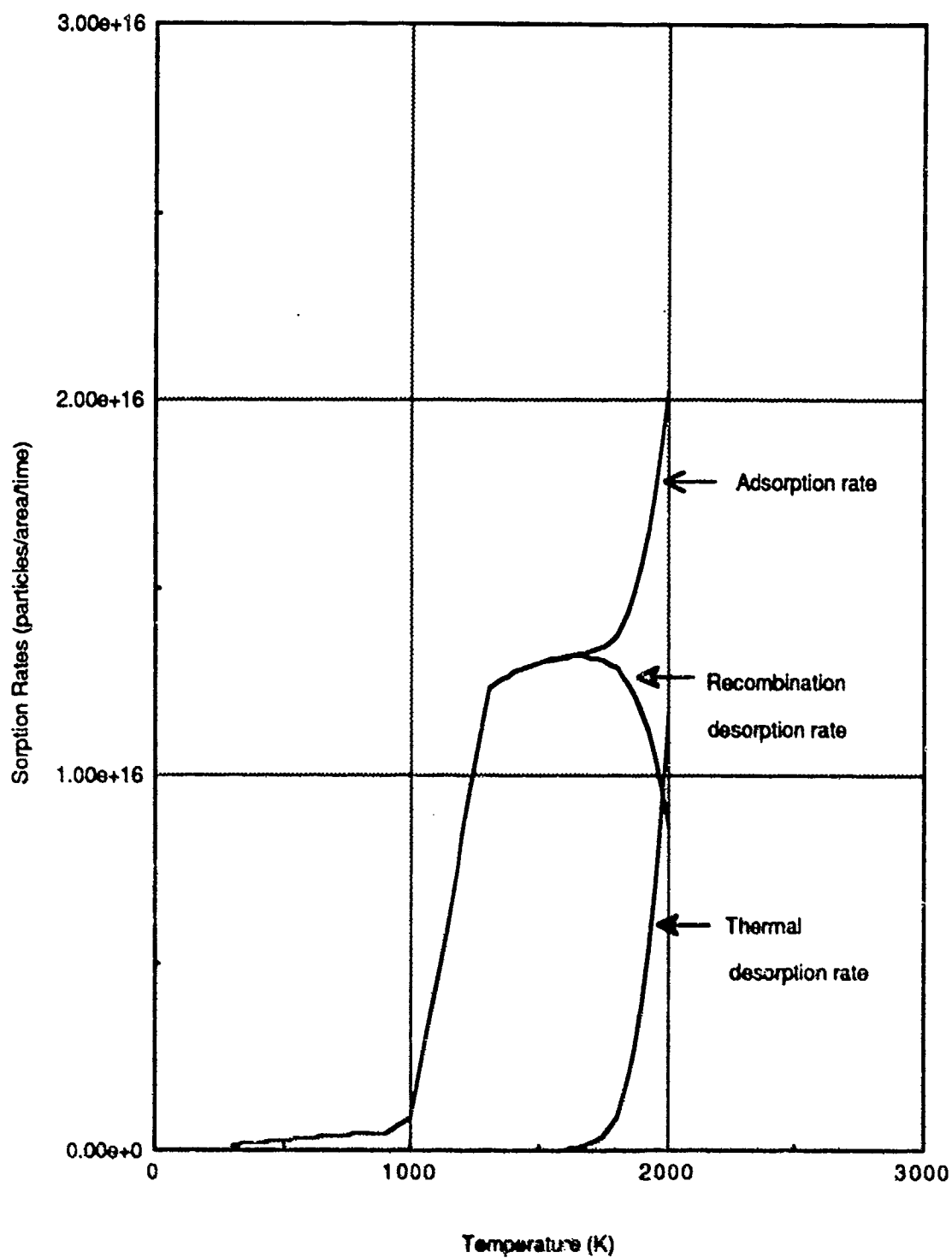


Figure 29. The Sorption Rates vs. Temperature for Nitrogen on Silicon Dioxide at a Dissociation Energy of 105 Kcal/Mole.

The computer routine calculated the values of the sorption rates, which are presented below in Table 14.

Table 14

Calculated Values of the Sorption Rates for a Dissociation Energy of 105 Kcal/Mole

<u>Temperature(K)</u>	<u>Adsorption Rate</u>	<u>Thermal Desorption Rate</u>	<u>Recombination Desorption Rate</u>
300	0.130E+15	0.000E+00	0.130E+15
400	0.197E+15	0.000E+00	0.197E+15
500	0.258E+15	0.000E+00	0.258E+15
600	0.315E+15	0.000E+00	0.315E+15
700	0.367E+15	0.499E-05	0.367E+15
800	0.416E+15	0.716E-01	0.416E+15
900	0.461E+15	0.124E+03	0.461E+15
1000	0.887E+15	0.416E+05	0.887E+15
1100	0.453E+16	0.546E+07	0.453E+16
1200	0.841E+16	0.316E+09	0.841E+16
1300	0.123E+17	0.969E+10	0.123E+17
1400	0.127E+17	0.186E+12	0.127E+17
1500	0.129E+17	0.239E+13	0.129E+17
1600	0.132E+17	0.224E+14	0.131E+17
1700	0.133E+17	0.159E+15	0.131E+17
1800	0.137E+17	0.889E+15	0.128E+17
1900	0.156E+17	0.387E+16	0.117E+17
2000	0.203E+17	0.116E+17	0.861E+16

The three sorption rates affect the kinetics of the reaction, depending on the relative magnitude of each rate. These rates were discussed in Chapter II and are briefly discussed below to facilitate the presentation.

The adsorption rate is given by the following expression:

$$\text{Adsorption rate} = \text{Initial sticking coefficient } (S_0) \times \text{Impingement rate } (N) \times \text{Fraction of surface that is bare of atoms } (1 - \theta).$$

(97)

The thermal desorption rate is given by:

$$\begin{aligned} \text{Thermal desorption rate} &= \text{Thermal desorption rate} \\ &\text{per unit area } (\delta) \times \text{Fractional surface} \\ &\text{concentration } (\theta) \end{aligned} \quad (98)$$

As the temperature increases from 300K, thermal energy is supplied to the system. The surface atoms, acting as simple harmonic oscillators, respond to this increase in energy through an increase in the vibrations about their equilibrium positions. As thermal energy continues to be supplied, a point will occur, however, where the vibrations become strong enough and the atoms begin to desorb. This is known as thermal desorption.

$$\begin{aligned} \text{The Recombination desorption rate is given by:} \\ \text{Recombination desorption rate} &= \text{Steric factor } (P) \times \\ &\text{Impingement rate } (N) \times \text{Fractional surface concentration} \\ &(\theta) \times \text{Fraction of collisions with enough energy to} \\ &\text{react} \end{aligned} \quad (99)$$

The recombination desorption rate is simply the number of atoms that are recombining via Langmuir-Rideal and desorbing as a molecule.

Referring to Figure 28, the adsorption rate and the recombination desorption rate are essentially equal up to and including 1300K, with only slight differences between

the two occurring from 1200-1300K. From say, 1300-2000K, these terms are no longer equal, since the thermal desorption rate begins to enter into the reaction at about 1300K and becomes a dominant influence at the higher temperatures.

These results follow directly from the development of the rate equations in Chapter II, specifically equation (1), repeated below.

$$\begin{array}{lclcl} \text{Time rate} & & & & \\ \text{of change of} & & & & \\ \text{adatoms} & = & \text{Adsorption} & - & \text{Thermal} & - & \text{Recombination} & & \\ \text{per unit area} & & \text{rate} & & \text{desorption} & - & \text{desorption} & & \\ & & & & \text{rate} & & \text{rate} & & \end{array} \quad (100)$$

Under steady-state conditions, the time rate of change is equal to zero, and for low values of temperature, the thermal desorption rate is much less than the adsorption rate and the recombination desorption rate, so the thermal desorption rate can be safely neglected at these low temperatures. Letting the thermal desorption rate go to zero and rearranging equation (100) results in the adsorption rate being equal to the recombination desorption rate. This equality is shown graphically in Figure 28 and numerically in the corresponding columns in Table 13.

As the temperature continues to increase from 1300K, the following occurs (again with reference to Figure 28 and Table 13):

- a. At 1400K, the recombination-desorption rate is a maximum at $0.0125E+17$ and begins to decrease as the

temperature increases. This is due to a low surface coverage at these high temperatures. That is, since the mechanism for recombination is that of Langmuir-Rideal (which requires a gas phase atom striking and recombining with a surface atom), then clearly, if the surface is sparsely covered with atoms, then the recombination rate will be low and thus so too will be the recombination desorption rate.

b. At a temperature of 1700K, the thermal desorption rate has reached a maximum and from 1700-2000K, it decreases. This decrease is again due primarily to the low surface coverage. Also at 1700K, the adsorption rate has reached a maximum and decreases as temperature increases. For $T > 1700K$, the adsorption rate is equal to the thermal desorption rate.

The Effect of the Denominator Terms on the Recombination Mechanism

Recall from Chapter II equation (52) which is shown again below as equation (101) and which presents the denominator terms; the chemisorption term, thermal desorption term, and the exponential term.

$$\gamma = \frac{2 P \dot{N} S_0 \exp \left[\frac{-E_a}{kT} \right]}{\dot{N} S_0 + \delta + P \dot{N} \exp \left[\frac{-E_a}{kT} \right]} \quad (101)$$

The chemisorption term, $\dot{N} S_0$, can be viewed as the rate at which the gas phase atoms are striking and adsorbing; the thermal desorption term, δ , is the rate at which the atoms leave the surface due solely to the added thermal energy; the exponential term provides a measure of the rate at which the surface atoms are leaving the surface due to recombination.

The computer routine calculated the values of each term which are shown below in Table 15 for a dissociation energy of 79 kcal/mole and in Table 16 for a dissociation energy of 105 kcal/mole. The column heading "Theta" corresponds to the fractional surface coverage and is included to facilitate the discussion and analysis.

The two tables below provide information regarding the order of the recombination reaction. Recall from Chapter II that first (second) order behavior meant that the recombination rate was dependent on the pressure to the first (second) power. Also, since the pressure was shown to be related to the impingement rate, similar statements

can be made with regard to the order and the impingement rate.

Table 15

Calculated Values of the Denominator Terms of
Equation (101) for a Dissociation
Energy of 79 Kcal/Mole

<u>Temp.</u> (K)	<u>Chemisorption</u> <u>Term</u>	<u>Thermal</u> <u>Desorption</u> <u>Term</u>	<u>Exponential</u> <u>Term</u>	<u>Theta</u>
300	0.439E+18	0.000E+00	0.130E+15	0.999E+00
400	0.415E+18	0.000E+00	0.197E+15	0.999E+00
500	0.380E+18	0.636E-07	0.259E+15	0.999E+00
600	0.341E+18	0.436E-01	0.315E+15	0.999E+00
700	0.301E+18	0.658E+03	0.368E+15	0.998E+00
800	0.264E+18	0.912E+06	0.417E+15	0.998E+00
900	0.229E+18	0.257E+09	0.462E+15	0.998E+00
1000	0.198E+18	0.202E+11	0.891E+15	0.996E+00
1100	0.169E+18	0.824E+12	0.465E+16	0.973E+00
1200	0.145E+18	0.183E+14	0.893E+16	0.942E+00
1300	0.124E+18	0.254E+15	0.137E+17	0.899E+00
1400	0.105E+18	0.243E+16	0.145E+17	0.862E+00
1500	0.891E+17	0.173E+17	0.152E+17	0.733E+00
1600	0.753E+17	0.966E+17	0.159E+17	0.401E+00
1700	0.636E+17	0.443E+18	0.166E+17	0.122E+00
1800	0.536E+17	0.172E+19	0.173E+17	0.299E-01
1900	0.451E+17	0.581E+19	0.179E+17	0.768E-02
2000	0.378E+17	0.174E+20	0.185E+17	0.217E-02

The values above show the chemisorption term larger than both the thermal desorption rate and the exponential term up to 1500K. The results of the dominant chemisorption term are that the fractional surface coverage is essentially unity (i.e., a fully covered surface) over this temperature range and also, the recombination process displays first order behavior. However, at temperatures greater than 1500K, the chemisorption term is decreasing with increasing temperature and the thermal desorption term

begins to dominate, being larger than the chemisorption term and exponential term. This results in the recombination rate being functionally dependent on the pressure to the second power, or second order kinetics.

The values above correspond to a dissociation energy of 79 kcal/mole; changing to a higher dissociation energy, thereby increasing the strength of the well in terms of binding the particle, alters the temperature at which the first-to-second order transition order occurs. Table 16, below, provides the calculated values of the denominator

Table 16

Calculated Values of the Denominator Terms of
Equation (101) for a Dissociation
Energy of 105 Kcal/Mole

<u>Temp.</u> <u>(K)</u>	<u>Chemisorption</u> <u>Term</u>	<u>Thermal</u> <u>Desorption</u> <u>Term</u>	<u>Exponential</u> <u>Term</u>	<u>Theta</u>
300	0.439E+18	0.000E+00	0.130E+15	0.999E+00
400	0.415E+18	0.000E+00	0.197E+15	0.999E+00
500	0.380E+18	0.000E+00	0.259E+15	0.999E+00
600	0.341E+18	0.000E+00	0.315E+15	0.999E+00
700	0.301E+18	0.499E-05	0.368E+15	0.999E+00
800	0.264E+18	0.717E-01	0.417E+15	0.998E+00
900	0.229E+18	0.124E+03	0.462E+15	0.998E+00
1000	0.198E+18	0.418E+05	0.891E+15	0.996E+00
1100	0.169E+18	0.561E+07	0.465E+16	0.973E+00
1200	0.145E+18	0.336E+09	0.893E+16	0.942E+00
1300	0.124E+18	0.108E+11	0.137E+17	0.900E+00
1400	0.105E+18	0.211E+12	0.145E+17	0.879E+00
1500	0.891E+17	0.281E+13	0.152E+17	0.854E+00
1600	0.753E+17	0.271E+14	0.159E+17	0.825E+00
1700	0.636E+17	0.201E+15	0.166E+17	0.791E+00
1800	0.536E+17	0.119E+16	0.173E+17	0.744E+00
1900	0.451E+17	0.592E+16	0.179E+17	0.654E+00
2000	0.373E+17	0.250E+17	0.185E+17	0.465E+00

terms of equation (101) for a dissociation energy of 105 kcal/mole.

In this case, the chemisorption term dominates both the thermal desorption term and the exponential term for all temperatures 300-2000K. The dominance of the chemisorption term yields a recombination rate that is first order throughout the range 300-2000K. At the higher temperatures, say those greater than 1600K, the calculated values show the chemisorption term decreasing and the thermal desorption term less than the exponential term. However, the chemisorption term is still greater than the desorption term. Taken together, since more atoms are chemisorbing than are thermally desorbing, the surface tends to remain more fully covered over a broader temperature range than that in the previous case. Again, this is consistent with the higher value of the dissociation energy used in the calculation of the values in Table 14. Note that if the calculated values showed a dominant exponential term, the recombination rate would again be first order with respect to temperature.

Hence, in contrast to the situation in which a dissociation energy of 79 kcal/mole was used, resulting in the recombination rate exhibiting a first-to-second order transition, with a higher dissociation energy of 105 kcal/mole, the recombination rate is first order throughout the temperature range 300-2000K. The higher dissociation

energy also yielded a surface that remained covered over a broader temperature range.

Since the values of the dissociation energy were not those resulting from hard, experimental data, it is important to address the issue of the impact on the results if experimental data existed.

If empirical data existed showing strictly first order behavior throughout the temperature range 300-2000K, this would lend credence to a larger dissociation energy since the particle would be more tightly bound within the potential well. On the other hand, if empirical data existed providing first order behavior at low temperatures and a transition to second order at higher temperatures, this would imply a lower dissociation energy was in operation, since a lower well-depth provides the particle with a lower potential barrier to surmount. Then, the particle having overcome the barrier, the kinetics are subject to influence from other factors, such as the thermal desorption rate in the case above.

Experimental efforts would go far in providing a resolution to these questions. For instance, assuming that the Langmuir-Rideal mechanism is the recombination mechanism in operation for nitrogen on silicon dioxide, then two observations can be made from experiment. The first is that if the dissociation energy is known from experiment, then the order of the reaction can be

substantiated. On the other hand, and this is the second observation, if the order is experimentally known, then the dissociation energy can be inferred or substantiated. Moreover, without regard for any particular recombination mechanism, knowledge of the dissociation energy and the order would lend support to a specific recombination mechanism, be it Langmuir-Rideal, Langmuir-Hinshelwood, or some as yet unknown mechanism.

The Effect of Varying the Initial Sticking Coefficient on the Recombination Reaction

The resulting plot of the calculated recombination coefficient as a function of temperature and using an initial sticking coefficient, S_0 , of $0.05 \times \exp(-0.002 \times T)$ and $0.95 \times \exp(-0.002 \times T)$ and, where T is the temperature (K), is shown below in Figure 30. The value of the dissociation energy is 79 kcal/mole.

The initial sticking coefficient used was $0.95 \times \exp(-0.002 \times T)$. The reason for this choice is evident from a comparison of the two curves of the recombination coefficient shown in Figure 30. The larger value of the initial sticking coefficient clearly yielded a maximum value of the recombination coefficient that matched and passed through the maximum of the empirical data. Whereas any lower values of the initial sticking coefficient gave a maximum much less than the corresponding empirical value.

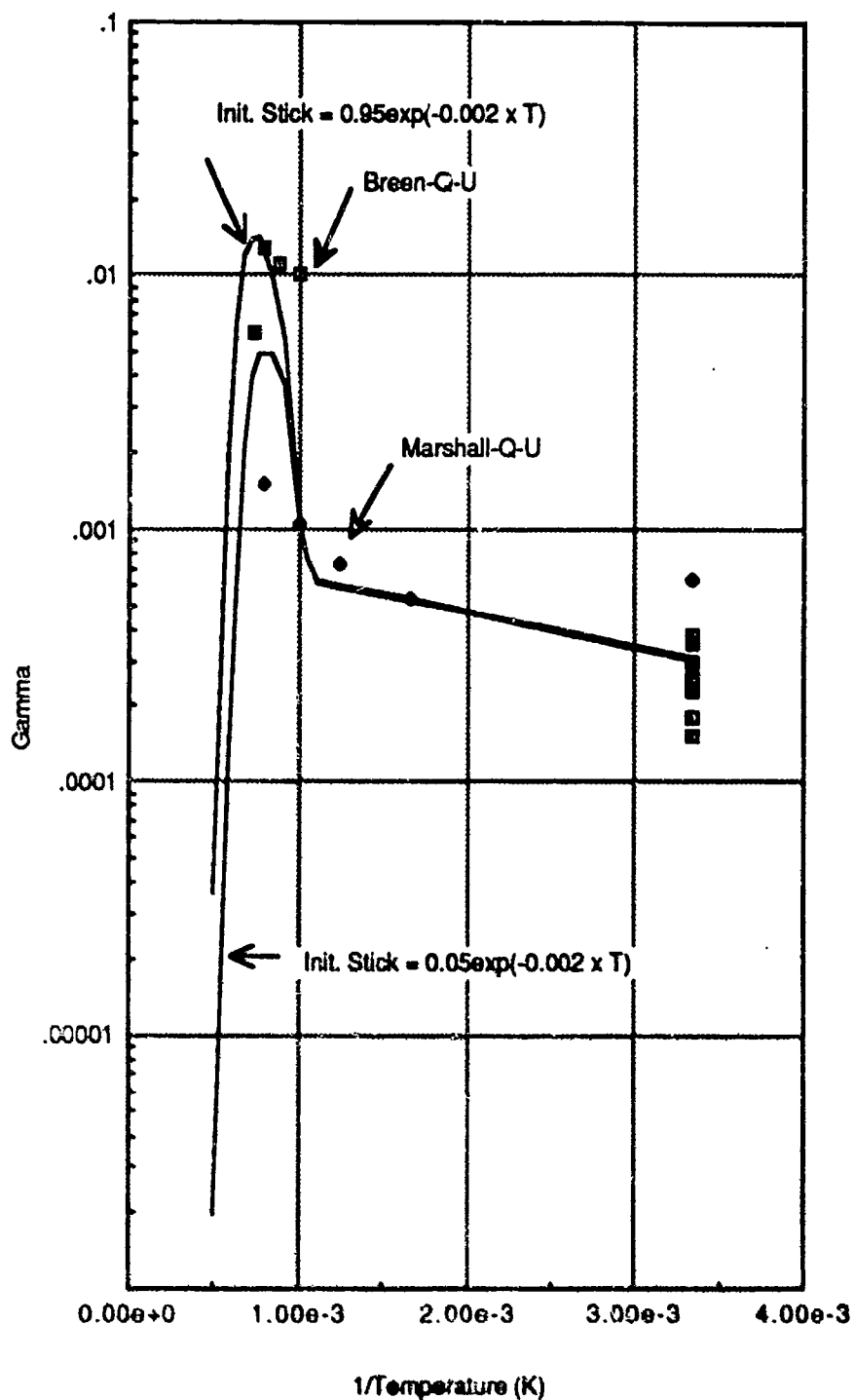


Figure 30. The Recombination Coefficient as a Function of Temperature for Initial Sticking Coefficients of $0.05 \times \exp(-0.002 \times T)$ and $0.95 \times \exp(-0.002 \times T)$.

Similarly, any higher values resulted in a maximum for γ that exceeded the maximum from the empirical data.

The Effect of Holding the Pressure Constant vs. Pressure Being a Function of Temperature

The resulting plot of the calculated recombination coefficient as a function of temperature and allowing the gas pressure of atomic nitrogen to vary with the temperature combined with a plot of a value of 0.00155 torr for the gas pressure of atomic nitrogen is shown below in Figure 31. The value of the dissociation energy is 79 kcal/mole and the value of the initial sticking coefficient, S_0 , was $0.95 \times \exp(-0.002 \times T)$, where T is the temperature (K).

To facilitate the following discussion, the calculated values of the recombination coefficient for the two cases are presented in Table 17.

As stated in Chapter III, since Marshall (51) did not state whether the number density varied or if the atomic gas pressure varied, for the purposes of this thesis, it was assumed that the gas pressure increased as the temperature increased, for a constant number density. However, since gas pressures do in fact vary with temperature according to Boyle's Law, it was felt that this issue could not merely be ignored; hence the decision to include it in this research task.

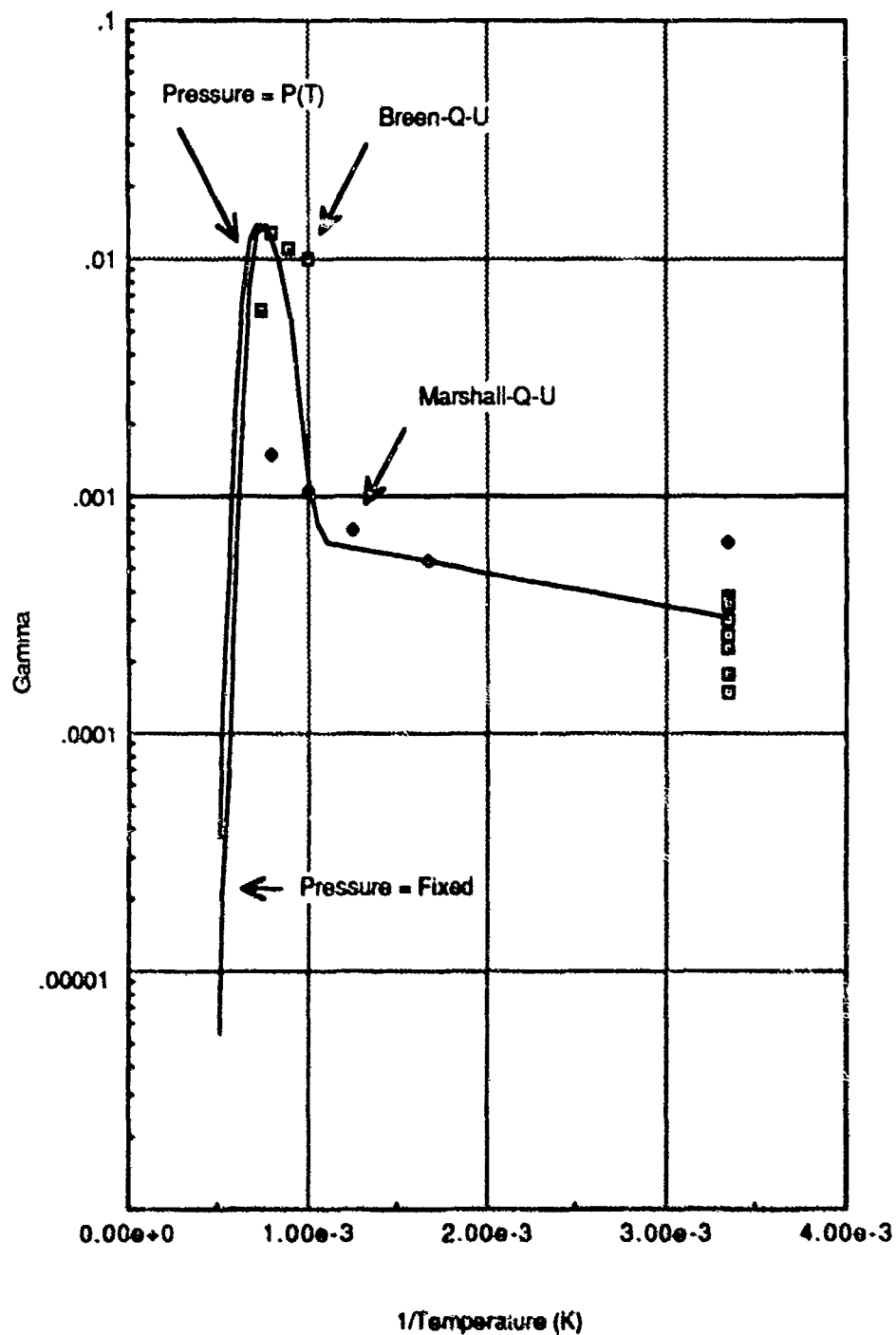


Figure 31. The Recombination Coefficient as a Function of Temperature. The Gas Pressure Varied as the Temperature and a Fixed Value of the Pressure.

Table 17

Gamma vs. Temperature for Fixed and Varying Pressure

<u>Temperature (K)</u>	<u>Gamma, Fixed Pressure (torr)</u>	<u>Gamma, Varying Pressure (torr)</u>
300	0.309E-03	0.309E-03
400	0.405E-03	0.405E-03
500	0.475E-03	0.475E-03
600	0.529E-03	0.529E-03
700	0.571E-03	0.571E-03
800	0.605E-03	0.605E-03
900	0.632E-03	0.632E-03
1000	0.115E-02	0.115E-02
1100	0.562E-02	0.562E-02
1200	0.998E-02	0.999E-02
1300	0.139E-01	0.140E-01
1400	0.128E-01	0.139E-01
1500	0.753E-02	0.118E-01
1600	0.203E-02	0.656E-02
1700	0.405E-03	0.201E-02
1800	0.861E-04	0.500E-03
1900	0.206E-04	0.129E-03
2000	0.554E-05	0.369E-04

The Fractional Surface Concentration of Nitrogen on Silicon Dioxide

The resulting plot of the fractional surface concentration, θ , of nitrogen on silicon dioxide as a function of temperature is shown below in Figure 32. All parameters (pressure, initial sticking coefficient, etc.) used by the computer routine in the calculation of θ are those shown in Table 10 of Chapter III.

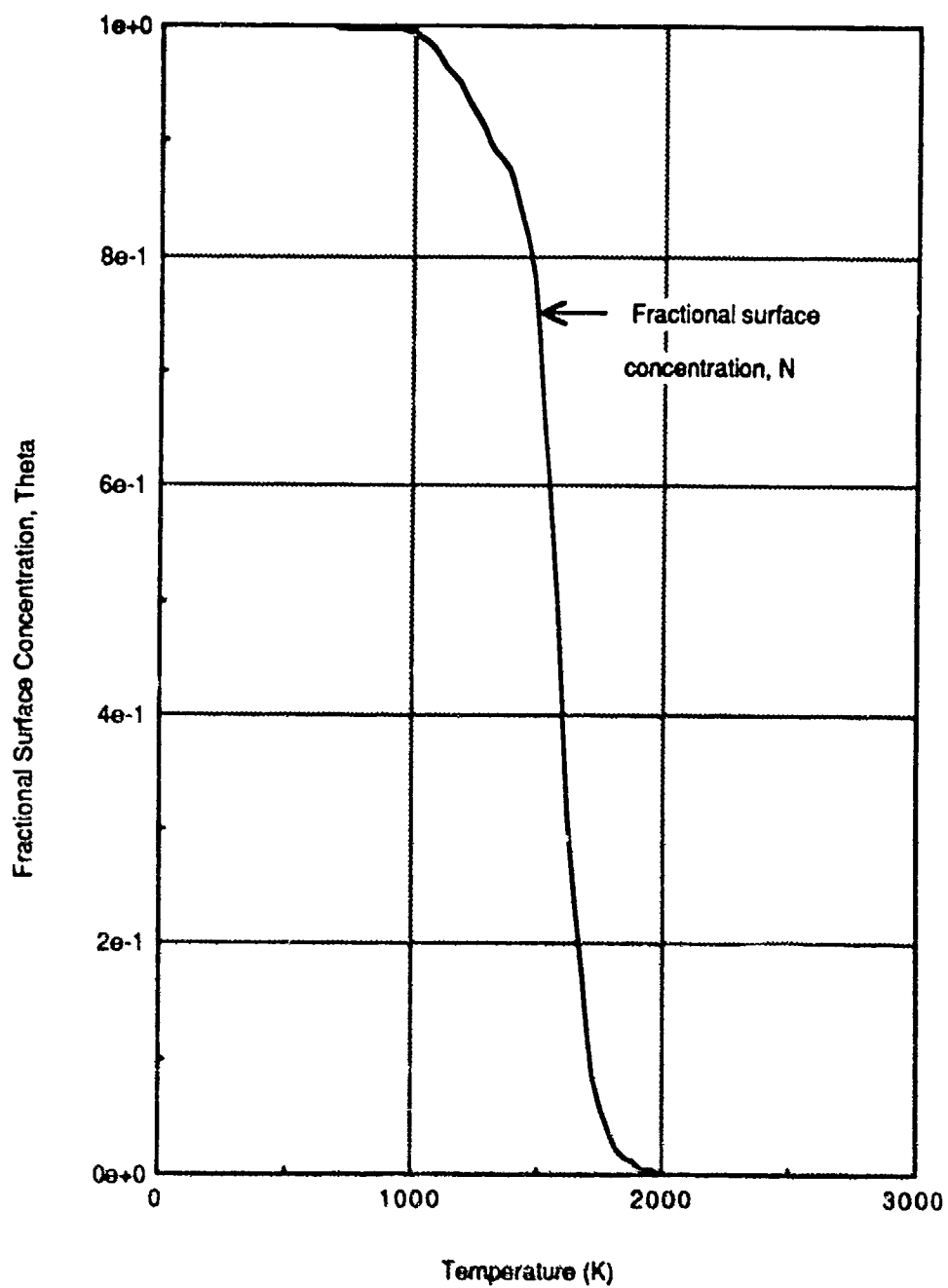
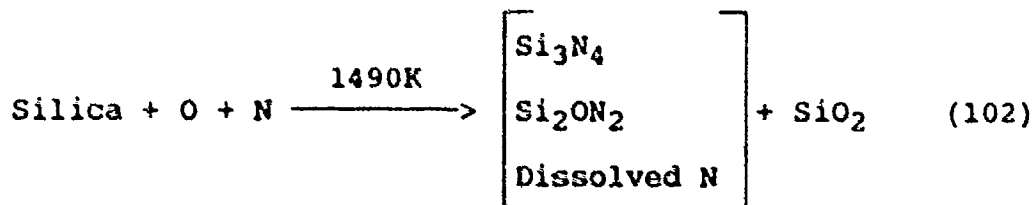


Figure 32. Fractional Surface Concentration as a Function of Temperature for Nitrogen on Silicon Dioxide.

The numerical values of θ were given previously in Table 15. Figure 32 illustrates the dependence of the nitrogen surface concentration on temperature. Theta is essentially unity (i.e., a fully covered surface) up to -1000K before it begins to decline, yielding a relatively bare surface due to thermal desorption.

From the literature, only Breen and others (5) provided some discussion on the character or coverage of the surface following exposure to a mixture of atomic nitrogen and atomic oxygen. (He also discussed coverage following exposure to molecular oxygen and this will be addressed shortly.)

According to Breen and others (5:64), a sample of silica was exposed to a mixture of atomic nitrogen and atomic oxygen at elevated temperatures of about 1490K. Analysis via X-ray photoelectron spectroscopy (XPS) showed that nitrogen was incorporated into the silica in the form a silicon nitride (Si_3N_4), silicon oxynitride (Si_2ON_2), or dissolved nitrogen. In terms of a chemical equation,



Specific details of the nature of the surface in terms of coverage or amounts of atomic species were not provided. Furthermore, whether the above action was reversible or not

was not mentioned. However, the reaction above does show that nitrogen, rather than oxygen, is incorporated into the silica at the high temperatures.

It is interesting to view the effect that a larger dissociation energy has on the fractional surface coverage. One expects that under such conditions the surface will retain its coverage over a broader temperature range. This is indeed the case, as shown in Figure 33, which provides the fractional surface concentration of nitrogen on silicon dioxide as a function of temperature for a dissociation energy of 105 kcal/mole. As shown, for a larger dissociation energy, the atoms remain on the surface longer, thereby increasing the surface concentration. For instance, at 2000K and for $D = 79$ kcal/mole, $\theta = 0.00217$, whereas at 2000K, $D = 105$ kcal/mole, $\theta = 0.465$, roughly a difference of two orders of magnitude.

The Fractional Surface Concentration of Oxygen on Silicon Dioxide

Although this thesis is concerned with heterogeneous recombination of nitrogen on silicon dioxide, a consideration of the surface coverage of oxygen may yield some insight into the relative surface coverage of the two atomic species, nitrogen vs. oxygen.

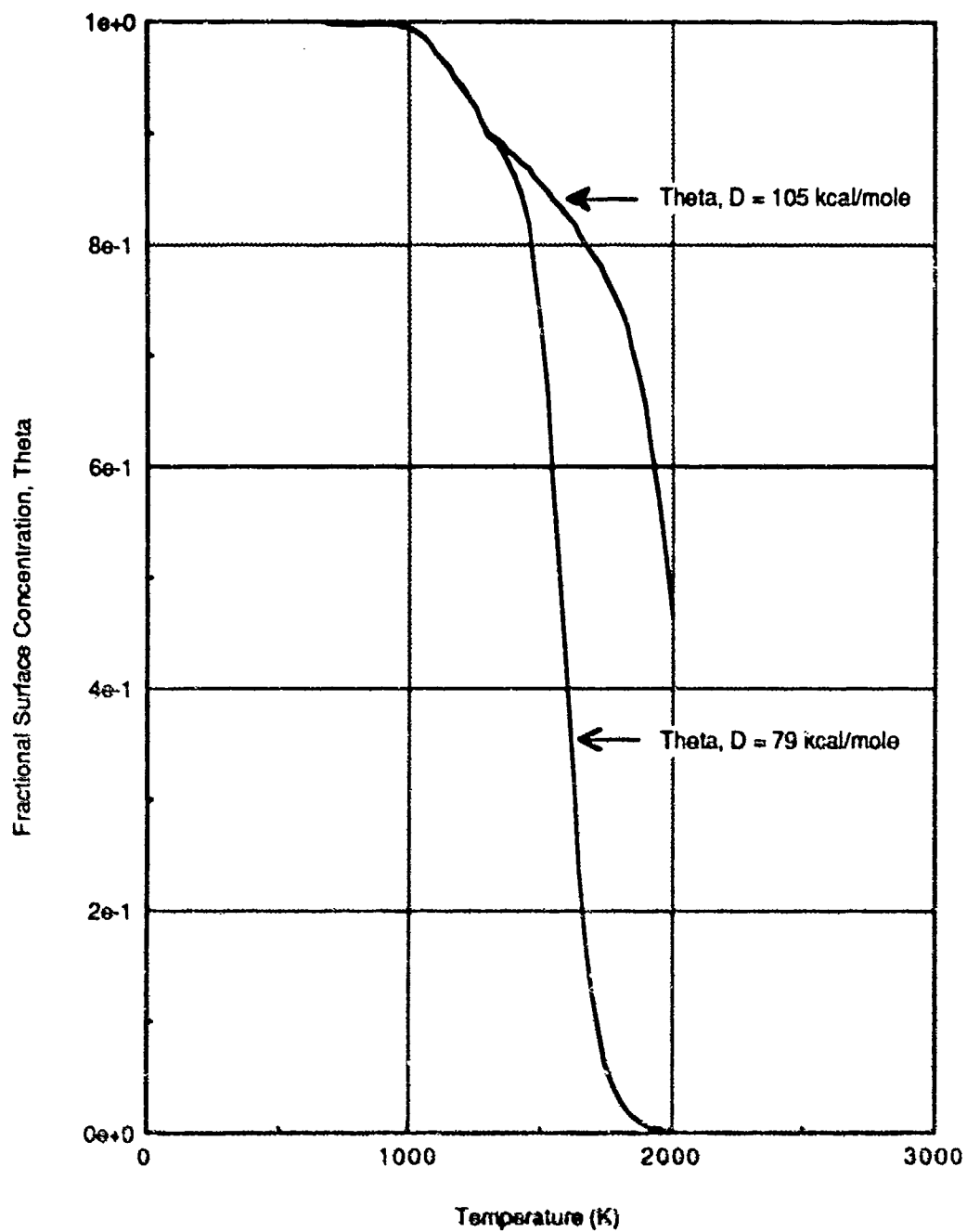


Figure 33. Fractional Surface Concentration as a Function of Temperature for Nitrogen on Silicon Dioxide for a Dissociation Energy of 79 and 105 Kcal/Mole.

The fractional surface concentration as a function of temperature for oxygen on silicon dioxide was calculated by the routine in Appendix A but using the following set of input parameters (72:50):

Table 18

Input Parameters to Calculate the Fractional Surface Concentration for Oxygen Chemisorption on Silicon Dioxide

<u>Parameter</u>	<u>Value</u>
Activation Energy	1 kcal/mole
Pressure	0.01 torr
Initial Sticking Coefficient	$0.05 \exp(-0.002 \times \text{Temp. (K)})$
Number of Surface Sites	5×10^{14} sites/cm ²
Steric Factor	$0.0000224 \times \exp(0.00908 \times \text{Temp. (K)})$
Dissociation Energy	81 kcal/mole

The resulting plot of the fractional surface concentration for oxygen on silicon dioxide in the temperature range 300-2000K is shown below in Figure 34.

Figure 34 shows that θ is essentially unity (i.e., a fully covered surface) up to ~500K before it begins to decline, yielding a relatively bare surface as the temperature increases. From the literature, Breen and others (5) provided some discussion on the character or coverage of the surface following exposure to molecular oxygen.

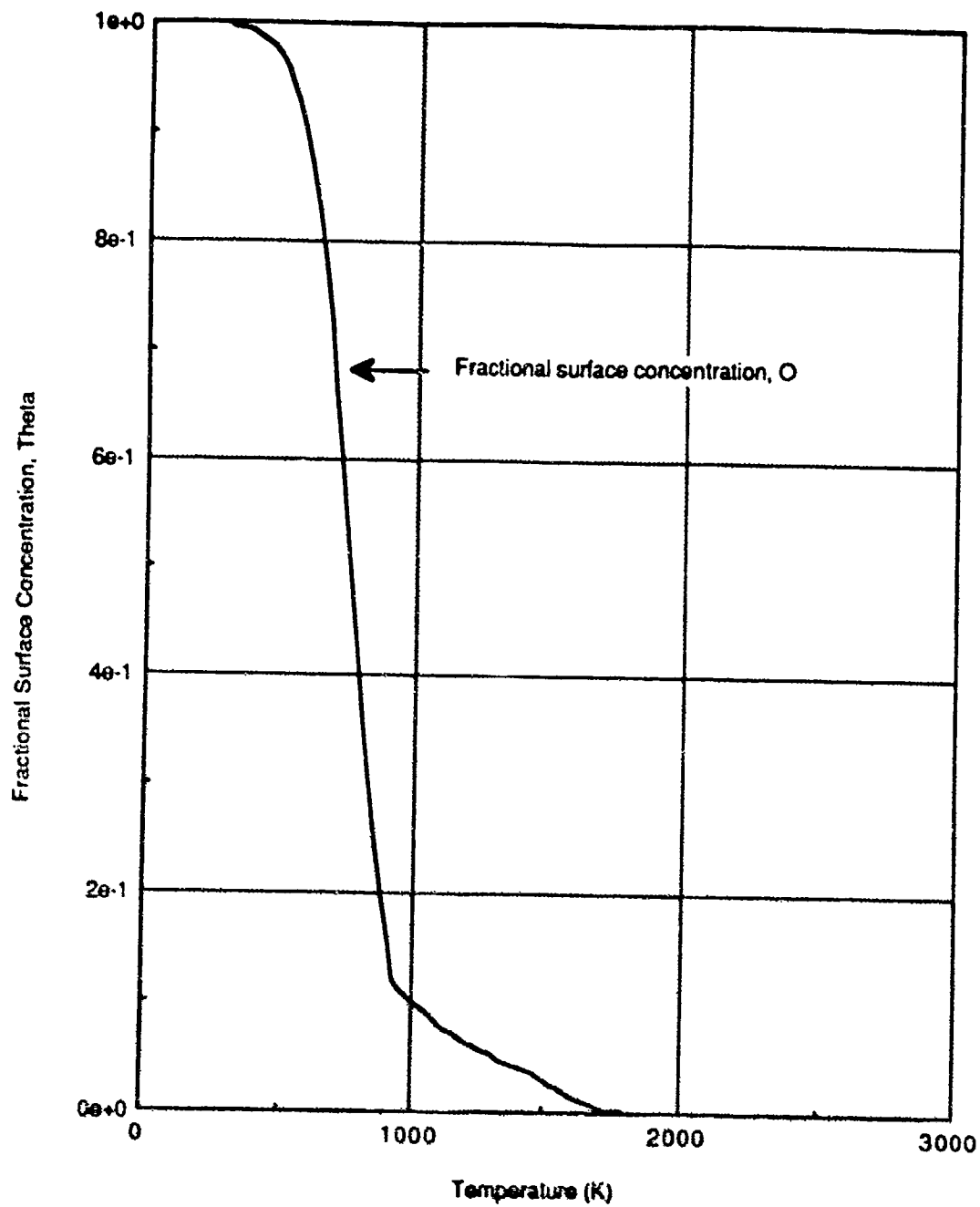


Figure 34. Fractional Surface Concentration for Oxygen on Silicon Dioxide.

According to Breen and others (5:64), a sample of silica was exposed to molecular oxygen at elevated temperatures of about 1270K. XPS analysis of the exposed samples "...showed only SiO_2 and there was no change in surface chemistry before or after reaction" (5:64). Breen and others (5) did not provide information regarding exposure of atomic oxygen on silica.

Figure 35, below, shows an overlay of Figures 33 and 34. A strong note of caution is required with respect to Figure 35: this plot is an overlay of the fractional surface concentration of nitrogen onto that of oxygen. Figure 35 is not the fractional surface concentration of nitrogen and oxygen together in a competing system.

Although no quantitative analysis can be obtained from Figure 35 regarding the surface concentration of nitrogen and oxygen acting in competing system, Figure 35, coupled with equation (97), does at least suggest the possibility that given a system in which atomic oxygen and nitrogen react with a silicon dioxide surface, nitridation may be favored over oxidation. If this is so, does nitrogen displace atomic oxygen over the entire temperature range or are there certain ranges where nitridation is favored over oxygen and vice versa? Looking at Figure 35, showing nitridation occurring at the higher temperatures, then perhaps research efforts should begin to focus on nitrogen chemisorption rather than, or in conjunction with oxygen

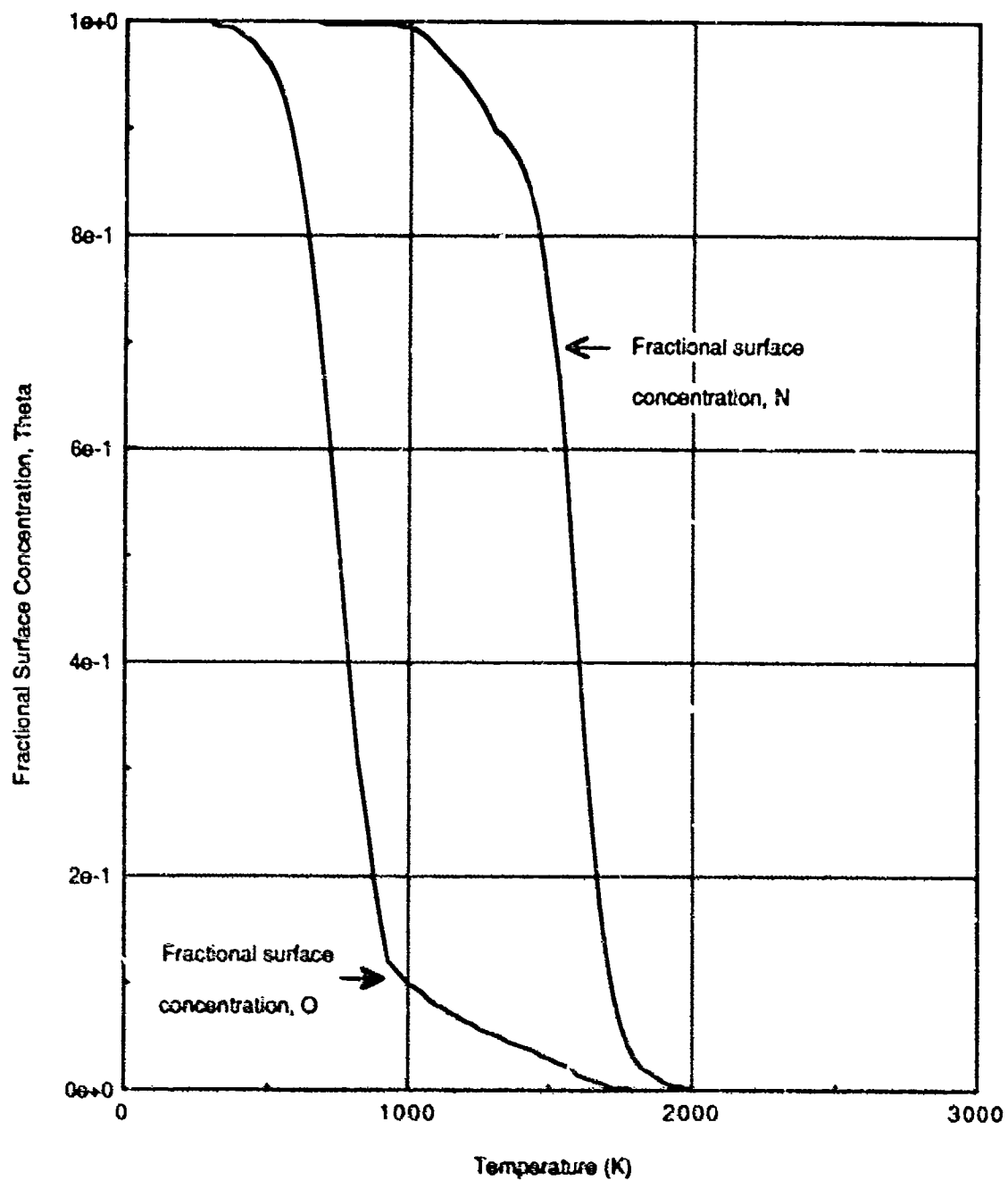


Figure 35. An Overlay of the Fractional Surface Concentration for Nitrogen onto that of Oxygen on a Silicon Dioxide Surface.

chemisorbing onto silicon dioxide. This type of reaction involves the two atomic species, nitrogen and oxygen, competing for surface sites and thus involves a whole new set of rate equations.

Let us extend the discussion and consider the recombination and subsequent nitridation of silicon dioxide and its application to the Shuttle's thermal protection tiles. Recall that the heating of the tiles increased by -20% from flights STS-2 to STS-5. Is this due to the exothermic nature of the recombination? What is the characteristic lifetime of the tiles based on the effects of nitrogen and/or oxygen recombination? What are the precise temperatures seen by the tiles? How do the recombination and time in flight affect the tiles? Do they undergo phase transformations in a manner similar to quartz? Under what temperature regimes do the tiles transition phases? How does nitrogen or oxygen accommodate to the new structure? What is the stoichiometry? That is, is it Si_xN_y ? Or is it some variant of $\text{Si}_x\text{N}_y\text{O}_z$?

Moreover, how resilient is a nitrided tile compared to an oxidized tile? According to Popper and Ruddlesden (63:619-621), silicon nitride (Si_3N_4) is chemically inert, and silicon nitride ceramics have oxidation resistance to 1673K, and a coefficient of thermal expansion of 2.5×10^{-6} per °C, compared to 0.5×10^{-6} per °C for silicon dioxide.

The majority of sources in the literature did not discuss the surface and its effect on the fractional surface concentration. Metals are relatively homogeneous; i.e., they can be characterized via crystal lattice constants, crystal packing forms, Miller indices, etc. Moreover, metallic crystals have a periodic array feature that allows for a homogeneous surface in terms of the number of potential surface sites and the spacings between the surface atoms. In addition, due to the periodic nature of the surface, there will be few, if any, domains which contain a larger number of potential sites than the neighboring domains. That is, one domain on the surface looks and therefore should behave exactly like any other domain on the surface.

This is not the case in amorphous materials such as a glass like silicon dioxide. The amorphicity extends throughout the bulk and to the surface. Therefore it is safe to expect that the surface will consist of a number of domains with potential sites interspersed among domains with little or no potential sites. These latter domains could be due to, say, the rotations of the tetrahedra as the temperature changes or due to the nature of the crystal. This view of the glass surface elicits certain questions. How is the fractional coverage affected? What is the effect on surface migration of the adsorbed atoms? Do they have a tendency to "skim" over the domains with

little or no active sites? What does a gas phase atom do when it strikes a domain with little or no sites? Does it recoil back into the gas phase? Does it displace one of the atoms lying close to the surface? As the temperature varies, the surface and the bulk undergo changes in their structure. Do these changes necessarily mean that the number of sites decreases?

Summary

This chapter presented the results and discussion of the activities involved in the attempt to develop a model for the heterogeneous recombination of nitrogen on a silicon dioxide surface in the temperature range of 300-2000K.

Langmuir-Rideal was assumed to be the mechanism of recombination. From the empirical recombination data in the literature, computational parameters were calculated and used as input parameters to a computer routine to calculate certain terms which could then be compared against those found in the literature.

Specifically, the objective was to determine if the calculated values of the recombination coefficient of nitrogen on silicon dioxide as a function of temperature matched those in the literature; the match between experiment and calculation was shown in Figure 26. Moreover, the analysis covered various aspects of the heterogeneous recombination of nitrogen on silicon dioxide.

The various aspects of the recombination and subsequent analysis included, but were not solely limited to

- a. The effect of varying the dissociation energy on the recombination coefficient.
- b. The sorption rates of nitrogen on silicon dioxide.
- c. The effect of the chemisorption term, thermal desorption term, and an exponential term on the recombination mechanism.
- d. The effect of varying the initial sticking coefficient on the recombination.
- e. The effect of holding the pressure constant as opposed to allowing it to vary with the temperature.
- f. The fractional surface concentration of nitrogen on silicon dioxide.

As an aside, the fractional surface concentration of oxygen on silicon dioxide was presented along with an overlay of the two fractional surface concentrations for nitrogen and oxygen. The latter provided the stimulus for speculating whether nitridation or oxidation of silicon dioxide is favored. This, however, can be resolved via experimental efforts, some of which are proposed in the next chapter.

V. Conclusions and Recommendations

Conclusions

At this point, it can be safely said that, when viewed macroscopically, the process of heterogeneous atomic recombination is relatively straightforward and understandable. However, when the attention is focused on the microscopic particulars such as the adsorbate atomic species and the adsorbent surface, the ability to understand the recombination becomes more complex.

The complexities arise due to several related issues: the mechanism of the recombination; the bond formed between the adsorbed gaseous atom and the surface; activation and dissociation energies; the nature of the surface and its behavior under varying temperatures; as well as the number of atoms that adsorb, recombine, and desorb as molecules. These issues are interrelated and can be suitably resolved after having some idea of how the gaseous atoms mechanistically interact with the surface.

The objective of this thesis was to develop a mechanism for the heterogeneous recombination of atomic nitrogen on a silicon dioxide surface in the temperature range of 300-2000K. The Langmuir-Rideal model was used as the basic mechanism to explain nitrogen recombination on silicon dioxide. However, this basic mechanism was extended under

the plausibility argument that the silicon dioxide surface is an active participant in the recombination process. Specifically, the surface silicon atoms were assumed to be the active centers for recombination with the gas phase nitrogen atoms.

From this, kinetic rate equations and a corresponding computer routine were developed for nitrogen recombining on silicon dioxide, empirical data of the recombination coefficient of nitrogen on silica surfaces were obtained, and the computer routine was executed to calculate the recombination coefficient of nitrogen on silicon dioxide as a function of temperature. The calculated values of the recombination coefficient were plotted against those from the literature and it was shown that the calculated values satisfactorily matched the empirical data set. This correspondence lends strong support to the position that Langmuir-Rideal is the basic mechanism by which atomic nitrogen heterogeneously recombines on silicon dioxide in the temperature range 300-2000K.

Recommendations

The computer routine was also used to calculate the recombination coefficient under conditions of varying well-depths and to calculate the values of the fractional surface concentration. However, as stated in Chapter IV, numerous issues remain to be determined with a better

degree of certainty. An experiment can be performed to address these and other, as yet unknown issues.

The experimental procedure would include, but not be limited to the following:

- a. Expose a silicon sample to atomic oxygen at elevated temperatures, say greater than 1200K to oxidize the sample yielding SiO_2 .
- b. Introduce the sample to atomic nitrogen at these elevated temperatures.
- c. Analyze the surface via Auger, X-ray photoelectron spectroscopy, or some other suitable technique.
- d. Fracture the nitrated silicon dioxide sample and perform another set of surface analyses.
- e. The analyses and observations should address those questions in Chapter IV and others posed by the experimentalists.

The next iteration in the experiment could then involve the same steps as above except instead of exposing the silicon dioxide sample to only atomic nitrogen, the sample would be exposed to known quantities of atomic oxygen and nitrogen. This would provide information of the recombination for the case of a competing system of two atomic species.

Moreover, using a mass analyzer on the exposed silica sample could provide values of the fractional surface concentration.

To apply the results of this thesis and the above experiment to a real-world situation, accomplish the same procedure on a new thermal protection tile designed for use on a reentry vehicle such as the Space Shuttle. In this case, if nitriding of the tile is confirmed and the reaction is strongly exothermic, one could consider doping the tile with an element that would either render the tile inert to nitrogen recombination or would form a surface complex with the nitrogen that is less exothermic and perhaps more resilient to temperature cycling. Special emphasis should be placed in ensuring that the experiment subject the tile to an environment that is as close as possible to the atmospheric environments seen by the vehicle during the launch and reentry phases of flight.

For example, vary the temperatures, pressures, concentrations of atomic nitrogen and oxygen and other atmospheric species, wind velocity, etc. This would tend to confirm or refute the supposition that nitridation is favored over oxidation as well as providing specific temperature ranges where the recombination of one species occurs instead of the other.

Evidently, to maintain the re-use capability of earth orbiting reentry vehicles, much more needs to be understood regarding the recombination reaction and the proposed materials that may comprise any future thermal protection system.

The Langmuir-Rideal mechanism was shown to be a very reasonable mechanism to explain atomic nitrogen recombination on silicon dioxide. The basic research in this thesis simulated real-world situations. The next logical step is in the laboratory to begin work to better understand the recombination reaction, energetic state of the desorbed species, and the effects of varying pressure and temperature. Moreover, experimental work would go far in advancing the current knowledge of thermal protection materials and the chemical species formed on them due to recombination of atmospheric gases.

Appendix A

This Appendix contains the program developed to calculate the recombination coefficient of nitrogen on silicon dioxide as a function of temperature. The program was written in Fortran 77 (also termed Fortran 5) on a Macintosh Plus, using the MicrosoftTM Fortran 77 compiler and is presented below.

c This program computes the recombination coefficient, Gamma,
c for nitrogen atoms recombining on a silicon dioxide surface
c in the temperature range of 300K to 2000K. The recombina-
c tion mechanism is assumed to be Langmuir-Rideal.

c GLOSSARY OF TERMS USED IN THIS PROGRAM

c Actnrg = The activation energy, Joules.
c 1 kcal/mole=6.949E-21 Joules/atom.
c Adrate = The adsorption rate, particles per area-time.
c Atwgt = The atomic weight of nitrogen, grams/mole.
c Avogdr = Avogadro's number, particles per mole.
c Boltzc = The Boltzmann constant, Joules/degree K.
c Chemr = The chemisorption term (denominator term).
c Delta = The thermal desorption rate of atoms per unit area,
c atoms/cm squared-sec.
c Derate = The thermal desorption rate, particles/area-time.
c Extern = The exponential term in the denominator.
c Gamma = The recombination coefficient at the wall, dimensionless.
c Ndot = The surface impingement rate of atoms per unit
c area, atoms/cm squared-sec.
c Peecon = The leading constant for the pressure = (number
c density*8.21E-5*760). Units: torr
c Pi = The ratio of the circle's circumference to its diameter.
c Planck = The Planck constant, Joule-sec.

```

c      Press = The pressure, Torr.
c      RecDes = The recombination desorption rate.

c      Sterfa = The steric factor, dimensionless.
c      Stick = The initial or clean surface sticking coefficient,
c              dimensionless.
c      Surfsi = The number of surface sites per unit area,
c              sites/cm squared. (See Thesis, chapter 3.)
c      Temp = The temperature, Kelvin scale.
c      Theta = The fractional surface concentration of atoms,
c              dimensionless.
c      Welldp = The thermal desorption energy for atoms,
c              Joules/atom.

c      DECLARE VARIABLES-----
Real Actng,Atmgt,Avogdr,Boltzc,Delta,Gamma,Ndot,Pi
Real Planck,Sterfa,Stick,Surfsi,Temp,Thetc,Welldp
Real Press,Chemi,Extern,Adrate,Desrate,RecDes,Peecon

c      DEFINE CONSTANTS-----
Actng = 0.640*6.949E-21
Atmgt = 14.0067
Avogdr = 6.02252E23
Boltzc = 1.38054E-23
Peecon = 3.11930E18/Avogdr
Pi = 3.141593
Planck = 6.6256E-34

c      The following value of pressure obtained by  $P=nRT$ ,
c      using Marshall's (RD438419,p 84) atomic number density of
c      SE13, at a temperature of 300K.
c      Press = 0.00155.       $P(T=2000K) = 0.01$  torr.
c      Welldp = 5.489710E-19
c      The above Welldp corresponds to 79 Kcal/mole.
c      That is,  $XX \text{ kcal/mole} * 6.249E-21 \text{ J/atom}$ 

c      WRITE OUT HEADERS-----
Write(6,*)
Write(6,*) ' Nitrogen Recombination Data '
Write(6,*)
Write(6,2) 'Temp', 'Gamma', 'Ndot', 'Delta', 'Theta'
Write(6,3) 'Temp', 'Chemi-RS', 'Delta', 'Extern'
Write(6,4) 'Temp', 'AdsRate', 'DesRate', 'RecDes'

2      Format(//,IX,2R10,3R13,/)
3      Format(//,IX,2R10,2R13,/)
4      Format(//,IX,2R10,2R13,/)

Do 100 N = 1,69
Temp = 275. + 25.*Real(N)
If(Temp.LT.900)Sterfa = 0.000453
If(Temp.LE.1000.and.Temp.GE.900) Then
Sterfa = ((1000.-Temp)/100.)*0.000453-((900.-Temp)/100.)
*0.0008
Endif
If(Temp.LE.1300.and.Temp.GT.1000) Then

```

```

      Sterfa = ((1300.-Temp)/300.)*.0008-((1000.-Temp)/300.)*.01
    Endif
    If(Temp.GT.1300) Sterfa = Sterfa
    Stick = 0.95*Exp(-0.002*Temp)

c    ACCOUNT FOR PHASE TRANSITION-----
    If(Temp.LE.900) Surfsi = 2.12E14
    If(Temp.GT.900) Surfsi = 1.80E14

c    ACCOUNT FOR PRESSURE VARYING AS THE TEMPERATURE-----
    Press = Peecon*Temp

c    CALCULATE RECOMBINATION PARAMETERS-----
    Ndot = Press*1333.2*(6.023E16/(2.*Pi*Atmwt*Boltzc*Temp))**.5
    Delta = (Surfsi*Boltzc*Temp/Planck)*Exp(-He11dp/(Boltzc*Temp))
    Theta = (Ndot*Stick)/(Ndot*Stick+Delta+Ndot*Sterfa*Exp(-Actnrg
1/(Boltzc*Temp)))
    Gamma = 2.*Sterfa*Theta*Exp(-Actnrg/(Boltzc*Temp))

c    ADDITIONAL PARAMETERS TO CONSIDER-----
c    These are the denominator (eq.52, Ch.11) terms-----
    Chemi = Ndot*Stick
    Extern = Sterfa*Ndot*Exp(-Actnrg/(Boltzc*Temp))
c    These are the sorption rate terms-----
    Adrate = Stick*Ndot*(1.-Theta)
    Derate = Delta*Theta
    Recdes = Sterfa*Ndot*Theta*Exp(-Actnrg/(Boltzc*Temp))

c    PRINT OUT THE RESULTS-----

c    Recombination parameters-----
    Write(6,5)Temp,Gamma,Ndot,Delta,Theta
5    Format(1X,5E12.4)

c    Denominator terms-----
    Write(6,6)Temp,Chemi,Delta,Extern
6    Format(1X,4E12.4)

c    Sorption Rate terms-----
    Write(6,7)Temp,Adrate,Derate,Recdes
7    Format(1X,4E12.4)

100  Continue

      End

```

Bibliography

1. Adamson, A. W. Physical Chemistry of Surfaces (Third Edition). New York: John Wiley & Sons, 1976.
2. Back, R. A. and others. "The Decay of Active Nitrogen at High Temperatures," Canadian Journal of Chemistry, 37: 2059-2063 (September 1959).
3. Berkowitz-Mattuck, J. B. Research to Determine the Effects of Surface Catalyticity on Materials' Behavior in Dissociated Gas Streams: Final Report. October 1968. AFML-TR-68-306. Air Force Materials Laboratory, Wright-Patterson AFB, OH, October 1968.
4. Bond, G. C. Heterogeneous Catalysis: Principles and Applications. Oxford: Clarendon Press, 1974.
5. Breen, J. and others. "Catalysis Study for Space Shuttle Vehicle Thermal Protection Systems." NASA CR-134124, Washington: National Aeronautics and Space Administration, 1973.
6. Brennen, W. and M. E. Shuman. "A New Example of Formal Non-Steady-State Kinetics. A Model of Heterogeneous Atom Recombination," The Journal of Physical Chemistry, 79: 741-746 (January-June 1975).
7. Brennen, W. and M. E. Shuman. "Kinetics of the Langmuir-Rideal Mechanism for Heterogeneous Atom Recombination," The Journal of Physical Chemistry, 82: 2715-2719 (July-December 1978).
8. Brennen, W. and E. C. Shane. "The Nitrogen Afterglow and the Rate of Recombination of Nitrogen Atoms in the Presence of Nitrogen, Argon, and Helium," The Journal of Physical Chemistry, 75: 1552-1564 (April-June 1971).
9. Campbell, I. M. and B. A. Thrush. "The Recombination of Nitrogen Atoms and the Nitrogen Afterglow," Proceedings of the Royal Society of London. Series A, 296: 201-221 (February 1967).
10. Clyne, M. A. A. and D. H. Stedman. "Rate of Recombination of Nitrogen Atoms," The Journal of Physical Chemistry, 71: 3071-3073 (July 1967).

11. Cottrell, T. L. The Strengths of Chemical Bonds (Second Edition). London: Butterworths, 1958.
12. Dickens, P. G. and M. B. Sutcliffe. "Recombination of Oxygen Atoms on Oxide Surfaces. Part 1 -- Activation Energies of Recombination," Transactions of the Faraday Society, 60: 1272-1285 (July 1964).
13. Evenson, K. M. and D. S. Burch. "Atomic-Nitrogen Recombination," The Journal of Chemical Physics, 45: 2450-2460 (October 1966).
14. Finster, J. and others. "Characterization of Amorphous SiO_x Layers with ESCA," Surface Science, 162: 671-679 (May 1985).
15. Flowers, O. and D. A. Stewart. "Catalytic Surface Effects on Contaminated Space Shuttle Tiles in a Dissociated Nitrogen Stream." NASA TM-86770, Washington: National Aeronautics and Space Administration, November 1985.
16. Gasser, R. P. H. An Introduction to Chemisorption and Catalysis by Metals. Oxford: Clarendon Press, 1985.
17. Ghosh, S. N. and S. K. Jain. "Catalytic Efficiency of Pyrex Glass for the Recombination of Nitrogen Atoms," British Journal of Applied Physics, 17: 765-767 (June 1966).
18. Golde, M. F. and B. A. Thrush. "Afterglows," Reports on Progress in Physics, 36: 1285-1356 (September 1973).
19. Gray, H. B. Chemical Bonds. An Introduction to Atomic and Molecular Structure. Menlo Park: Benjamin Cummings Publishing Company, 1973.
20. Green, B. D. "Atomic Recombination into Excited Molecular - A Possible Mechanism for Shuttle Glow," Geophysical Research Letters, 11: 576-579 (June 1984).
21. Green, B. D. and others. "The Shuttle Environment Gases, Particulates, and Glow," Journal of Spacecraft and Rockets, 22: 500-511 (September-October 1985).
22. Gupta, R. N. and others. "Space Shuttle Heating Analysis with Variation in Angle of Attack and Surface Condition," AIAA Paper 83-0486, New York: American Institute of Aeronautics and Astronautics, 1983.

23. Haaze, J. "NEXAFS and SEXAFS Studies of Chemisorbed Molecules," Applied Physics A--Solids and Surfaces, **38**: 181-190 (November 1985).
24. Hacker, D. S. and others. "Recombination of Atomic Oxygen on Surfaces," The Journal of Chemical Physics, **35**: 1788-1792 (October 1961).
25. Hayward, D. O. and B. M. W. Trapnell. Chemisorption (Second Edition). London: Butterworth and Company Ltd., 1964.
26. Helms, C. R. "Electron Spectroscopy Studies of the Si-SiO₂ Interface," Surfaces and Interfaces in Ceramic and Ceramic-Metal Systems, Volume 14, edited by J. Pask and A. Evans. New York: Plenum Press, 1981.
27. Herron, J. T. and others. "Kinetics of Nitrogen Atom Recombination," The Journal of Chemical Physics, **30**: 879-885 (April 1959).
28. Hersh, C. K. "Nitrogen," The Encyclopedia of the Chemical Elements, edited by C. A. Hampel. Skokie, IL: Reinhold Book Corporation, 1966.
29. Himpsel, F. J. "Electronic Structure of Semiconductor Surfaces," Applied Physics A--Solids and Surfaces, **38**: 205-212 (November 1985).
30. Hinshelwood, C. N. The Kinetics of Chemical Change. Oxford: Clarendon Press, 1949.
31. Hirschfelder, J. "Semi-Empirical Calculations of Activation Energies," Journal of Chemical Physics, **9**: 645-653 (August 1941).
32. Hobson, J. P. "Physical Adsorption of Nitrogen on Pyrex at Very Low Pressures," The Journal of Chemical Physics, **34**: 1850-1851 (April 1961).
33. Hu, S. M. "Properties of Amorphous Silicon Nitride Films," Journal of the Electrochemical Society, **113**: 693-698 (July 1966).
34. Jumper, E. J. and others. "A Model for Fluorine Atom Recombination on a Nickel Surface," The Journal of Physical Chemistry, **84**: 41-50 (January 1980).

35. Kelly, R. and C. A. Winkler. "The Kinetics of the Decay of Nitrogen Atoms as Determined from Chemical Measurements of Atom Concentrations as a Function of Pressure," Canadian Journal of Chemistry, 37: 62-78 (September 1959).
36. Kingery, W. D. Introduction to Ceramics. New York: John Wiley and Sons, 1960.
37. Klinger Educational Products Corporation. Product Bulletin 115-116. Jamaica, NY, 1986.
38. Kofsky, I. L. and J. L. Barrett. "Surface-Catalyzed Recombination into Excited Electronic, Vibrational, Rotational, and Kinetic Energy States: A Review," NASA N86-13253, Washington: National Aeronautics and Space Administration, 1986.
39. Kretschmer, C. B. and H. L. Petersen. "Kinetics of Three-Body Atom Recombination," The Journal of Chemical Physics, 39: 1772-1778 (October 1963).
40. Laidler, K. J. Chemical Kinetics (Second Edition). New York: McGraw-Hill Book Company, 1965.
41. Laidler, K. J. "Kinetic Laws in Surface Catalysis," Catalysis. Volume I, edited by P. H. Emmett. New York: Reinhold Publishing Corporation, 1954.
42. Liebau, F. Structural Chemistry of Silicates. New York: Springer-Verlag, 1985.
43. Linnett, J. W. and D. G. H. Marsden. "The Recombination of Oxygen Atoms at Salt and Oxide Surfaces," Proceedings of the Royal Society of London. Series A, 234: 504-515 (March 1956).
44. Loehman, R. E. Basic Research on Oxynitride Glasses: Final Report. July 1982. Contract DAAG-29-79-C-0007. SAI International, Menlo Park, CA, July 1982.
45. Lund, R. E. and H. J. Oskam. "Studies of the Nitrogen Afterglow. I. Surface Catalytic Efficiency and Diffusion Controlled Decay of Atomic Nitrogen," The Journal of Chemical Physics, 48: 109-115 (January 1968).
46. Marinelli, W. J. and J. P. Campbell. Spacecraft-Metastable Energy Transfer Studies: Final Report. 31 July 1986. Contract NAS9-17565. Physical Sciences Inc., Andover, MA, July 1986.

47. Marshall, T. and E. A. McLennan. "Interaction of Recombining Atomic Nitrogen with Gaseous Plasmas," IEEE Transactions on Nuclear Science, NS-10: 124-135 (January 1963).
48. Marshall, T. C. "Studies of Atomic Recombination of Nitrogen, Hydrogen, and Oxygen by Paramagnetic Resonance," The Physics of Fluids, 5: 743-753 (July 1962).
49. Marshall, T. C. "Surface Recombination of Nitrogen Atoms on Quartz," The Journal of Chemical Physics, 37: 2501-2502 (November 1962).
50. Marshall, T. C. and R. A. Kawcyn. "Thermal and Radiative Properties of Recombining Atomic Nitrogen," The Physics of Fluids, 5: 1657-1660 (December 1962).
51. Marshall, T. C. and others. Molecular Storage and Transfer of Electromagnetic Energy in Gaseous Plasmas: Final Report. April 1964. RADC-TDR-63-275. Contract AF30(602)-2650. Rome Air Development Center, Griffiss AFB, NY, April 1964 (AD-438419).
52. Menzel, D. "Electronically Stimulated Desorption," Applied Physics A--Solids and Surfaces, 38: 191-192 (November 1985).
53. Metals and Ceramics Information Center. Engineering Property Data on Selected Ceramics Volume III Single Oxides. MCIC-HB-07-Vol. III. Columbus, OH, July 1981.
54. National Aeronautics and Space Administration. Second Workshop on Spacecraft Glow. NASA CP-2391. Washington: Scientific and Technical Information Office, 1985.
55. National Aeronautics and Space Administration. Space Shuttle. NASA SP 407. Washington: Scientific and Technical Information Office, 1976.
56. Nishijima, M. and others. "Reactions of NO with the Si(111)(7 x 7) Surface: EELS, LFED and AES Studies," Surface Science, 137: 473-490 (February 1984).
57. Norton, F. H. Elements of Ceramics (Second Edition). Reading: Addison-Wesely Publishing Company, 1974.
58. Outred, M. and M. E. Pillow. "The Logarithmic Decay of the Lewis-Rayleigh Afterglow in Nitrogen," The Journal of Physics B--Atomic and Molecular Physics, 3: 399-404 (January 1970).

59. Owen, D. A. "A Spectroscopic Experimental and Computer Assisted Empirical Model for the Production and Energetics of Excited Oxygen Molecules Formed by Atom Recombination on Shuttle Tile Surfaces," NASA N82-23128, Washington: National Aeronautics and Space Administration, 1982.
60. Park, C. "Collisional Ionization and Recombination Rates of Atomic Nitrogen," AIAA Journal, 7: 1653-1654 (August 1969).
61. Parr, N. L. and others. "Preparation, Micro-structure, and Mechanical Properties of Silicon Nitride," Special Ceramics, edited by P. Popper. New York: Academic Press, 1972.
62. Pauling, L. The Nature of the Chemical Bond and the Structure of Molecules and Crystals (Third Edition). Ithaca: Cornell University Press, 1960.
63. Popper, P. and S. N. Ruddelsen. "The Preparation, Properties, and Structure of Silicon Nitride," Transactions of the British Ceramic Society, 60: 603-626 (June 1961).
64. Rahman, J. L. and J. W. Linnett. "Recombination of Atoms at Surfaces. Part 10--Nitrogen Atoms at Pyrex Surfaces," Transactions of the Faraday Society, 67: 170-178 (January 1971).
65. Rosner, D. E. and R. Cibrian. Nonequilibrium Stagnation Region Aerodynamic Heating of Hypersonic Glide Vehicles, 1975. AFOSR-TR-76-0965. Air Force Office of Scientific Research, Bolling AFB, DC, 1975.
66. Rossington, D. R. "Surface Chemistry of Glass," Introduction to Glass Science, edited by L. D. Pye and others. New York: Academic Press, 1972.
67. Sancier, K. M. and others. "Luminescence of Solids Excited by Surface Recombination of Atoms. II. Recombination Coefficients," The Journal of Chemical Physics, 37: 860-864 (August 1962).
68. Schwab, G. M. "Introductory Lecture," Solid/Gas Interface. New York: Academic Press, 1957.
69. Scott, C. D. "Catalytic Recombination of Nitrogen and Oxygen on High-Temperature Reusable Surface Insulation," AIAA Paper 80-1477, New York: American Institute of Aeronautics and Astronautics, 1980.

70. Scott, C. D. "Catalytic Recombination of Nitrogen and Oxygen on Iron-Cobalt-Chromia Spinel," AIAA Paper 83-0585, New York: American Institute of Aeronautics and Astronautics, 1983.
71. Scott, C. D. "Effects of Nonequilibrium and Wall Catalysis on Shuttle Heat Transfer," Journal of Spacecraft and Rockets, 22: 489-499 (September-October 1985).
72. Seward, W. A. A Model for Oxygen Recombination on a Silicon Dioxide Surface. Dissertation, AFIT/DS/AA/85-1. School of Engineering, Air Force Institute of Technology (AU), Wright-Patterson AFB, OH, December 1985.
73. Shand, E. B. Glass Engineering Handbook (Second Edition). New York: McGraw-Hill Book Company, 1958.
74. Shugler, A. "On the Equivalency of Si-O Bonds n Silicon Dioxide," Journal of Physics and Chemistry of Solids, 47: 659-664 (August 1986).
75. Shuman, M. E. and W. Brennen. "Heterogeneous Recombination of Nitrogen Atoms by the Smith Side Tube Method: Effects of Tube Length and Homogeneous Recombination," The Journal of Chemical Physics, 68: 4077-4085 (May 1978).
76. Shustorovich, E. "Coverage Effects Under Atomic Chemisorption: Morse-Potential Modeling Based on Bond Order Conservation," Surface Science, 163: L645-L654 (May 1985).
77. Smith, W. F. Principles of Materials Science and Engineering. New York: McGraw-Hill Book Company, 1986.
78. Sze, S. M. Semiconductor Devices. Physics and Technology. New York: John Wiley & Sons, 1985.
79. Tompkins, F. C. Chemisorption of Gases on Metals. New York: Academic Press Inc. 1978.
80. Vedeneyev, V. I. and others. Bond Energies, Ionization Potentials and Electron Affinities. New York: St. Martin's Press, 1966.
81. Vincenti, W. G. and C. H. Kruger, Jr. Introduction to Physical Gas Dynamics. Malabar, Florida: Robert E. Krieger Publishing Co., Inc., 1986.

82. Wells, F. A. Structural Inorganic Chemistry (Third Edition). Oxford: Clarendon Press, 1962.
83. Wentink, T. Jr. and others. "Nitrogen Atomic Recombination at Room Temperature," The Journal of Chemical Physics, 29: 231-232 (July 1958).
84. Wright, A. N. and C. A. Winkler. Active Nitrogen. New York: Academic Press, 1968.
85. Yamashita, T. "Rate of Recombination of Nitrogen Atoms," The Journal of Chemical Physics, 70: 4248-4258 (May 1979).
86. Young, R. A. "Pressure Dependence of the Absolute Catalytic Efficiency of Surfaces for Removal of Atomic Nitrogen," The Journal of Chemical Physics, 34: 1292-1294 (April 1961).
87. Zhandov, V. P. "Effect of Lateral Interaction of Adsorbed Particles on the Average Kinetic Energy of Desorption of Reaction Products," Surface Science, 165: L31-L34 (May 1986).

VITA

Michael Newman was born on 20 November 1951 in Niagara Falls, New York. He graduated from Niagara Falls High School in 1969 and attended Niagara County Community College from which he received two Associate Degrees: one in Liberal Arts and Humanities, 1972; the other in Applied Science, 1974. He then relocated to Tucson, Arizona, in 1979 and earned a Bachelor of Science in Mathematics from the University of Arizona, 1981. He received his commission through Officer Training School in August 1982 and began study in the Undergraduate Degree Conversion Program at the Air Force Institute of Technology, Dayton, Ohio, in September, 1982. He graduated in March 1984 with a Bachelor of Science in Electrical Engineering. He then served at Sunnyvale Air Force Station (now called Onizuka Air Force Station), HQ-AFSCF/VXTA, until July 1986, when he returned to the Air Force Institute of Technology. While stationed at Onizuka Air Force Station, he completed a graduate program in management offered by the University of Southern California, graduating in June 1986 with a Master of Science in Systems Management.

Permanent address: 963 Shauna Lane

Palo Alto, California 94301

A189843

REPORT DOCUMENTATION PAGE

Form Approved
OMB No. 0704-018

1. REPORT SECURITY CLASSIFICATION UNCLASSIFIED			1b. RESTRICTIVE MARKINGS		
2a. SECURITY CLASSIFICATION AUTHORITY			3. DISTRIBUTION/AVAILABILITY OF REPORT Approved for public release; distribution unlimited.		
2b. DECLASSIFICATION/DOWNGRADING SCHEDULE					
4. PERFORMING ORGANIZATION REPORT NUMBER(S) AFIT/GE/ENG/87D-50			5. MONITORING ORGANIZATION REPORT NUMBER(S)		
6a. NAME OF PERFORMING ORGANIZATION School of Engineering		6b. OFFICE SYMBOL (If applicable) AFIT/ENG		7a. NAME OF MONITORING ORGANIZATION	
6c. ADDRESS (City, State, and ZIP Code) Air Force Institute of Technology Wright-Patterson AFB, Ohio 45433				7b. ADDRESS (City, State, and ZIP Code)	
8a. NAME OF FUNDING/SPONSORING ORGANIZATION		8b. OFFICE SYMBOL (If applicable)		9. PROCUREMENT INSTRUMENT IDENTIFICATION NUMBER	
8c. ADDRESS (City, State, and ZIP Code)				10. SOURCE OF FUNDING NUMBERS	
		PROGRAM ELEMENT NO.		PROJECT NO.	TASK NO.
					WORK UNIT ACCESSION
11. TITLE (Include Security Classification) A Model for Nitrogen Atom Recombination on a Silicon Dioxide Surface (U)					
12. PERSONAL AUTHOR(S) Michael Newman, B. S., M. S., Capt, USAF					
13a. TYPE OF REPORT Thesis		13b. TIME COVERED FROM _____ TO _____		14. DATE OF REPORT (Year, Month, Day) 1987 December	
15. PAGE COUNT 186					
16. SUPPLEMENTARY NOTATION					
17. COSATI CODES			18. SUBJECT TERMS (Continue on reverse if necessary and identify by block number)		
FIELD	GROUP	SUB-GROUP	Heterogeneous Recombination, Adsorption, Recombination Coefficient, Space Shuttle Heating, Catalytic Nitrogen Recombination, Nitrogen Chemisorption		
20	13	8			
19. ABSTRACT (Continue on reverse if necessary and identify by block number) Title: A MODEL FOR NITROGEN ATOM RECOMBINATION ON A SILICON DIOXIDE SURFACE Thesis Chairman: Donald R. Kitchen, Major, USAF Professor of Electrical Engineering (See reverse for Abstract.)					
20. DISTRIBUTION/AVAILABILITY OF ABSTRACT <input checked="" type="checkbox"/> UNCLASSIFIED/UNLIMITED <input type="checkbox"/> SAME AS RPT <input type="checkbox"/> DTIC USERS					
21. ABSTRACT SECURITY CLASSIFICATION UNCLASSIFIED					
22a. NAME OF RESPONSIBLE INDIVIDUAL Donald R. Kitchen, Major, USAF			22b. TELEPHONE (Include Area Code) 513-255-4960		22c. OFFICE SYMBOL AFIT/ENG

UNCLASSIFIED

Security Classification of this Page

19. ABSTRACT

A model which describes the heterogeneous recombination of atomic nitrogen on a silicon dioxide surface in the temperature range 300-2000K was developed. The model accounts for surface participation in the recombination and uses Langmuir-Rideal as a basic mechanism to describe gas phase nitrogen atoms recombining with adsorbed nitrogen atoms. Silicon atoms were assumed to be the active surface sites upon which the nitrogen atoms adsorb.

Rate equations were derived from first principles and incorporated into a computer routine which calculated the recombination coefficient and other recombination parameters. The maximum value of the recombination coefficient was calculated to be 0.014 at 1300K. The number of surface sites was calculated to be 2.12×10^{14} per square cm. The results show that the model agrees satisfactorily with the empirical data.

CV.

Security Classification of this Page
UNCLASSIFIED